JOURNAL OF THE AERONAUTICAL SCIENCES

VOLUME 5 SEPTEMBER, 1938 NUMBER 11

CONTENTS

Flat Plates under Pressure . . . . . ELIAS MONESS 421

Dynamic Errors of the Rate-of-Climb Meter . . C. S. DRAPER AND G. V. SCHLIESTETT 426

Analytical Comparison of Helicopter and Airplane in Level Flight . MONTGOMERY KNIGHT 431

Range and Take-Off Calculations for Planes with Continuously Controllable Pitch Propellers ALBERT B. SCOLES AND WILLIAM A. SCHOECH 436

Some Remarks on the Physical Aspects of the Aircraft Icing Problem . . A. R. STICKLEY 442

Stainless Steel in Aircraft . . . . . HERBERT V. THADEN 447

Letters to the Editor 454
(*Max M. Munk, Richard C. Molloy*)

Institute Notes 455
Exchanges 456
Aeronautical Reviews 457
Books Received 455

Book Reviews

Airplane Structures, Vols. I and II, (*Alfred S. Niles and Joseph S. Newell*) . . . . . E. E. SECHLER 425

Flight Handbook, (*W. O. Manning*) 435

Yahrbuch der Deutsche Luftfahrtforschung, 1937 . . . . . J. C. HUNSAKER 441

Published by the

INSTITUTE OF THE AERONAUTICAL SCIENCES, INC.

JOURNAL OF THE AERONAUTICAL SCIENCES

VOL. 5 SEPTEMBER, 1938 NO. 11

Editor: J. C. HUNSAKER, *Massachusetts Institute of Technology*

Associate Editor: ARNOLD M. KUETHE, *Institute of the Aeronautical Sciences*

PUBLISHED MONTHLY BY THE INSTITUTE OF THE AERONAUTICAL SCIENCES, INC. AT 20TH AND NORTHAMPTON STS., EASTON, PA.

The JOURNAL OF THE AERONAUTICAL SCIENCES is the official publication of the Institute of the Aeronautical Sciences, Inc., and prints papers of scientific and technical interest to members and subscribers. In general, it provides an opportunity for members to publish articles disclosing new knowledge and new applications in the field of the aeronautical sciences. The Journal prints a few complete professional papers in each issue and a large number of short notes and critical comments. The Journal restricts itself to the aeronautical aspects of advances in science and engineering. New knowledge in physics, metallurgy, meteorology, etc., having aeronautical applications is reported and discussed in the Journal. Papers read at meetings of the Institute are presented in full or digested. Reviews of aeronautical literature and a digest of current aircraft books and magazines form a section of the publication. The news of the Institute is furnished members through the Journal.

SUBSCRIPTION RATES

United States and Possessions		Foreign Countries, Including Canada	
1 Year	$5.00	1 Year	$6.00
Single Copies	.50	Single Copies	.60

Manuscripts for publication, proofs, and all correspondence should be addressed to the Editorial Secretary of the JOURNAL.

Correspondence regarding subscriptions may be addressed to Publication Office, 20th and Northampton Sts., Easton, Pa., or to the Editorial Office of the JOURNAL OF THE AERONAUTICAL SCIENCES, 30 Rockefeller Plaza, Rockefeller Center, New York, New York. Cable Address: INSAEROSCI.

Entered as Second Class Matter at the Post Office, Easton, Pa., May 1, 1937. Acceptance for mailing at a special rate of Postage provided for in the Act of August 24, 1912. Authorized April 29, 1937.

JOURNAL OF THE AERONAUTICAL SCIENCES

Volume 5 SEPTEMBER, 1938 Number 11

Flat Plates under Pressure

ELIAS MONESS, *Douglas Aircraft Company*

(Received April 18, 1938)

Introduction

CURVES and equations are given for the maximum deflection and stress in rectangular sheets under pressures encountered in airplane practice. The object of this paper is to supply the designer of high altitude airplanes with systematic information for the design of thin sheets which have to withstand a given pressure differential. For the underlying theory for the equations given, reference is made to the work of A. and L. Föppl.[1]

"Thick," "Thin," and "Very Thin" Plates

A "thick" plate resists loads only by bending; its middle surface does not stretch; its deflection is negligible compared to its thickness. A "very thin" plate has no bending strength; it resists loads entirely by tension; its middle surface stretches; its deflection under load is so large that the thickness becomes negligible compared to it. The "thin" plate resists load both by bending and tension; its deflection is of the same order as its thickness. A plate of given dimensions does not always belong to the same category. A "thick" plate will become a "thin" one if the load applied to it is sufficiently large to cause it to deflect several times the thickness; similarly, a "thin" plate will behave as a "very thin" one under large loads.

In order to find approximately what class a given plate belongs to, the following assumptions will be made: The maximum deflection f of a "thick" plate should be $^1/_{20}$ of its thickness h; the minimum deflection of a "very thin" plate should be ten times its thickness. The equations for the deflection of "thick" and "very thin" square plates are, respectively:

$$f = 0.23pa^4/Eh^3, \text{ and } f = .804a\sqrt[3]{pa/Eh}$$

where a is half the length of the side of the panel, in inches; p is the pressure in lbs. per sq. in.; E is the modulus of elasticity. Inserting the values $f/h = {}^1/_{20}$ into the first equation and $f/h = 10$ into the second,

$$a/h = 38.9/(p)^{1/4} \text{ and } a/h = 377.1/(p)^{1/4}, \text{ respectively.}$$

These are plotted in Fig. 1 and define the region of "thick" and of "very thin" plates. Between these two curves is the region of "thin" plates. Tests have shown that panels encountered in airplane practice usually lie in this region. Fig. 1 also gives a "mean" curve of this region. This is plotted by finding that value of f/h for which the same deflection results from either of the two equations given above; this value is $f/h = 1.51$. The equation for the deflection of "thin" plates is

$$p = E(f/h)(h/a)^4\,[4.35 + 1.92(f/h)^2]$$

the "mean" curve is obtained by inserting $f/h = 1.51$ into this equation. Fig. 1 shows how a plate of a given a/h ratio moves into the "thin" or "very thin" region as the pressure increases.

Deflection of Thin Plates

The deflection of square thin plates can be calculated from the equation:

$$(a/h)^4p = E(f/h)[1.37 + 1.92\,(f/h)^2]$$

[1] Föppl, August and Ludwig. *Drang und Zwang*, Vol. I, R Oldenburg, München und Berlin, 1924.

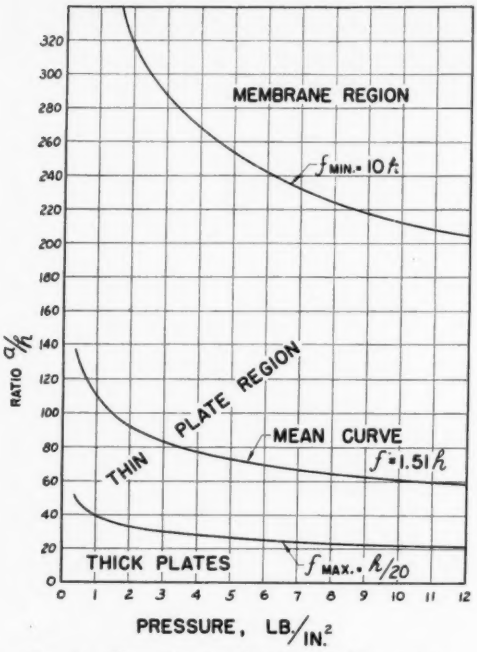

FIG. 1. Chart for classification of plates under pressure.

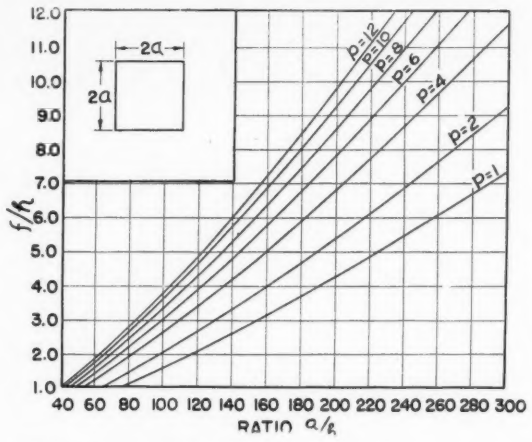

FIG. 2. Deflection of square Dural plate under pressure.

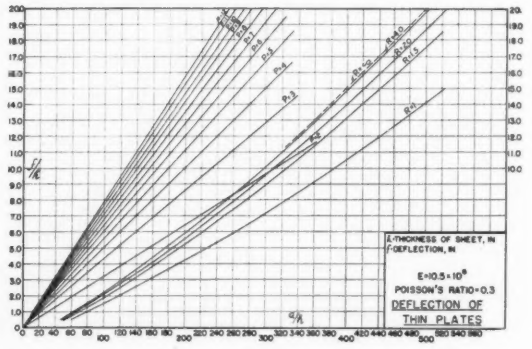

FIG. 3. Deflection of rectangular plates under pressure.

From this equation f/h is plotted against a/h for various pressures in Fig. 2. The deflection of rectangular thin plates is a function of their aspect ratio R. A combination of the equations for thick and for very thin rectangular plates gives the equation:

$$(a/h)^4 p = E(f/h)[1/s + (1/n^3)(f/h)^2]$$

where s and n are constants depending on R. In Fig. 3, f/h is plotted against a/h for various values of R. The pressure is assumed to be 1 lb. per sq. in. The deflection for any pressure p may be found by using instead of a/h the "equivalent" value $[(a/h)(p)^{1/4}]$. This equivalent a/h can be found in Fig. 3 by following a vertical at the actual a/h to the intersection with the required pressure line and then scaling the distance from this point of intersection to the origin of co-ordinates. Fig. 3 shows that an increase in R from 2.0 to 4.0 means approximately only a 25 percent change in the deflection, while any further increase in R has practically no effect on the deflection. It should be kept in mind that these deflections are only for panels with rigid boundaries.

Stresses in Thin Plates

In rectangular panels the maximum stresses occur at the center of the plate. High local stresses may occur near the rivets but, as a rule, they are not critical for the design of the panel. The maximum stress is on the tension side of the sheet and represents the sum of the bending and tension stress. For square panels it can be found from the equation:

$$\sigma_{max.} = (Ef/a^2)(1.76h + 0.635f)$$

for rectangular panels the maximum stress can be found from the equation:

$$\sigma_{max.} = .406E \frac{f/h}{(a/h)^2} [(3.33 + 1/R^2) + 2.55(f/h)(3.33k_1 + k_2/R)]$$

where k_1 and k_2 are constants depending on R. These stresses act parallel to the short sides of the panel. Figs. 4, 5, 6, and 7 give the maximum transverse stress for $R = 1.0$, 1.5, 2.0, and 4.0, respectively. The stresses in the longitudinal direction are always smaller than the transverse ones; but in combination with stresses arising from sources other than pressure they may become critical; they are found from the equation:

$$\sigma_{max.} = .406E \frac{f/h}{(a/h)^2} [(3.33/R^2 + 1) + 2.55(f/h)(k_1 + 3.33\ k_2/R)]$$

These stresses are plotted in Figs. 8, 9, and 10.

Theoretical Considerations

The equations for the deflection of thick and very thin plates are arrived at by equating the work done

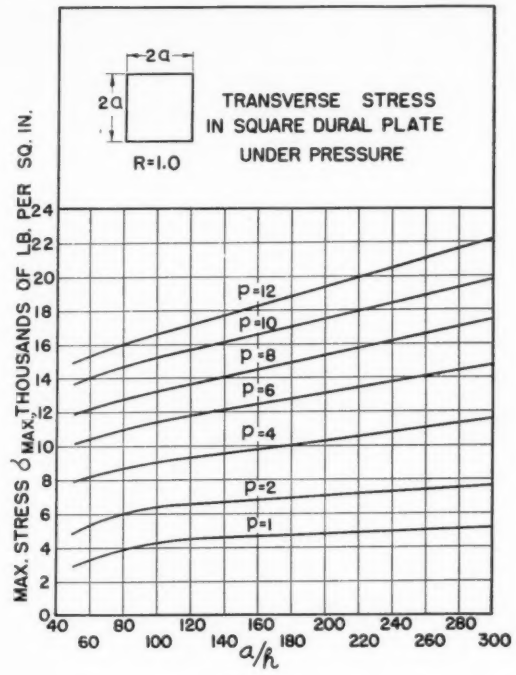

FIG. 4.

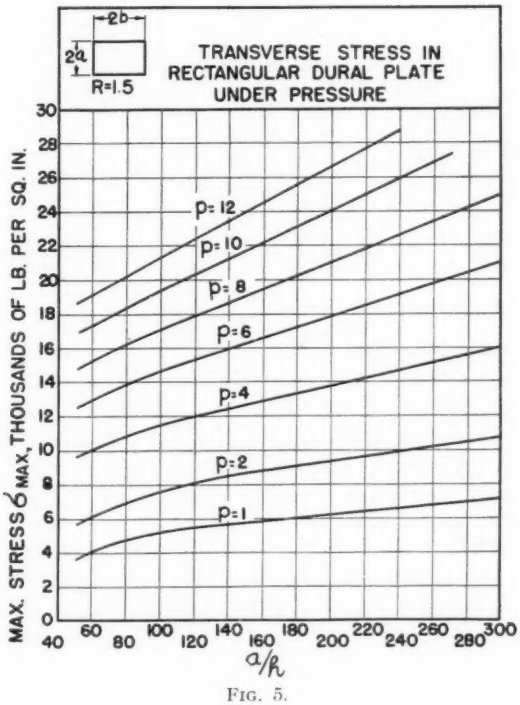

FIG. 5.

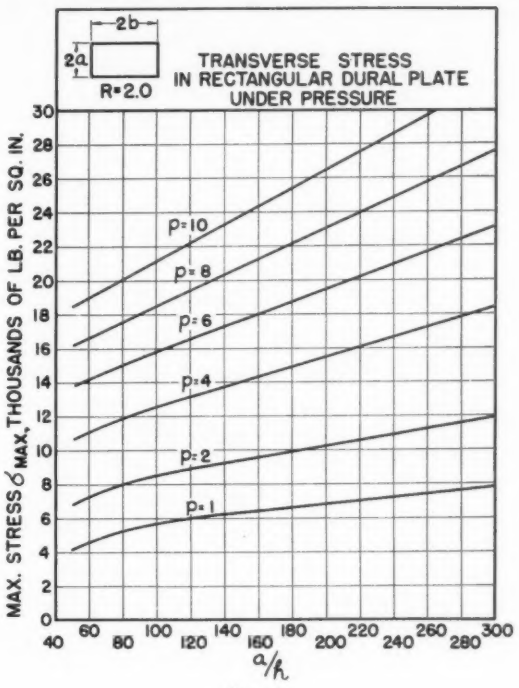

FIG. 6.

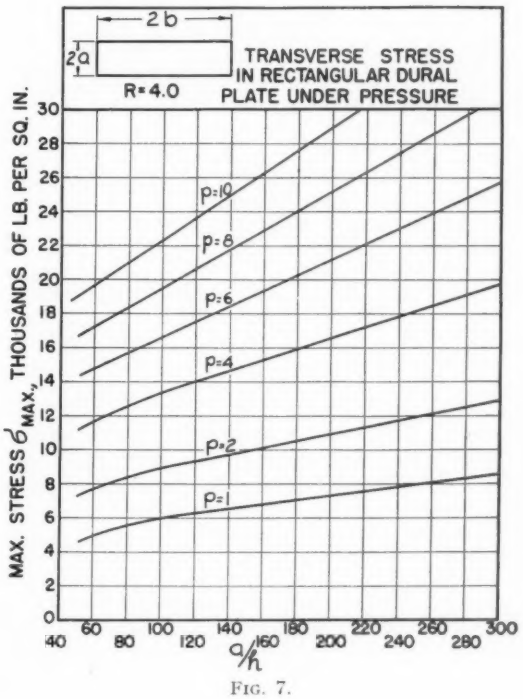

FIG. 7.

by the applied forces to the internal work of deformation of the plate. To facilitate these calculations the shape of the deflected plate is assumed, as a first approximation, to be such that both the longitudinal and the transverse fibers are cosine curves. The equations for the deflection of thin plates are obtained by combining the equations for thick plates with those for membranes.

In this paper the numerical coefficients of the equations are based on Poisson's ratio 0.3, which is the value for dural. The coefficient for the deflection of simply supported thick plates is about three times that for

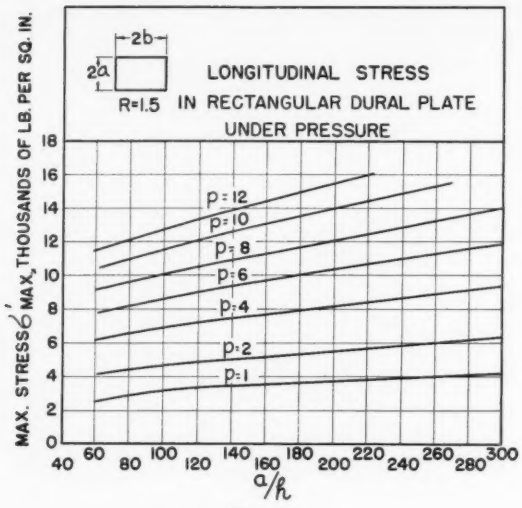

FIG. 8.

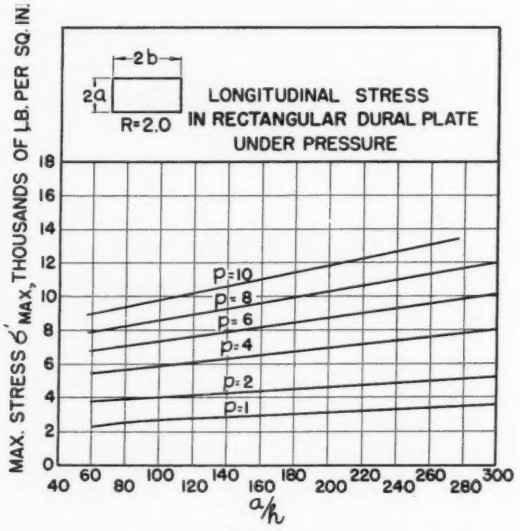

FIG. 9.

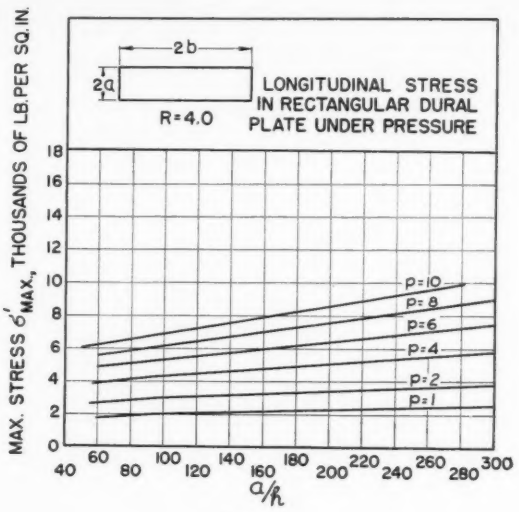

FIG. 10.

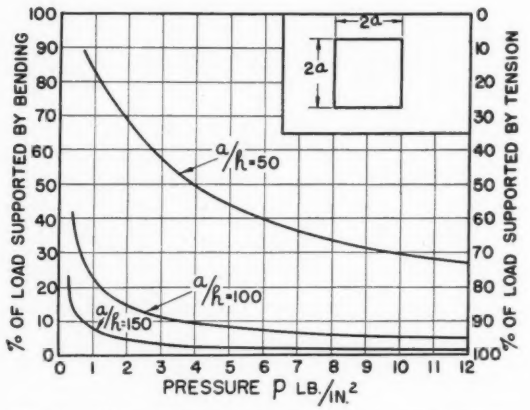

FIG. 11. Distribution of total carrying strength between bending and tension.

thick plates with clamped edges. The question arises as to which value is to be used for the derivation of the equation for the deflection of thin plates. For square plates the coefficient for simply supported thick plates has been used because clamping the edges of a thin plate will not raise the center of the plate appreciably, but will only cause a local turning-over of the edges. For rectangular plates the coefficient used is an average between that for simply supported and clamped plates; this is done to allow for the fact that there is more boundary support per unit area than in the case of the square plate. It might be added that the choice of the one or the other coefficient would affect the final result but little since it deals only with the term depending on bending, and this term is small compared to that depending on tension. In deriving the equation for the maximum stress in a thin plate the coefficient for the simply supported thick plate was used. This is conservative since the maximum stress in simply supported thick plates is higher than that in clamped ones; moreover, the term depending on bending is of the same order as that depending on tension and it remains a significant part of the total even under relatively high pressures. Fig. 12 brings out this fact clearly.

Figs. 4 to 10 give the maximum stress as a function of the ratio a/h for various pressures and aspect ratios R; however, the equations for the maximum stress do not include the pressure directly; they contain the term f/h which is a function of the pressure. These equations were first solved for a number of values of a/h and the maximum stress was plotted against f/h for various values of R; with the aid of Fig. 3 which connects the quantities f/h and a/h with pressure the above curves were then re-plotted to give the stresses directly as a function of the pressure.

The total load on a thin plate is supported partly by bending and partly by tension. It is possible to find the percentage of support offered by either; Fig. 11 shows this percentage for various ratios a/h and for a

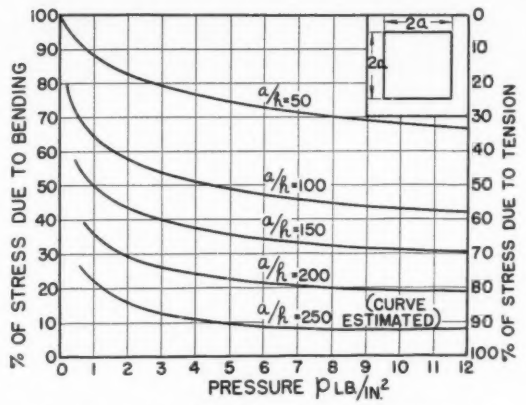

FIG. 12. Ratio of bending stress and tensile stress to total stress.

square plate. The above percentages are determined as follows: For the part of the pressure resisted by bending, p_1, there is the relation

$$f/h = 0.73\ (p_1/E)(a/h)^4$$

(the coefficient 0.73 is for clamped square thick plates); for the part p_2 resisted by tension

$$f/h = .804(a/h)^{3/4}(p_2^2/E)^{1/3}$$

for a given f/h the two right sides of the above equations must be equal. Since p_1 and p_2 together make up the total pressure p, it is easy to express either of them in terms of p. It will be seen from Fig. 11 that already at $a/h = 100$ the bending support becomes negligible; the plate is a "membrane"; it takes the load only in tension. The total stress in a thin plate is due partly to bending and partly to tension. The percentage of either stress in a square plate is plotted in Fig. 12. It will be seen that the stress due to bending remains a considerable part of the total stress, long after the support offered by bending has vanished.

A plate will deflect most under the first several pounds of pressure. As the pressure continues to increase the corresponding increases in deflection become smaller and smaller. The reason for this is that the plate begins to behave more and more like a membrane, and for the latter the deflections increase as the cube root of the pressure.

Book Review

Airplane Structures, Vols. I and II, by ALFRED S. NILES and JOSEPH S. NEWELL, John Wiley and Sons, Inc.; 451 pages and 177 pages, respectively; $5.00 and $2.75, respectively.

The publication of the revised edition of this text has bridged an important gap between classical strength of materials and practical airplane design. Although primarily a textbook on airplane structural design and analysis, it will be a valuable reference book for the use of the experienced designer. This is particularly true because of the fact that the authors have not sponsored any one method of analysis but have attempted to give at least an outline of all of the methods in common use and to show the advantages and limitations of each.

The first two chapters give a short discussion of the aerodynamic and flying considerations which affect the structural design. These include such items as the specifications, the performance, the location and use of various aerodynamic parts of the airplane, and the loads and loading conditions on the structure. No effort is made to give a complete aerodynamic discussion; however, enough of such material is included in these two chapters so that the young designer will realize that there are definite interlocking requirements between the aerodynamic and the structural design.

The next four chapters are devoted to a discussion of beam analysis methods. The authors have given one of the most complete treatments of beams under various types of loading that has ever been collected in one volume. The mathematical treatment of beams is explained in simple terms so that a designer with limited ability in the use of calculus and differential equations can use the equations with confidence and a feeling that he understands the physical picture behind the derivations. Nearly all of the discussion is on beams which follow the fundamental laws of the simple beam theory, and only a limited amount of space is given to beams made up of thin sheet material for which special design methods must be used.

Chapter VII contains a comprehensive discussion of the problems of torsion, starting with the classical theory of a circular bar and then going to the more complicated cases such as torsion of open sections and thin-walled structures. Combined stresses are covered by a somewhat unusual but quite understandable treatment using Mohr's circle.

The analysis of statically determinate plane and space trusses is treated in detail in Chapters VIII and IX. All common methods of truss analysis are covered, the merits of each method being illustrated by detailed examples. Chapter IX covers the use of graphical methods for beam and truss analysis; methods which if properly used, are a great time saver in certain structural problems.

Structures, the failure of which is primarily caused by some form of instability failure, are briefly treated in the next chapter. Column failure is discussed in detail and a short and very incomplete treatment of instability failures of thin-sheet structures is given.

Chapter XI is a review of the various means of attachment of structural elements with particular emphasis being placed on welding and riveting. The treatment of welding is of a somewhat general nature and would not, in general, be sufficient to use for design. On the other hand, the use of rivets with standard (not countersunk) heads is complete with tabulated strength values of all of the commonly used rivet materials. Short paragraphs on other forms of attachment give a picture of the other methods which are now used and which have been used in the past.

The final chapter in the first volume considers deflection in structures as a design problem. Energy methods of analysis are treated for beams and trusses, as well as some of the other more commonly used solutions. At the end of the chapter a short comparison of methods is made which is intended to guide the designer in his choice for any given problem.

The second volume, containing two chapters, is entirely devoted to the problem of indeterminate structures. In the first chapter is discussed, in detail, the problem of the indeterminate truss and the various manners in which an analysis can be made.

(continued on page 435)

Dynamic Errors of the Rate-of-Climb Meter

C. S. DRAPER and G. V. SCHLIESTETT, *Massachusetts Institute of Technology*

Presented at the Instruments Session, Sixth Annual Meeting, I. Ae. S.
January 24, 1938

Introduction

RATE-OF-CLIMB meters* were first described in 1910 by Bestelmeyer,[1] who recognized the existence of errors due to rapidly changing conditions. However, little quantitative information is available even at the present time on the magnitude of the errors to be expected in particular maneuvers. These "dynamic errors" can be negligible or relatively large depending upon the time required for changes in the actual rate of climb as compared with a period called the "characteristic time" of a particular instrument. If the forcing changes occur in a time much less than the characteristic time, large dynamic errors will appear while slower changes have progressively less effect.

The present paper outlines the general theory of the conventional "capillary leak" rate-of-climb meter and describes a laboratory method for determining the coefficients necessary to predict performance in flight. Theoretical and laboratory results in the form of curves are compared with data taken from flight tests. Special attention is paid to the case of sinusoidal changes, and non-dimensional curves applicable to any frequency are given.

General Theory

Fig. 1 shows the essential parts of a rate-of-climb meter as considered by several previous investigators.[1,2,3,4,5,6] A pressure gage is connected to a chamber and passages having a total volume V when the pressure P_1 inside is equal to the external pressure P. The system is sealed from the atmosphere except for a capillary element having the property of passing air at a rate of Q mass units per unit time, where

$$Q = C(\rho_2/\eta_2)(P - P_1) = (C/\nu_2)(P - P_1) \quad (1)$$

C = capillary coefficient
ρ_2 = mass density of air in capillary
η_2 = viscosity of air in capillary
ν_2 = kinematic viscosity of air in capillary

This capillary coefficient C may be constant or may be changed in an arbitrary manner by a temperature or pressure sensitive control element. However, it can ordinarily be considered as constant over the short time intervals in which dynamic errors are important. The chamber is usually so constructed that internal temperature changes are minimized.

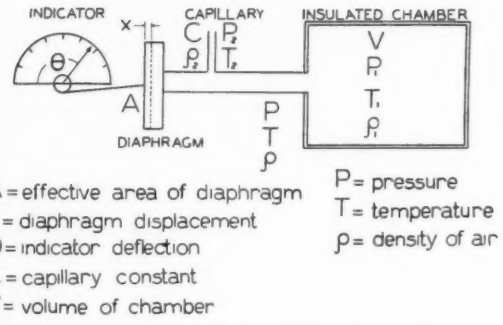

FIG. 1. Diagram of a rate-of-climb meter.

To set up the equation associated with indications of the rate-of-climb meter, the mass of gas inside the system is expressed in terms of volume V, internal pressure P_1, internal temperature T_1, effective diaphragm area A, and diaphragm deflection x. This expression is differentiated to find the rate of change of internal mass in terms of the variables given, and this rate of change is equated to the rate of flow through the capillary element as given by Eq. (1). The diaphragm deflection is expressed in terms of the elastic coefficient k, the damping coefficient b, the effective area A of the pressure gage element and the pressure difference $(P - P_1)$. Mechanical inertia effects are assumed to be negligible compared with the other forces involved. Finally, the rate of change of external pressure is related to the rate of change of altitude by differentiating the hydrostatic equation to obtain

$$dP/dt = -\rho g(dz/dt) = -\rho g v_a \quad (2)$$

in which z is the altitude, g is the acceleration of gravity, and v_a is the actual rate of climb. After combining terms the result is a differential equation relating the indicated rate of climb v_i to v_a.

$$a_2 \frac{d^2 v_i}{dt^2} + a_1 \frac{dv_i}{dt} + a_0 v_i = a_3 v_a + a_4 \frac{dT_1}{dt} \quad (3)$$

in which

$$a_0 = \frac{1}{DE} \frac{R}{M} \frac{C}{\nu_2} \frac{k}{A}$$

* Rate-of-climb meters are considered to include the class of instruments which give a direct indication of the rate of change of altitude. Two companies make these instruments in the United States. By one, they are known as "Rate of Climb Meters," by the other, as "Vertical Speed Meters."

TABLE 1
Coefficients of Typical Rate-of-Climb Meters Measured at an Average Altitude of 4000 Ft.

Meter	n	τ (Seconds)
A	8.5	3.0
B	7.2	3.5
C	136	6.4

$$a_1 = \frac{1}{DE}\left(\frac{R}{M}\frac{C}{\nu_2}\frac{b}{A} + \frac{V}{T_1}\frac{k}{A} + \frac{AP_1}{T_1}\right)$$

$$a_2 = \frac{1}{DE}\frac{V}{T_1}\frac{b}{A}$$

$$a_3 = \frac{MgPV}{RTT_1}$$

$$a_4 = -\frac{P_1V}{T_1^2}$$

where

R = universal gas constant
M = molecular weight of air

$$D = \frac{\theta}{x} = \frac{\text{angular deflection of indicator hand}}{\text{linear deflection of diaphragm}}$$

$$E = \frac{v_i}{\theta} = \frac{\text{meter reading}}{\text{angular deflection of indicator hand}}$$

If the effect of internal temperature changes can be neglected, Eq. (3) becomes

$$(d^2v_i/dt^2) + b_1(dv_i/dt) + b_0v_i = b_0v_a \qquad (4)$$

The equality of the coefficients of v_i and v_a is the result of a proper static calibration; *i.e.*, the instrument is made to read correctly for constant rates of climb. In flight the rate of climb v_a is not constant but varies with time in a manner depending upon the particular maneuver considered. If the coefficients b_1 and b_0 are known, the behavior of the rate-of-climb meter can be calculated for any range over which these coefficients are substantially constant. The essential information can either be computed directly from design constants or determined from the response of a complete instrument to a "step forcing function" in which the applied rate of climb is suddenly changed from one constant value to another.

For an instrument which does not oscillate under a step function, that is, one that has more than critical damping, Eq. (4) can be written as

$$\frac{d^2v_i}{dt^2} + \frac{n+1}{\tau}\frac{dv_i}{dt} + \frac{n}{\tau^2}v_i = \frac{n}{\tau^2}v_a \qquad (5)$$

where τ is called the "characteristic time" of the instrument and n is the "characteristic damping number." The value of n is unity for an instrument which is just critically damped and becomes larger as the damping is increased.

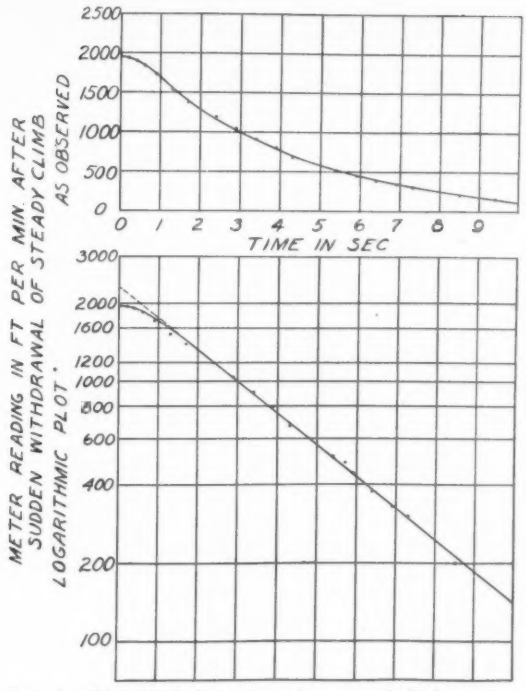

FIG. 2. Characteristic curves of a rate-of-climb meter. (Meter B.)

In general, the solution of Eq. (5) has the form

$$v_i = Ae^{-t/\tau} + Be^{-nt/\tau} + v_s \qquad (6)$$

in which A and B are constants to be determined by initial conditions and v_s is the steady state response to a particular forcing function v_a. For the case of a step function with v_a suddenly changing from a constant value v_{i_0} to 0, Eq. (6) becomes

$$v_i/v_{i_0} = [n/(n-1)](e^{-t/\tau} - \frac{1}{n}e^{-nt/\tau}) \qquad (7)$$

With the value of n always greater than unity the second term will decrease faster than the first term until finally v_i/v_{i_0} behaves as a simple exponential. Under this condition

$$\ln(v_i/v_{i_0}) \cong \ln[n/(n-1)] - (t/\tau) \qquad (8)$$

A plot with the logarithm of v_i/v_{i_0} (or v_i) as ordinate and time as abscissa will be a straight line when Eq. (8) becomes true. The slope of this straight line is the reciprocal of the characteristic time τ, while extension of the line to its intersection with the $t = 0$ axis permits the determination of n. Fig. 2 shows an example of this procedure Table 1 gives values of n and τ for three typical modern rate-of-climb indicators

As the actual rate of climb in many practical cases can be approximated by the use of sinusoidal curves, it is useful to find the steady state solution of Eq. (5) for this type of forcing function. This solution

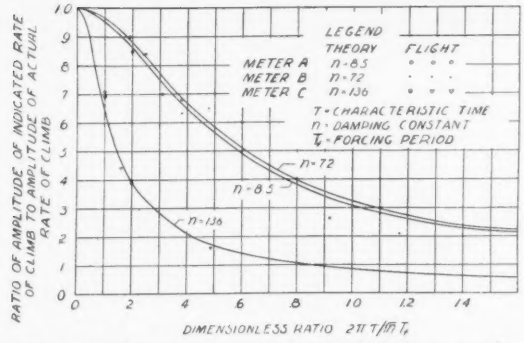

FIG. 3. Performance curves of rate-of-climb meters for sinusoidal changes.

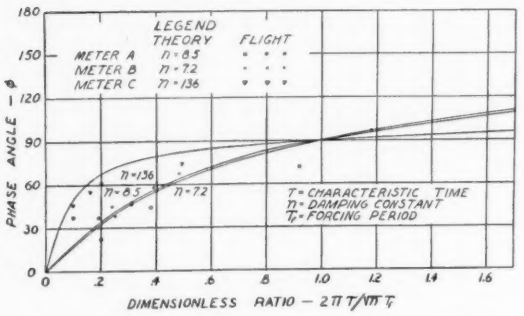

FIG. 4. Phase-angle curves of rate-of-climb meters.

is found by the straight forward application of well known mathematical processes with the result

$$\frac{v_i}{v_{am}} = \frac{\sin\left[\frac{2\pi t}{T_f} - \phi\right]}{\sqrt{\left[1 - \frac{1}{n}\left(\frac{2\pi\tau}{T_f}\right)^2\right]^2 + \left[\frac{n+1}{n}\frac{2\pi\tau}{T_f}\right]^2}} \qquad (9)$$

in which the subscript m denotes amplitude and

T_f = period of forcing motion

$$\phi = \tan^{-1}\left(\frac{n+1}{n}\frac{2\pi\tau}{T_f}\right) \Big/ \left[1 - \frac{1}{n}\left(\frac{2\pi\tau}{T_f}\right)^2\right]$$

The curves of Fig. 3 show the amplitude of v_i/v_{am} as a function of $(1/\sqrt{n})(2\pi\tau/T_f)$ for the three meters listed in Table 1. On this same figure are shown the experimental check points of five flight tests. Corresponding theoretical and flight test values of the phase angle ϕ are given in Fig. 4.

EXPERIMENTAL RESULTS

As a check on the accuracy of the theoretical analysis, two types of experiments were carried out.

(1) In the laboratory, the meters were placed in a chamber and subjected to a sinusoidal pressure variation by means of a cam-operated bellows.[7]

(2) In flight tests, the instruments were mounted on a special board and subjected to sinusoidal changes of altitude about a level course. Fig. 5 is a photograph showing the equipment installed in a Fairchild 24 airplane. A continuous photographic record of meter readings was taken for each run by means of a motion picture camera. Modern sensitive altimeters, shown by previous tests to have negligible dynamic errors, were used to record the actual altitude changes. Rate-of-climb data were found by taking slopes from the altitude curves.

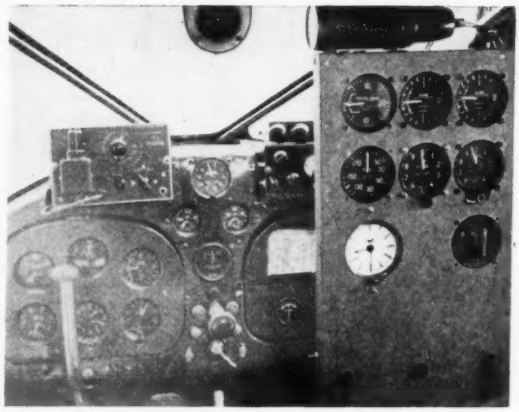

FIG. 5. Special installation for flight tests of instruments.

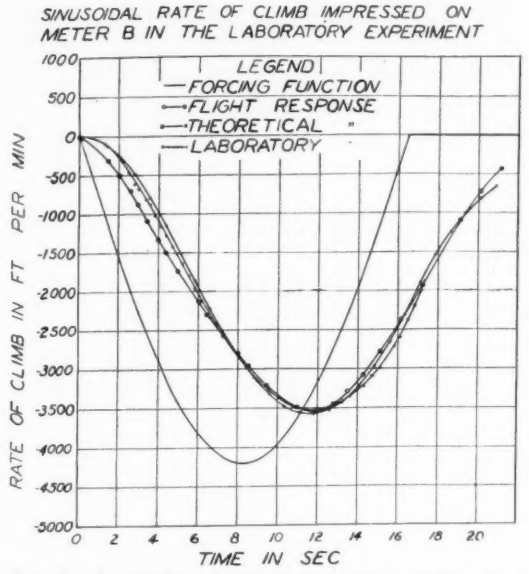

FIG. 6. Comparison of rate-of-climb meter response in a flight maneuver with laboratory test and theory.

A sinusoidal approximation to the rate of climb occurring when an airplane changes altitude by means of a steep glide is shown in the forcing function curve of Fig. 6. The response curves as predicted by theory based on step-function tests, as given by an artificially produced sinusoidal rate of climb and as measured in flight are seen to be substantially identical. This case includes a transient at the initial instant since the rate of climb was constant at zero when the forcing function was applied.

Figs. 7, 8, and 9 show the results of flight tests which included sections with approximately sinusoidal

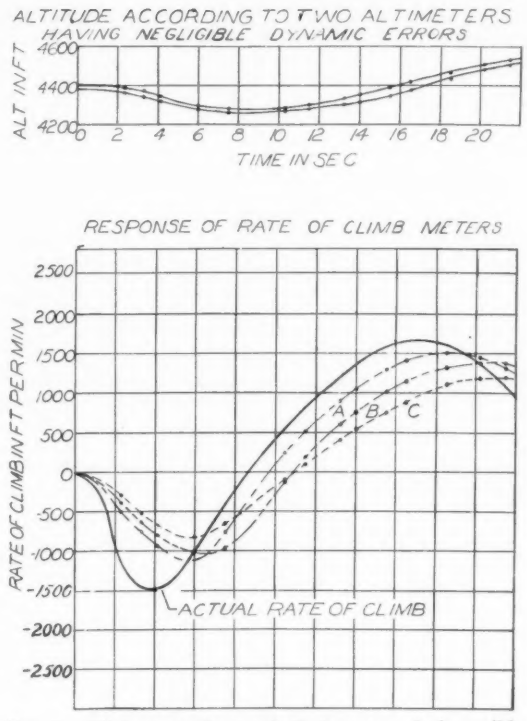

FIG. 7. Flight test of rate-of-climb meters during mild maneuver.

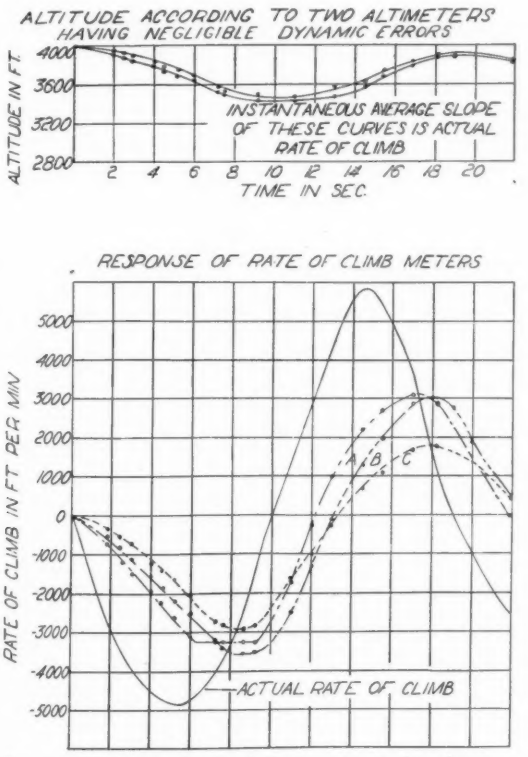

FIG. 8. Flight test of rate-of-climb meters during vigorous maneuver.

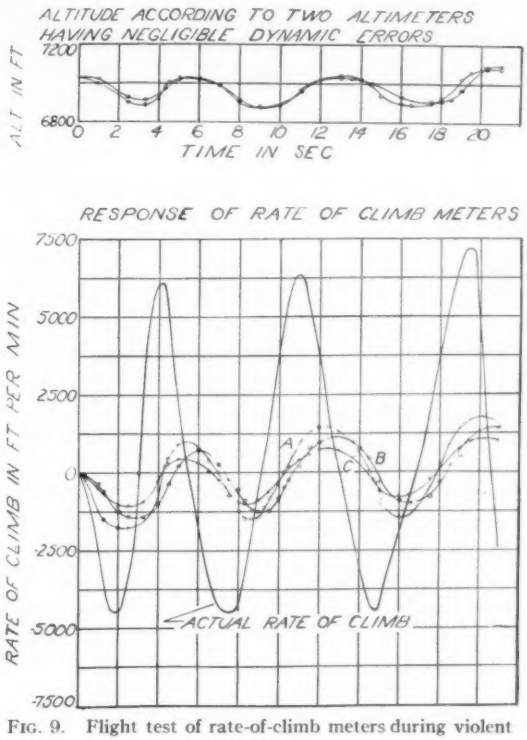

FIG. 9. Flight test of rate-of-climb meters during violent maneuver.

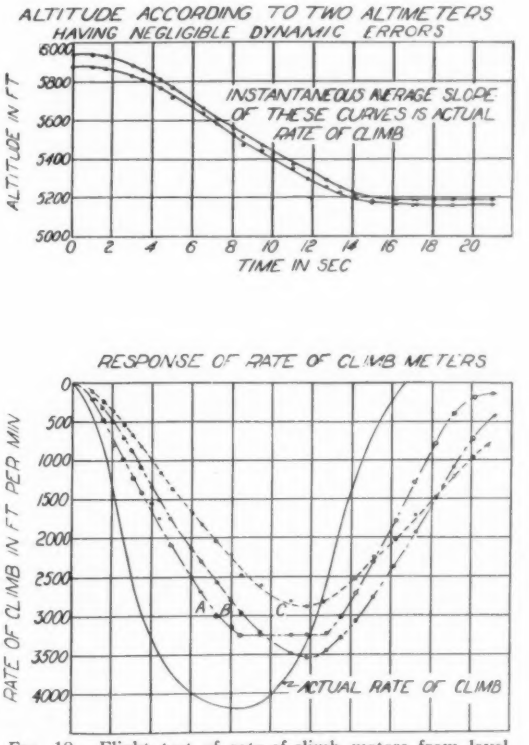

FIG. 10. Flight test of rate-of-climb meters from level flight to steep glide to level flight.

rates of climb. In each case sufficient time elapsed after the variation started for a comparison of peak values to represent the steady state condition in amplitude and phase. Points taken from these figures for each of the rate-of-climb meters of Table 1 are indicated on Figs. 3 and 4. The points show close enough agreement with the calculated curves to insure the general method will give reliable results.

The behavior of meters A, B, and C during a steep glide between two flight levels is shown in Fig. 10. Meter A, which has the shortest characteristic time, has the smallest dynamic error, except when the reading is limited by a stop at a rate of descent of 3250 ft. per min. The meter C, with a characteristic time of 6.4 sec. and an n value of 136 as compared with 3.0 sec. and 8.5, respectively, for meter A, has a considerably greater error during the whole maneuver. This result is in agreement with the curves of Fig. 3 even though the rate of climb was not exactly sinusoidal and included a transient at the initial instant. From the upper curve of Fig. 2 which is typical of the transient in any case it is apparent that after a time interval equal to twice the characteristic time transient effects have almost disappeared. For the case of Fig. 10, the period involved is several times the characteristic time for each instrument so the indications have certainly reached the steady state before the maneuver ends.

Discussion

Eaton,[2] Stewart,[3] and Brombacher[5] have given treatments of dynamic errors in the rate-of-climb meter which differ from that outlined above in that the transient is represented by a single exponential term instead of two terms as given in Eq. (6). Taking the typical case of Eq. (7) as the transient it is apparent that as the number n is increased, the response tends toward a simple exponential. In Table 1, meter C is of the type tested by the previous investigators and has a ratio n equal to 136 as compared with values of 8.5 and 7.2, respectively, for meters A and B which represent more recently designed instruments. It follows that for the older type of instrument it was valid to treat the transient as a simple exponential but such a procedure will involve an appreciable calculation error with the newer types.

The maneuvers studied above are for the most part artificial in the sense that they would never be used in ordinary flight. However, the experiments demonstrate the validity of the analysis and illustrate the trend to be expected in dynamic errors of the rate-of-climb meter. These errors become increasingly greater as rate-of-climb changes become more rapid. In an extreme case such as that of Fig. 9 the meter may get so far "out of phase" that a maximum upward rate of climb is indicated when the airplane actually has a considerable downward velocity. This result is merely a confirmation of the well known fact that a rate-of-climb meter is unreliable during violent maneuvers. In any case a rate-of-climb meter will substantially recover from the effects of any disturbance in a time period equivalent to twice the characteristic time.

In normal use, rate-of-climb meters are subjected to much slower changes than those used in the flight tests. Any variation in rate of climb occurring while the pilot is attempting to hold constant altitude can be considered as the start of a sinusoidal change of long period with relatively small transient effects. Referring to Figs. 3 and 4 this condition corresponds to a very low value of the argument for which the plots show substantially correct readings as regards both phase and amplitude.

W. G. Brombacher of the Bureau of Standards, and Charles H. Colvin of the Kollsman Instrument Company, have pointed out five principal conditions under which a rate-of-climb meter is used; (1) to maintain level flight; (2) to attain a maximum rate of climb; (3) to attain a minimum rate of descent; (4) to maintain a constant rate of climb; and (5) to maintain a constant rate of descent. All these operations involve such relatively slow changes in rate of climb that the present-day instruments will all give satisfactory service if properly used. It is only necessary for the pilot to remember that he must make his control adjustments slowly if he wishes to rely on his rate-of-climb meter.

Reference

[1] Bestelmeyer, A., *Zur Theorie des Ballonmanometers*, Physikalische Zeitscrift, Vol. II, pp. 736–768, 1910.

[2] Eaton, H. N., *Aircraft Instruments*, pp. 46–52, Ronald Press, 1926.

[3] Stewart, C. J., *Aircraft Instruments*, pp. 42–51, John Wiley & Sons, 1930.

[4] Mears, A. H., *Statoscopes and Rate of Climb Indicators*, N.A.C.A. Technical Report No. 126, Part 3, 1922.

[5] Brombacher, W. G., *Measurement of Altitude in Blind Flying*, N.A.C.A. Technical Note No. 503, pp. 31–33, 1934.

[6] McKay W., *Dynamic Characteristics of Pressure Operated Aircraft Instruments*, Thesis, Massachusetts Institute of Technology, 1935.

[7] Weems, W. R., *The Effect of Tubing on the Indications of an Airspeed Meter*, Journal of the Aeronautical Sciences, Vol. 3, No. 5, p. 165, March, 1936.

Analytical Comparison of Helicopter and Airplane in Level Flight*

MONTGOMERY KNIGHT, *Georgia School of Technology*

Presented at the Rotary-Wing and Lighter-than-Air Session, Sixth Annual Meeting, I. Ae. S. January 25, 1938

SUMMARY

The general power equation is obtained for the helicopter rotor in level flight on the assumption that the circulation about the rotor blades is independent of radius and forward velocity.

The power required by the rotor is then compared with that required by a wing whose span is equal to the rotor diameter. Curves are given showing the variation of this power ratio with forward speed for three different rotor solidities and for a wing of aspect ratio 6, both for the lifting surfaces only and for the complete helicopter and airplane.

The analysis indicates the superiority of the helicopter rotor over the airplane wing at high speeds and its inferiority in the climbing range.

INTRODUCTION

MUCH uncertainty still exists as to the relative merits of the helicopter and the airplane. To clarify this situation to some extent, the following analysis dealing with a comparison of the two aircraft types in level flight has been prepared.

When expressed mathematically, the problem of the helicopter becomes extremely cumbersome unless certain general simplifying assumptions are made as follows:

(1) The number of blades may be taken as infinite.

(2) All angles associated with the induced velocity are small, thus permitting the usual approximations.

(3) Rotational and radial components of velocity and tip effects may be neglected.

(4) The slipstream contraction may be neglected.

(5) The fluctuating airflow over the blades does not affect their profile characteristics.

Moreover, the special case of level flight requires two more assumptions in order that the analysis may be reduced to its simplest form:

(1) The rotor axis remains vertical.

(2) The circulation about the individual blades is independent of radius and forward velocity.

INDUCED AXIAL VELOCITY

The induced velocity relationships have been obtained previously by R. A. Hefner and the author[1] for the case of static thrust by using a new application of the vortex theory. Fig. 1 shows this concept with the vortices which emanate from the blade tips forming a cylindrical surface of vorticity extending to infinity below the rotor.

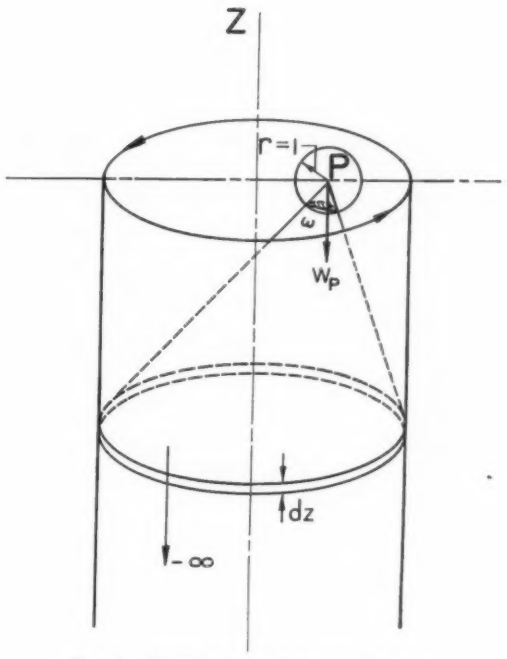

FIG. 1. Vortex system for static thrust.

It has been shown[1] that the induced velocity under these conditions may be expressed as

$$w_p = \frac{d\Gamma/dz}{4\pi}\,[\omega(Z_2) - \omega(Z_1)] \qquad (1)$$

where w_p = axial induced velocity, Γ = total circulation about the blades, $\omega(Z)$ = solid angle subtended at P by element of circulation dz, and $d\Gamma/dz$ = constant. However, since $Z_2 = \infty$ and $Z_1 = 0$, $\omega(Z_2) = 0$ and $\omega(Z_1) = 2\pi$. Therefore

$$w_p = -\,(1/2)(d\Gamma/dz) = \text{constant} \qquad (2)$$

This merely means that, for constant circulation along the blade, the induced axial velocity over the entire rotor circle will be constant and of the value given by Eq. (2).

When the rotor is given a horizontal velocity, V, the vortex cylinder is blown back as shown in Fig. 2. Moreover, in the reversed velocity region over the retreating blades, a small inverted cylinder forms. The size of this cylinder is a function of the forward motion

* Released by the Director, State Engineering Experiment Station of Georgia.

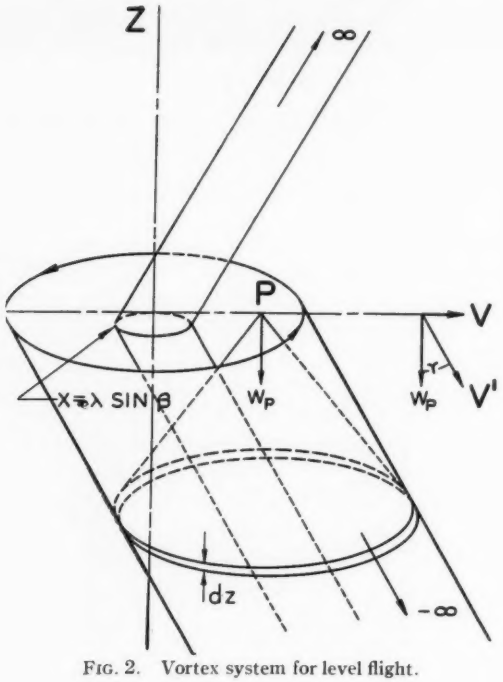

FIG. 2. Vortex system for level flight.

and its inclination is equal and opposite to that of the large cylinder.

It is obvious that, for a given element, dz, of the vortex cylinders, the solid angle at P will decrease with increasing forward velocity. The nature of this decrease may be determined by noting that, for very large values of Z, the solid angle will be (see Fig. 2) $\omega(Z) = \omega_0(Z) \cos \gamma$, where $\omega_0(Z)$ = solid angle for static thrust condition. Hence for horizontal motion at a given speed Eq. (1) becomes

$$w_p = -(\cos \gamma)/2(d\Gamma/dz) = \text{constant} \qquad (3)$$

This signifies that, for forward motion as well as hovering, the axial velocity is uniform over the rotor disc. Therefore, the circulation gradient in the z direction is

$$d\Gamma/dz = -2w/\cos \gamma = -2V'$$

where $V' = \sqrt{w^2 + V^2}$ and $\cos \gamma = w/\sqrt{w^2 + V^2}$.

The vertical distance between adjacent turns of the vortical helix has been shown in reference 1 to be $d = \dfrac{2\pi w}{\Omega B}$, where B = number of blades and Ω = blade angular velocity. Since the circulation gradient is $d\Gamma/dz = \Gamma/Bd$, the following important relationship emerges, if Ω = constant,

$$\Gamma\Omega/4\pi = -w\sqrt{w^2 + V^2} = w_0^2 \qquad (4)$$

where w_0 = induced velocity for hovering flight. This may be reduced to the non-dimensional form

$$\varphi^4 + \lambda^2\varphi^2 - \varphi_0^4 = 0$$

by putting $\varphi = w/\Omega R$, $\varphi_0 = w_0/\Omega_0 R$, and $\lambda = V/\Omega R$

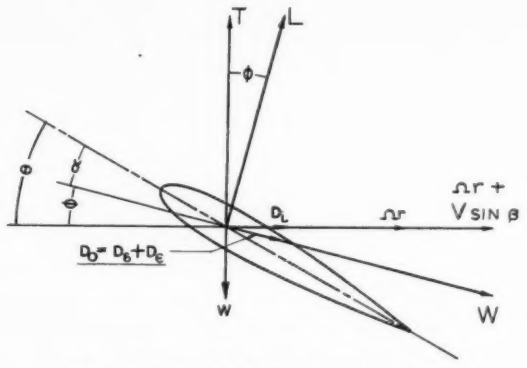

FIG. 3. Forces and velocities on blade element.

the subscript zero referring to the case of static thrust. Fortunately, for practical values of the rotor parameters and tip speeds, the first term in Eq. (4) is negligible for $\lambda > 0.10$ and it is sufficient to write the induced angle as

$$\varphi = \varphi_0^2/\lambda$$

and $$\varphi_\sigma = (T_{\sigma_0}/4\lambda)\sigma \quad \text{(reference 1)} \qquad (5)$$

where σ = solidity = $Bc/\pi R$.

LIMITING LIFT COEFFICIENT

The thrust on a blade element (see Fig. 3) is

$$dT = \rho(\Gamma/B)wdr = (\rho/2)ca_0(\theta - \varphi)W^2dr$$

where T = thrust, W = resultant velocity, r = radius of element, c = blade chord, a_0 = profile lift curve slope, and θ = blade incidence angle. Thus

$$\Gamma = \frac{Bca_0(\theta - \varphi)W}{2} = \text{constant} \qquad (6)$$

In reference 1, it has been shown for static thrust that the blade twist for constant circulation is $\theta = \theta_{tip}/r$ and, therefore,

$$\alpha = \frac{R}{r}(\theta_0 - \varphi)_{tip}$$

where α = effective angle of attack of element. It is evident that this type of rotor will begin to stall at the center. However, as Glauert has stated,[2] stalling is unimportant within the circle $r = {}^1/_3R$. From reference 1, $\alpha_{max.} = .25$ may be taken as the full scale limit and hence the non-dimensional limiting thrust coefficient (*ibid.*) is seen to be

$$(C_{T_0})_{max.} = (\sigma a_0/2)(\theta_0 - \varphi_0)_{max.} = \sigma a_0/24$$

where $C_{T_0} = (2L/\rho\pi R^2\Omega^2R^2)$ and L = weight of helicopter. Putting $T_{\sigma_0} = C_{T_0}/\sigma^2$, this becomes $(T_{\sigma_0})_{max.} = a_0/24\sigma$ and, since $a_0 = 6$ (approximately),

$$(T_{\sigma_0})_{max.} = 1/4\sigma \qquad (7)$$

THRUST

The thrust on each blade element as shown above is

$$dT = \rho(\Gamma/B)Wdr$$
$$= \rho(\Gamma/B)\Omega R^2(x + \lambda \sin \beta)dx$$

where $x = r/R$ and β = azimuth angle measured from downwind.

The mean thrust on the entire rotor thus becomes

$$T = \frac{\rho\Gamma\Omega R^2}{2\pi}\int_0^{2\pi}\int_0^1 (x + \lambda \sin \beta)dxd\beta$$

$$T_\sigma = \Gamma/\pi\Omega R^2\sigma^2$$

Since Ω is to be held constant

$$T_\sigma = T_s \tag{8}$$

TORQUE

The torque coefficient may be defined as

$$Q_\sigma = 2Q/\rho\pi R^2\Omega^2R^3\sigma^3$$

From Fig. 3 it is evident that the torque is composed of three parts so that

$$Q_\sigma = Q_{\sigma_i} + Q_{\sigma_\epsilon} + Q_{\sigma_\delta}$$

where Q_{σ_i} = induced torque coefficient, Q_{σ_ϵ} = profile variation torque coefficient, and Q_{σ_δ} = minimum profile torque coefficient.

Induced torque: The induced torque on a blade element is due to the inclination of the lift vector and hence

$$dQ_i = (w/W)rdT$$
$$= \rho(\Gamma/B)\Omega R^3\varphi xdx$$

For the entire rotor

$$Q_i = \frac{\rho\Gamma\Omega R^3\varphi}{2\pi}\left[\int_0^{2\pi}\int_0^1 xdxd\beta - 2\int_\pi^{2\pi}\int_0^{\lambda \sin \beta} xdxd\beta\right]$$

and

$$Q_{\sigma_i} = T_{\sigma_0}\varphi_\sigma\left(1 - \frac{\lambda^2}{2}\right) = \frac{\sigma T_{\sigma_0}^2}{4\lambda}\left(1 - \frac{\lambda^2}{2}\right)$$

It is necessary to split up the integration in this and the following cases because the sign of the integrand is always positive and therefore does not give the correct torque in the reversed flow region.

Profile variation torque: As in reference 1, the profile variation drag coefficient can be expressed as

$$C_{D_\epsilon} = \epsilon C_L^2 = \epsilon\, a_0^2(\theta - \varphi)^2$$

Thus on an element (see Eq. 6),

$$dQ_\epsilon = (\rho/2)\cdot c\ \epsilon\ a_0^2(\theta - \varphi)^2W^2rdr$$

$$= \frac{\rho}{2}\frac{4\Gamma^2\epsilon R^2}{B^2c}xdx$$

Then, for the rotor,

$$Q_\epsilon = \frac{2\rho\Gamma^2}{2\pi}\frac{R^2\epsilon}{Bc}\left[\int_0^{2\pi}\int_0^1 xdxd\beta - 2\int_\pi^{2\pi}\int_0^{\lambda \sin \beta} xdxd\beta\right]$$

and $Q_{\sigma_\epsilon} = 2\epsilon T_{\sigma_0}^2[1 - (\lambda^2/2)]$

Minimum profile torque: For the blade element this is

$$dQ_\delta = (\rho/2)c\delta W^2rdr$$
$$= (\rho/2)c\delta\Omega^2R^4(x + \lambda \sin \beta)^2xdx$$

Then, for the rotor,

$$Q_\delta = \frac{\rho}{2}\frac{Bc\delta\Omega^2R^4}{2\pi}\left[\int_0^{2\pi}\int_0^1 (x + \lambda \sin \beta)^2xdxd\beta - 2\int_\pi^{2\pi}\int_0^{\lambda \sin \beta}(x + \lambda \sin \beta)^2xdxd\beta\right]$$

and $Q_{\sigma_\delta} = (\delta/4\sigma^2)[1 + \lambda^2 - (51/24)\lambda^4]$

DRAG

The drag coefficient will be defined as

$$D_\sigma = 2D/\rho\pi R^2\Omega^2R^2\sigma^2$$

The drag on a blade element is

$$dD = (\rho/2)cC_DW^2 \sin \beta dr$$

Thus it will be seen that the drag coefficients for the entire rotor are obtained merely by substituting sin β for the moment arm in the torque equations giving the following results:

$$D_{\sigma_i} = \sigma T_{\sigma_0}\varphi_\sigma\lambda = \sigma^2T_{\sigma_0}^2/4$$
$$D_{\sigma_\epsilon} = 2\sigma\epsilon T_{\sigma_0}^2\lambda$$
$$D_{\sigma_\delta} = (\delta/4\sigma)[\lambda + (7/2)\lambda^3]$$

POWER REQUIRED

Rotor: The total power required by the rotor will be

$$P_R = Q\,\Omega + D_RV \tag{9}$$

where D_R = rotor drag. But

$$D_RV = (D_\sigma/\sigma)(\rho/2)\pi R^2\Omega^3R^3\sigma^3\lambda$$

and $$Q\,\Omega = Q_\sigma(\rho/2)\pi R^2\Omega^3R^3\sigma^3$$

Substituting the individual torque and drag terms in Eq. (9) the rotor power becomes

$$P_R = \left[\left(\frac{\sigma T_{\sigma_0}^2}{4\lambda} + 2\epsilon T_{\sigma_0}^2\right)\left(1 + \frac{\lambda^2}{2}\right) + \frac{\delta}{4\sigma^2}\left(1 + 2\lambda^2 + \frac{11}{8}\lambda^4\right)\right]\frac{\rho}{2}\pi R^2\Omega^3R^3\sigma^3 \tag{10}$$

Wing: For purposes of comparison the span of the wing of the "corresponding" airplane will be taken as equal to the rotor diameter. This is reasonable since existing autogiros and helicopters have rotor "diameter-loadings" that approximate the span-loadings of present-day airplanes of moderate size.

The power required by a wing having a span equal to the diameter of the rotor will be

$$P_W = D_WV = (C_{D_i} + C_{D_\epsilon} + \delta_W)(\rho/2)SV^3$$

where δ_W = minimum profile drag coefficient of wing. However, keeping in mind that, for level flight,

$$T_\sigma = T_{\sigma_0} = \frac{2L}{\rho\pi R^2\Omega^2R^2\sigma^2} = \text{constant}$$

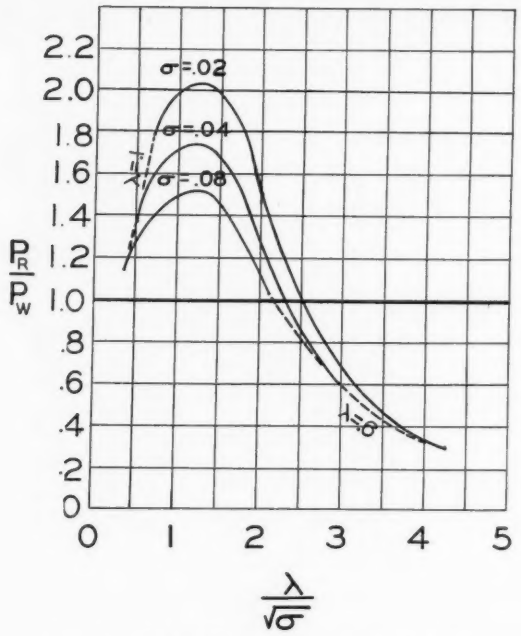

FIG. 4. Level flight comparison, rotor vs. wing.

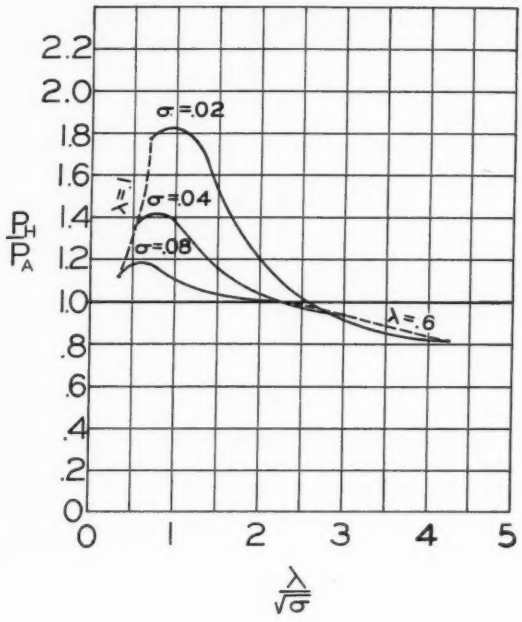

FIG. 5. Level flight comparison, helicopter vs. airplane.

and $C_L = 2L/\rho SV^2$ it is evident that

$$C_L = (\sigma^2/\sigma_w)(T_{\sigma_0}/\lambda^2)$$

where $\sigma_w = S/\pi R^2 = 4/\pi \text{A.R.}$

The drag coefficients may be written as follows:

$$C_{D_i} = \frac{C_L{}^2}{\pi \text{A.R.}} = \frac{\sigma^4}{\sigma_W{}^2}\frac{T_{\sigma_0}{}^2}{\lambda^4}\frac{\sigma_W}{4}$$

and

$$C_{D_\epsilon} = \epsilon_W C_L{}^2 = \epsilon_W \frac{\sigma^4}{\sigma_W{}^2}\frac{T_{\sigma_0}{}^2}{\lambda^4}$$

where ϵ_W = constant. Therefore

$$P_W = \left[\delta_W + \frac{\sigma^4}{\sigma_W{}^2}\frac{T_{\sigma_0}{}^2}{\lambda^4}\left(\frac{\sigma_W}{4} + \epsilon_W\right)\right]\frac{\rho}{2}SV^3 \quad (11)$$

Power ratio: Eqs. (10) and (11) may now be combined to obtain the power ratio for the wing and rotor only, in terms of the static thrust coefficient, T_{σ_0}, as follows:

$$\frac{P_R}{P_W} = \frac{\sigma^3\left[T_{\sigma_0}{}^2\left(\frac{\sigma}{4\lambda} + 2\epsilon\right)\left(1 + \frac{\lambda^2}{2}\right) + \frac{\delta}{4\sigma^2}\left(1 + 2\lambda^2 + \frac{11}{8}\lambda^4\right)\right]}{\delta_W\sigma_W\lambda^3 + \frac{\sigma^4 T_{\sigma_0}{}^2}{\sigma_W\lambda}\left(\frac{\sigma_W}{4} + \epsilon_W\right)} \quad (12)$$

For maximum rotor efficiency, $T_{\sigma_0} = (T_{\sigma_0})_{max.} = 1/4\sigma$ and

$$\frac{P_R}{P_W} = \frac{\left[\frac{1}{16}\left(\frac{\sigma}{4\lambda} + 2\epsilon\right)\left(1 + \frac{\lambda^2}{2}\right) + \frac{\delta}{4}\left(1 + 2\lambda^2 + \frac{11}{8}\lambda^4\right)\right]}{\delta_W\frac{\sigma_W}{\sigma}\lambda^3 + \frac{1}{16\lambda}\frac{\sigma}{\sigma_W}\left(\frac{\sigma_W}{4} + \epsilon_W\right)} \quad (13)$$

For the complete helicopter and airplane Eq. (13) must be modified by the addition of the parasite power terms in both numerator and denominator, thus:

$$\frac{P_H}{P_A} = \frac{P_R + \delta_P'(\sigma_W/\sigma)\lambda^3}{P_W + \delta_P(\sigma_W/\sigma)\lambda^3} \quad (14)$$

where δ_P' = helicopter parasite drag coefficient and δ_P = airplane parasite drag coefficient.

In order to use Eq. (13) and (14) for purposes of actual comparison it is necessary to make a choice of the wing and profile parameters and the most logical method is to select average values as follows:

Wing A.R. = 6, hence $\sigma_W = .212$

$\delta_W = \delta = .008$

$\delta_P = \delta_P' = .022$

$\epsilon_W = .0062$ (reference 3)

$\epsilon = \frac{5}{3}\epsilon_W = .0104$ (reference 1)

The results obtained by inserting these parametric values in Eq. (13) are given graphically in Fig. 4 for three rotor solidities, σ = .02, .04, and .08 covering practically all present autogiros and helicopters. These curves show clearly the power required by the rotor in terms of that required by the wing.

In Fig. 5, corresponding curves are given as obtained from Eq. (14) and afford a comparison of the complete helicopter and the complete airplane.

In both the above figures, the power ratio is plotted against $\lambda/\sqrt{\sigma}$ thus permitting direct comparison at various forward speeds.

Discussion of Results

As indicated in the curves, the present theory is limited to a range of values of λ from 0.10 to 0.60. Nevertheless, the curves show definite trends outside of these limits.

In Fig. 4, the notable superiority of the two rotors of smaller solidity at the higher speeds and their equally notable inferiority at the lower speeds as compared with the "corresponding" wing may be clearly seen.

A similar relationship, though less extreme, appears to exist also for the complete aircraft. The assumption that the parasite drags of the helicopter and airplane may be taken as the same will probably be criticized. However, the author believes that careful aerodynamic design of the parasite parts of future helicopters will result in a close approach to this equality.

Figs. 4 and 5 are not intended to furnish a complete comparative analysis of the power required by the airplane and the helicopter, for they represent only a set of average conditions. However, these curves indicate that a helicopter rotor of small solidity should be superior at high speeds to the fixed wing of average proportions, and inferior to it at low speeds.

Moreover, the inclusion of parasite-drag indicates that a cleanly designed helicopter having a rotor of small solidity will not necessarily be inferior at high speeds to the airplane and may eve nbe slightly superior. This fact, together with its ability to move vertically, appears to the author to make the helicopter worthy of further study and development.

References

[1] Knight, Montgomery, and Hefner, Ralph A., *Static Thrust Analysis of the Lifting Airscrew*, N.A.C.A. Technical Note No. 626, December, 1937.

[2] Glauert, H., *On the Horizontal Flight of a Helicopter*, British A.R.C. R. & M. No. 1157, March, 1928.

[3] Jacobs, Eastman N., Ward, Kenneth E., and Pinkerton, Robert M., *The Characteristics of 78 related Airfoil Sections from Tests in the Variable Density Wind Tunnel*, N.A.C.A. Technical Report No. 460, 1933.

Book Reviews

(*continued from page 425*)

Simple examples are carefully worked out and explained, tending to simplify this subject which has always been one which the young designer has dreaded, due largely to a lack of complete understanding of the principles involved. The second chapter deals with indeterminate beams covering such subjects as the three moment equations for beams under axial loads and the analysis of beam columns with constant and variable cross-sections.

From the standpoint of a compilation of the classical methods of analysis of beams, trusses, and other such conventional types of structure, these two volumes are a valuable addition to designers' libraries and to the field of structural textbooks. The separation into two volumes is somewhat unfortunate, inasmuch as the material in the second volume is directly related to that in the first and the separation tends to bring in a sense of discontinuity between the treatment of determinate and indeterminate structures which should be avoided whenever possible.

The treatment of what might be called unconventional types of structure, such as monocoque and semi-monocoque, is rather incomplete and unsatisfactory. It is realized that this subject is very controversial in nature and that design methods are constantly changing; however, it is necessary to give the designer all of the information which is available and to indicate to him the limitations of the various suggested analysis methods. A suggested method of doing this would be to have one volume which was entirely devoted to thin sheet structures and related structures, which would be frequently revised as more complete knowledge was gained on these matters.

The book is very ably and well written and contains a large number of illustrations. Many tables, charts, and nomograms will tend to simplify certain routine analyses such as column design, choice of rivet and bolt sizes, etc. Problems relating to the subject matter are given at the end of each chapter, and examples of typical analyses are liberally interspersed throughout the textual material.

E. E. Sechler
California Institute of Technology

Flight Handbook, by W. O. Manning; Flight Publishing Company, London; 142 pages, 3s. 6d.

Let no-one be misled by the title of this book. It is anything but a "Handbook" in the sense we are accustomed to use the term, but rather it is a non-mathematical introduction to Aeronautical Engineering.

As such it is a very readable and informative account of the principles of aerodynamics, structural design, gliders and sailplanes, balloons and airships, propellers, and instruments. The explanation of the lift of a wing, the principles underlying structural design, the chapter on balloons and airships, and the one on instruments are especially well done.

The general level of the book is such that the high-school student could understand it without difficulty.

Range and Take-Off Calculations for Planes with Continuously Controllable Pitch Propellers

ALBERT B. SCOLES and WILLIAM A. SCHOECH, *U. S. Navy and California Institute of Technology*

Presented at the Air Transport Session, Sixth Annual Meeting, I. Ae. S. January 27, 1938

Introduction

THE purpose of this paper is two-fold: first, to develop a method for evaluating the ultimate-range parameter in miles per pound of fuel consumption for planes equipped with continuously controllable pitch propellers; and second, to utilize this method in investigating the effect of several geometrical parameters of the airplane upon range. An excellent recent treatment of the problem, in which several of the parameters are replaced by mean values, is given in reference 1, while the procedure which has become classical in this country is outlined in reference 2.

Outline of the Method

The method consists of a more exact evaluation of the ultimate-range parameter, namely, miles per pound of fuel consumed, which, when integrated over the weight range of the fuel capacity, will give the range. This parameter is designated as C_R, and is defined by the equation

$$C_R = V/(\text{b.h.p.} \times c)$$

where V is in miles per hour (true airspeed), b.h.p. is the brake horsepower, and c is in pounds per brake horsepower per hour.

For convenience in evaluating this parameter, it is rearranged algebraically as follows:

$$C_R = V/(\text{b.h.p.} \times c) = [1/(\text{t.h.p.}/V)] \times \eta/c$$

where η = propulsive efficiency = t.h.p./b.h.p. But $Drag \times V$ = t.h.p.; therefore, (t.h.p./V) is proportional to $Drag$ and C_R is proportional to $(1/Drag) \times (\eta/c)$.

This will be recognized as a portion of the familiar Breguet formula for range:

$$R = \int (Lift/Drag) \times (\eta/c)(dW/W)$$

Here $Lift$ is equal to $Weight$; hence, they may be cancelled, and the formula becomes

$$R = \int (1/Drag) \times (\eta/c)dW = \int C_R\, dW$$

which must be evaluated between the limits of initial and final "Gross Weights."

Maximum range will correspond to maximum C_R, and, inasmuch as this is a non-analytical function of $Drag$, η, and c, all of which vary with altitude, the integral must be evaluated by a step-by-step process for a specific altitude. Generally the process is as follows: The limits of the integral being the initial and final Gross Weights, the maximum values of C_R are evaluated for these weights, and for as many intermediate weights as may be necessary to define a curve. For the altitude and weight chosen, a series of true airspeeds is selected. This fixes, for each speed, the term $1/Drag$, (*i.e.*, V/t.h.p.) of the integral. The remaining terms (η, c) of the integral, being dependent upon the engine-propeller combination, cannot be separated and must be evaluated as the ratio η/c. The maximum value of this ratio is determined for each speed and used in the basic equation to obtain the value of C_R for each speed. A plot of these values of C_R *vs.* speed will determine for the fixed weight and altitude the maximum value of C_R and the speed at which it will be obtained. The maximum value of C_R is plotted against the weight, and the area under the curve will give the maximum range.

The total thrust horsepower may be computed by Oswald's method[3] or from the full-scale polar of the airplane. Since η and c must be determined for a single engine, the total thrust horsepower is divided by the number of engines and a fictitious C_R, corresponding to one engine, is determined. The C_R for the complete airplane is then given by dividing this fictitious C_R by the number of engines.

Inasmuch as both η and c are dependent upon r.p.m., use is made of a parameter which is independent of r.p.m. and which is defined as follows:

$$C_{SJ} = C_S^5/J^2\eta = \frac{\rho V^5}{N^2 \text{ b.h.p.}} \frac{1}{\eta} \frac{N^2D^2}{V^2} = \frac{\rho V^3 D^2}{\text{b.h.p.} \times \eta} = \rho\, V^3D^2/\text{t.h.p.}$$

where C_S is the propeller speed-power coefficient, and J is the propeller advance ratio.

This parameter is evaluated from existing GALCIT* three-bladed propeller-efficiency charts. It is then plotted against propulsive efficiency for values of constant J (Fig. 1). Then, for a given W, V, and com-

* Guggenheim Aeronautics Laboratory, California Institute of Technology.

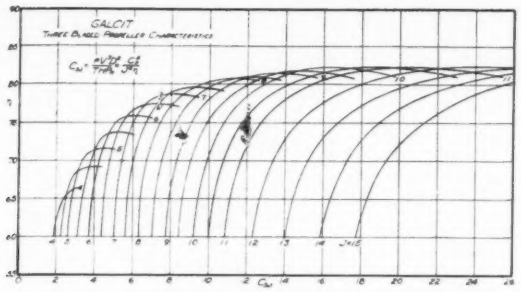

FIG. 1. C_{SJ} *vs.* η for constant J for three-bladed propellers replotted from Fig. 7 of reference 5.

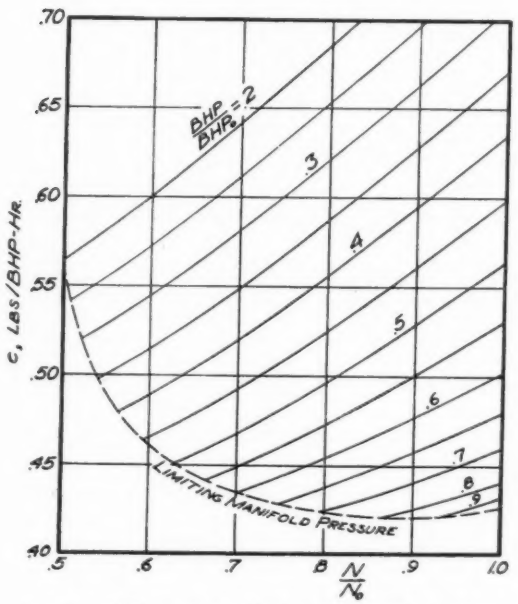

FIG. 2. N/N_{rated} *vs.* specific fuel consumption for constant b.h.p./b.h.p.$_{rated}$. These curves represent average values for modern aircraft engines.

puted t.h.p. the value of C_{SJ} is computed for entering the curves. A series of values of J is selected, and the N's corresponding to the assumed J's are computed. Then, for each C_{SJ} and J, the corresponding η is determined from the curve. With these η's and the computed t.h.p., values of b.h.p. are calculated from which, together with the corresponding N (converted to engine r.p.m.), the specific fuel consumption, c, is determined. It is found convenient to plot engine curves with the ratio of N/N_{rated} against specific fuel consumption, for constant values of b.h.p./b.h.p.$_{rated}$, as in Fig. 2. The data upon which Fig. 2 is based are discussed later in the paper. It will be noted that propeller r.p.m. can be used in the ratio, thus saving a step in the calculations. With the values of η and c thus determined for each N, the ratio of η/c is plotted against N, and, in general, there will be a maximum in this curve which will give the maximum η/c obtainable and the corresponding optimum N for the specified weight and velocity. Limiting manifold pressure or full throttle for the engine may prohibit the use of values of N which

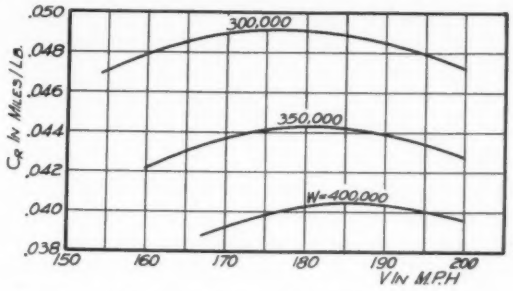

FIG. 3a. V in m. p. h. *vs.* C_R in miles/lb. for constant gross weight.

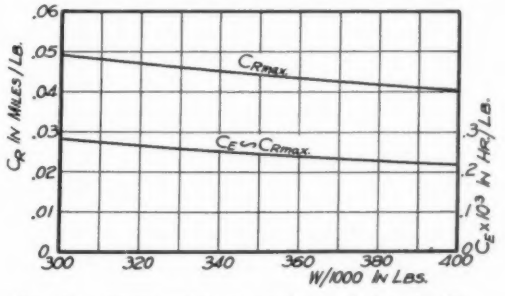

FIG. 3b. Gross weight *vs.* maximum C_R in miles/lb.

would give a true maximum to the η/c curve. In such cases, the curve of η/c *vs.* N ends at the value of N corresponding to the above restriction, and this will give the maximum attainable η/c. In general, the maximum η/c will not occur at either maximum η or at minimum c. This note is made because of the fact that in many cases the lowest possible specific fuel consumption has been assumed as the criterion for maximum range.

The above process may be repeated over the range of possible velocities from stall to maximum. Then, from the values of V, c (for maximum η/c), and b.h.p. (determined from t.h.p. and the η for maximum η/c), the value of C_R is computed. A plot of this value against V for the specified weight will, in general, reveal a maximum which will represent the maximum miles obtainable per pound of fuel consumed for the given weight of airplane (Fig. 3a). The maximum generally occurs at 1.1 to 1.4 $\times$ (V for L/D maximum). This curve will, of course, give the miles per pound of fuel consumed for any speed, provided the optimum r.p.m. is used.

These curves are obtained for initial and final gross weights and for some intermediate values. One intermediate value will usually be sufficient, but other values may be necessary if the proportionate weight of fuel carried is large.

If values of $C_{R_{max.}}$ for the given weights be plotted against weight, the area under the curve, between the initial and final Gross Weights, will be seen to represent the maximum range obtainable (Fig. 3b).

Endurance is also obtainable directly by this method. If C_R be divided by the velocity in miles per hour for

which it was determined, the result is hours per pound. Therefore, the endurance parameter is defined as $C_E = 1/(\text{b.h.p.} \times c)$. This, too, is plotted against V as before, and, in general, there will be a maximum on this curve which will represent the maximum hours obtainable per pound of fuel consumed for the given weight of airplane. Then, if values of $C_{E_{max.}}$ are plotted against weight, as before, the area under the curve represents the maximum endurance obtainable. Figs. 4a and 4b give typical endurance curves determined in this way.

If values of C_E are taken from Fig. 4a for the V corresponding to $C_{R_{max.}}$, and these values are integrated over the weight range, the result will be the time required to fly the maximum range.

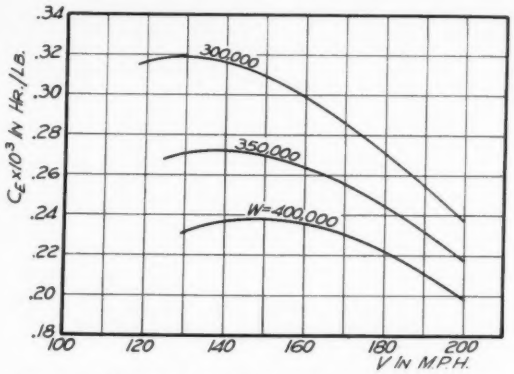

FIG. 4a. V in m.p.h. *vs.* C_E in hr./lb. for constant gross weight.

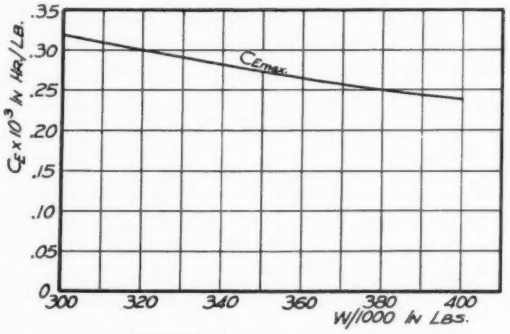

FIG. 4b. Gross weight *vs.* maximum C_E in hr./lb.

AN APPROXIMATE METHOD

If only maximum range and average cruising speed are desired, a very close approximation may be obtained by carrying out the calculations for a weight corresponding to half fuel load. If the L/D and η/c corresponding to the optimum V are substituted in the Breguet formula, the range obtained by this short method will be within two percent of that obtained by the longer method. The optimum V obtained is the average cruising speed, also within two percent.

LIMITATIONS OF THE METHOD

In the preliminary calculations, standard charts were used for determining propulsive efficiency. There is considerable evidence at present that there must be some sort of a multiplicative correction applied to make performance calculations consistent with flight test data. Correction curves have been proposed, as well as the use of arbitrary percentage corrections. However, recent torque indicator tests made to determine accurately the brake horsepower of engines in flight, suggest that the correction might possibly be more properly applied to the test-stand brake horsepower, in which case chart efficiencies will apply. The authors feel that further flight tests with the torque indicator will give the correct answer to this question. If, however, a multiplicative factor appears necessary, it can be applied directly to the range parameter C_R.

As for the variation of brake horsepower in flight and at altitude, it is felt that the torque indicator will again provide the answer. This in turn will permit charting of true specific fuel consumptions.

The specific fuel consumption curves shown in Fig. 2 represent the average of test-stand runs and flight-test reduction for several modern commercial and military aircraft engines. A close agreement exists with curves in reference 1 in the region of high horsepowers, but there is a consistent deviation in the low horsepowers. The authors have noted particularly that there is a great lack of data, both from test stand and from flight tests, on fuel consumption at low power and low engine speeds, where maximum C_R and C_E are likely to occur.

EFFECT OF PARAMETERS ON RANGE

In investigating the effect of geometrical parameters upon range, it is necessary to hold as many factors constant as possible, permitting variation in only those which logically must vary. The gross weight was first fixed at 300,000 lbs., due to current interest in airplanes of this size. A power plant was chosen which preliminary estimates indicated would produce maximum range. The effect of increasing the power will be discussed later.

The general data assumed for this airplane are as follows:

Gross weight	300,000 lbs.
Payload	25,000 lbs.
Power plant weight	30,500 lbs.
6 engines	2500 h.p. at 1200 r.p.m. (take-off) 2000 h.p. at 1000 r.p.m. (rated) 1500 h.p. at 955 r.p.m. (cruising)
Basic weight	141,000 lbs.
Structure, furnishings, payload, passengers, power plant, less wing weight and fuel weight	
Remaining weight	159,000 lbs.
For fuel weight and wing weight	

From the curve of Fig. 5 the wing weight is determined, using a design load factor of 5. The balance is

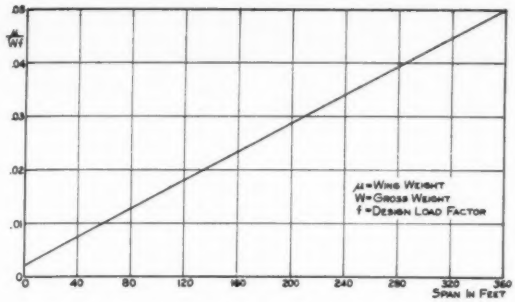

FIG. 5. Variation of wing weight with wing span.

then the weight available for fuel, oil, and tanks; and the actual fuel weight is assumed as 6/6.25 times the weight available for fuel, oil, and tanks. The curve of Fig. 5 is taken from a report on wing weights of contemporary airplanes by J. E. Lipp of the Douglas Aircraft Company, Inc., soon to be published. The particular curve used is based upon an allowable stress of 45,000 lbs./in.^{2}, which is in accord with modern practice in the construction of large airplanes. This linear variation of wing weight *versus* span checks very closely with a similar analysis made by A. E. Lombard of the Curtiss-Wright Corporation.

The procedure followed was to assume a constant aspect ratio and, for different wing spans, to compute the range and average cruising speed. This was carried out covering aspect ratios from 9 to 17, and wing spans from 210 ft. to 330 ft. Results are plotted in Fig. 6. The quantities

$$\text{A.R.} = b^2/S \text{ or } S = b^2/\text{ A.R.}$$

and

$$l_w = W/S = W \times \text{A.R.}/b^2$$

where A.R. is the aspect ratio, b the wing span, S the wing area, l_w the wing loading, and W the gross weight.

It is evident that, if the variation of range with aspect ratio and span is investigated, its variation with wing loading can be determined and curves of constant wing loading can be drawn in. This has been done in Fig. 6. The investigation was not carried beyond an aspect ratio of 17 because it was felt that wing weight data might no longer hold for the type of structure which would be necessary. Furthermore, the percentage increase in maximum range with higher aspect ratios is close to the limit of the accuracy of the calculations. Similarly, constant wing-loading lines are not carried beyond 70 because take-off and sea-level rate-of-climb requirements eliminate higher values from practical consideration, unless additional power is provided, and this in itself reduces maximum range. Fig. 6 also shows the variation of average cruising speed with the several parameters. On the lower set of curves one division on the ordinate corresponds to about a 3 percent variation in maximum range; on the upper set the same division corresponds to about a 6 percent variation in average cruising speed.

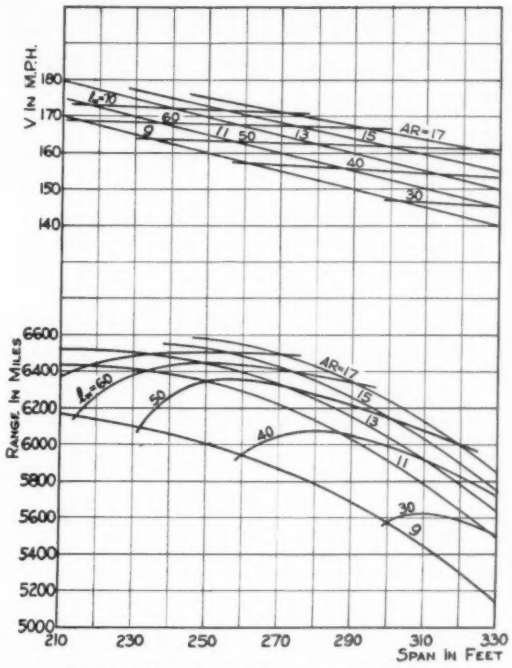

FIG. 6. Variation of maximum range and average cruising speed for maximum range, with wing span, for constant aspect ratio and constant wing loading.

A study of the figure indicates that in the range of values considered there is a gain in maximum range to be expected from increasing aspect ratio and from decreasing wing span, the combination producing optimum range. It follows, as further indicated on the figure, that one may expect increases in maximum range with increased wing loading, and, in general, there will be an optimum combination of aspect ratio and span for a given wing loading. However, the gain in range caused by increase in wing loading is relatively small for wing loadings above 50 lbs. per sq. ft.

Effect of Parameters on Take-Off

Since take-off requirements have a very powerful influence on range, some analysis of the take-off problem is necessary. Take-off calculations were carried out for the above airplane as a landplane, following the method of reference 2, to determine limiting wing loading for practical take-off. Inasmuch as present regulations require that landplanes climb over a fifty-foot obstacle after take-off, with the air temperature at 110°F., the additional distance required by these specifications is included in take-off distance. Calculations indicated that take-off distance is approximately independent of aspect ratio and depends principally on wing loading. Calculated take-off distances are given in Table 1.

Take-off distances in excess of 7000 ft. are considered as impractical for a landplane, and, therefore, further landplane considerations were restricted to airplanes with wing loadings of 50 or less.

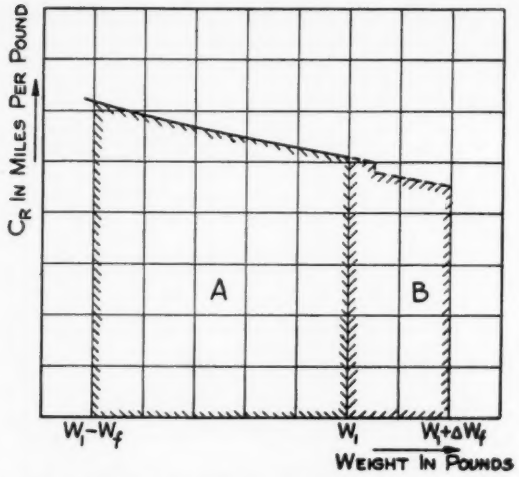

FIG. 7. Increase in maximum range due to 40 percent excess fuel, assuming assisted take-off with this weight. Area A is the normal range. Area B is the increase. W_1 is the normal gross weight. W_f is the normal fuel weight. ΔW_f is the excess fuel weight.

Seaplane (flying boat) take-off calculations were made for comparison with landplane take-offs. The method of reference 4 was used, noting that seaplanes are not subjected to the same temperature and climb-over-obstacle penalties as landplanes. Further, the effect of increased power on take-off of both seaplanes and landplanes, and on range and average cruising speed was determined. To compensate for increased power plant weight, fuel weight was deducted, keeping the gross weight constant.

All of the final take-off results are collected in Table 2 where range and cruising speed results are also included. For the range calculations landplanes are assumed to be aerodynamically equivalent to the corresponding seaplanes.

This tabulation indicates quite simply that increasing power to gain a better take-off invariably results in a considerable decrease in maximum range, with no gain in average cruising speed. Remembering that increased maximum range corresponds directly to increased payload for a fixed shorter range, it is apparent that with unassisted take-off the relatively low-wing-loading, low-powered airplane with satisfactory take-off, and with suitable cruising speed, is the more practical commercially. If increased speed is needed for express service, the penalty must be taken in payload. Further, the take-off differential between seaplanes (flying boats) and landplanes of large size for long range, is not as great as might be expected from analyses on smaller planes, and in some cases the seaplanes will have better take-off.

Fig. 6 indicates that the range of a large airplane with a wing loading of 20 to 30 and marginal take-off characteristics may be substantially increased by overloading with fuel to a wing loading of 40 to 50 and employing assisted take-off. However, the increase in range will not be directly proportional to the amount of fuel added, because the new average C_R over the range will be considerably lowered. This is shown qualitatively on Fig. 7 where the increased range is represented approximately by the area of the trapezoid produced by extending the C_R curve to the overload weight. The discontinuity in this curve results from a shift to a higher power combination. This area will be further reduced by an amount roughly proportional to the increased structural weight incident to stressing for the overload weight, and for assisted take-off.

TABLE 1

Wing Loading	Take-Off Distance
30 lbs./ft.^{2}	4745 ft.
40	5535
50	7075
60	8880
70	10230

TABLE 2

Power—6 Engines
Power Loading (lbs./b.h.p.) = 20

Wing Loading (Lbs./Sq. Ft.)	Type	Take-Off Time (Sec.)	Take-Off Distance (Ft.)	Range (Miles)	Speed (M.p.h.)
30	Sea	62	4360	5580	145
	Land	51	4745		
40	Sea	93	7430	6030	155
	Land	54	5535		
50	Sea	145	15400	6320	165
	Land	64	7075		

Power—8 Engines
Power Loading (lbs./b.h.p.) = 16.7

Wing Loading (Lbs./Sq. Ft.)	Type	Take-Off Time (Sec.)	Take-Off Distance (Ft.)	Range (Miles)	Speed (M.p.h.)
30	Sea	31	2200	4870	145
	Land	38	3525		
40	Sea	43	3430	5280	155
	Land	39	4285		
50	Sea	56	5460	5350	165
	Land	43	4695		

REFERENCES

[1] Bierman, David, *A Study of the Factors Affecting the Range of Airplanes;* N.A.C.A. Technical Note 592, 1937.

[2] Diehl, Walter Stuart, *Engineering Aerodynamics* (revised edition); The Ronald Press Company, New York, 1936.

[3] Oswald, W. Bailey, *General Formulas and Charts for the Calculation of Airplane Performance;* N.A.C.A. Technical Report 408, 1932.

[4] Shoemaker, J. M., and Parkinson, J. B., *A Complete Tank Test of a Model of a Flying Boat;* N.A.C.A. Technical Note 464, 1933.

[5] Russell, J. S., and McCoy, H. M., *Wind Tunnel Tests on a High Wing Monoplane with Running Propeller; Part 1;* Journal of the Aeronautical Sciences, Vol. 3, No. 3, January, 1936, p. 73.

Book Review

Yahrbuch der Deutsche Luftfahrtforschung, 1937: R. Oldenbourg, München and Berlin; 1095 pages, 30 RM.

This is a great volume of 1095 pages containing the scientific and technical contributions in 1937 of German workers in the various aeronautical sciences. As one advantage of national regimentation, we note the unification of effort obtained by an all inclusive publication of the work of all groups.

The volume is published under the auspices of the research division of the Air Ministry with the endorsement of Generals Göring, Milch, and Udet. It contains the contributions of the Deutsche Akademie der Luftfahrtforschung, the Lilienthal Society, the D.V.L. (Aldershof), the D.F.L. (Braunschweig), A.V.A. (Göttingen), D.F.S. (Darmstadt), F.F.O. (Oberfaffenhofen), and of the academic groups at Aachen, Berlin, Braunschweig, Darmstadt, Hannover, Munich, Stuttgart, Karlsruhe, Göttingen, etc.

General surveys of the state of knowledge serve to introduce the technical papers which constitute the bulk of the volume. These surveys, each by a well known expert, cover aerodynamics hydrodynamics, construction, strength, engines, materials, airports, gliders, radio, photography, and medicine.

Further, there are reports on organization, equipment, and program of the principal research laboratories.

It is impossible to review the 150 technical papers but the following comments may be helpful in giving readers an idea of the material.

Airfoil Theory. (Comments by Prof. M. Rauscher.)

(1) *Steady Incompressible Flows*

In this group, *A. Betz* and *F. Keune* give a generalized, and at the same time simplified, treatment of Kármán-Trefftz airfoils, including types with upturned trailing edges. *F. Keune*, in another paper, discusses the flow past the skeleton of an uncambered airfoil with flap, largely following Chapligin and Arjanikow. *W. Kochanowski's* article on the pressure distribution over arbitrary wing sections largely recounts the work of Theodorsen and Garrick on this subject.

(2) *Steady Compressible Flows*

A paper by *L. Prandtl*, after a broad discussion of the problem of lifting surfaces, deals with various types of singularities in a compressible medium, and leads to an approximate theory of flat airfoils at supersonic speeds. *H. Schlichting*, in a supplementary paper, elaborates on this theory and applies it to several concrete cases. *O. Walchner* analyzes the possibility of using two wings of finite thickness in biplane formation to secure a drag as low as that of a single thin plate at supersonic speeds; he comes to the conclusion that friction would destroy any scant advantages the scheme might otherwise offer.

(3) *Unsteady Incompressible Flows*

Wind tunnel tests to check flutter theory are reported in a paper by *H. Voigt*. Excellent agreement between experiment and theory was found on the whole. *H. G. Küssner* gives a concise review of the theory of unsteady flow on wings. The special question of the forces on a flapping control surface is studied by *F. Dietze*. Finally, *K. Leiss* discusses the problem of mass balancing a control surface against flutter in various modes, and shows that the order of the mode to be guarded against determines the minimum number of balancing weights that can be used.

Airplane Aerodynamics. (Comments by Prof. S. Ober.)

(1) *Airplanes and Airfoils*

Papers are included on general performance analysis by *G. Bock* (D.V.L.); on take-off computation by *B. Gothert* (D.V.L.); measurements of profile drag and lift by *H. Doetsch* and *M. Kramer* (D.V.L.) and by *Muttray*. These drag measurements confirm the fact, long realized, that variable density tunnel results are subject to correction for square tips and excessive stream turbulence. Pressure distribution results from wind tunnels are given for a tapered flap wing by *P. Ruden* (T. H. Hannover), from steady flight measurements by *G. Kiel* (D.V.L.) for wing tip and tail and also for one section of a flapped wing on another plane. Results of tests of end plates on sweptback wings are given by *J. Hubert* (Darmstadt). An important paper on the effect of slipstream or downwash at the tail from results of flight tests is given by *R. Schmidt* (Dornier). Total force on the horizontal tail was measured in flight and reported by *H. W. Kaul* and *W. Pretschner* (D.V.L.).

Drag and cooling with different radiator arrangements are discussed in two good papers, one, from wind-tunnel tests, by *Linke* (T.H., Aachen), the other from tunnel and flight tests, by *W. Barth* (Dornier).

(2) *Propellers*

The problem of designing propellers for high speed airplanes is discussed by *A. Betz*, (Göttingen), and *F. Weinig* (D.V.L.). Weinig also considers the use of guide vanes and contra-turning propellers. Propellers in yaw are analyzed by *G. Klingemann* and *F. Weinig* (D.V.L.). Lifting airscrews are discussed by *O. Walchner* (Göttingen), *A. Betz*,[1] and *H. G. Küssner*[2] (Göttingen).

Propeller and engine vibrations are discussed by *K. A. Lürenbaum* (D.V.L.).[3]

(3) *Floats and Hulls*

A general discussion of hull forms with some new data is given by *W. Sottorf* (D.V.L., Hamburg), who also presents a new analysis of tests of planing surfaces. Stability of seaplanes on the water is discussed by *W. Boccius* (D.V.L., Hamburg). Use of hydrovanes to assist take-off is reported by *W. Sottorf* and *O. Tietjens*.

(4) *Equipment for Aerodynamic Research*

The pressure wind tunnel at Göttingen is described by *H. Winter*. A combined wind and water tunnel is described by *M. A. Müller* (T.H., Berlin). Brief descriptions of flight instruments such as recording capsule type pressure gages, towable pitots, rate-of-climb meters, inclinometers, control force, and position

(*continued on page 446*)

[1] Translated in N.A.C.A. Technical Memorandum No. 836.
[2] Translated in N.A.C.A. Technical Memorandum No. 827.
[3] Very similar to S.A.E. Journal, Dec. 1936.

Some Remarks on the Physical Aspects of the Aircraft Icing Problem

A. R. STICKLEY, *U. S. Weather Bureau*

Presented at the Meteorology Session, Sixth Annual Meeting, I. Ae. S.
January 25, 1938

PREPARATORY to initiating an investigation with regard to the matter of aircraft icing, a survey of such of the existing literature on the subject as was available to the author has been conducted. The present paper deals with some of the more important aspects of the problem as revealed by this survey.

Some interesting relations result from a consideration of the passage of an airfoil through an atmosphere laden with water droplets. It is found in this case, that as the size of the droplets becomes smaller, the thickness of the layer which is cleared of droplets by the airfoil becomes vanishingly small. Considering droplets of various sizes to be suspended in the air together, this, in effect, means, of course, that almost all of the smaller droplets will fly around the airfoil with the air itself while the larger droplets, possessing more inertia, overcome the forces of viscosity and are deposited on the airfoil. As far as the author is aware, Noth[1] first called attention to this fact. A quantitative treatment of the problem has been worked out, it is understood, by Lacey in an unpublished thesis dealing with the aircraft icing problem which he presented at the Massachusetts Institute of Technology in 1936. Although the writer has not had access to this paper, the fundamental idea utilized in it has been described to him. Making use of this idea, the author has carried out the following rough analysis, which indicates the factors by which the thickness of the droplet-cleared region may be determined.

The problem is first simplified by assuming that air laden with droplets of a uniform size is flowing around a cylinder of infinite length. The results obtained by Bleeker[2] for a problem involving similar conditions are next made use of. He assumes that the cylinder has a radius of 25 cm. and that the air is moving along the lines of flow at an infinite distance from the cylinder with a speed of 50 meters per sec. Under these conditions, he finds that, "The centrifugal accelerations even at a great distance from the cylinder are much greater than the accelerations of gravity." Making similar assumptions here then, only the centrifugal accelerations are used in applying Stokes' law dealing with the motion of a droplet through the air. Now, consider a droplet lying at infinity on the boundary of the region cleared of droplets. It is evident that this droplet will impinge against the cylinder at the point B of Fig. 1, this point being the intersection with the surface of the cylinder of the locus of the points on the lines of flow at which the curvature of the lines of flow changes sign. Now if 2δ represents the thickness of the droplet cleared region, it is further evident that, if the compression suffered by the air in its flow around the cylinder is neglected, the quantity δ may be taken as the distance through which the droplet considered must move normal to the lines of flow in order to reach the cylinder. Next, let the line of flow running through the point A of Fig. 1 be the line of flow on which the droplet was initially situated. Also let the point A designate the point at which this line of flow may first be said to deviate from a straight line (the selection of such a point could be made, of course, by picking out the point on the line of flow at which this line of flow has some arbitrarily stipulated very small slope). Then, if u represents the component of the droplet's velocity normal to the lines of flow encountered by it in moving from A to B, and if t represents the time, while t_A and t_B designate the times at which the droplet arrives at A and B, respectively,

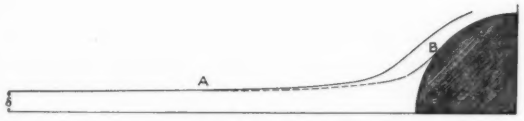

FIG. 1.

$$\delta = \int_{t_A}^{t_B} u\,dt \tag{1}$$

Applying Stokes' law and assuming the density of the droplet to be unity, u is given by the equation

$$u = (2/9)r^2v^2/\mu\rho \tag{2}$$

where r = the radius of the droplet in cm., v = the speed in cm. per sec. of the droplet with respect to the cylinder, ρ = the radius of curvature in cm. of the lines of flow intersected by the droplet along its path; the various radii are taken at the points where the droplet intersects the lines of flow, and μ = the viscosity of the air in gms. per cm. sec.

Substituting in Eq. (1)

$$\delta = (2/9)(r^2/\mu)\int_{t_A}^{t_B}(v^2/\rho)dt \tag{3}$$

from which it is seen that δ varies as the square of the radius of the droplet r and that δ is therefore an in-

finitesimal of higher order than r and will, as has been said, become vanishingly small as r diminishes.*

A second striking fact is that, under suitable conditions, the size of the drops can become too large to lead to an ice deposit of any consequence. This follows from considerations involving the "icing time" concept used by Bleeker.[2] To illustrate the meaning of this concept, he considers a drop which has been undercooled to the temperature of $-5°C$. When this drop is jarred on its impact with the airplane, freezing immediately sets in and causes the temperature of the mixture of ice and water to rise to 0°C. When the mixture reaches this temperature, about 6 percent of the quantity of water in the droplet will have frozen.

Bleeker then points out that the vapor pressure of the mixture of water and ice is now considerably in excess of the vapor pressure of the surrounding air, even though the latter vapor pressure be that of saturation at the existing air temperature. Therefore, in consideration of the strong ventilation which is taking place he contends that the important cooling-off factor is that due to a rapid evaporation of the water-ice mixture. In order to gain an idea of the amount of time required to convert all of the water in a droplet into ice and vapor in this manner, Bleeker first supposes that the process takes place while the droplet retains its spherical shape. He applies Trabert's formula for the rate of evaporation to a droplet which has a diameter of 10^{-3} cm., a temperature of 0°C. and which is surrounded by saturated air with a temperature of $-5°C$. Under these conditions he finds that 12 percent of the water in the droplet must evaporate in order to freeze the remainder and that the time required to complete the freezing in this manner is about 7 seconds.

Bleeker next points out that the icing time is proportional to the droplet radius. This is evident from the following considerations: First the time required to evaporate the 12 percent of the remaining liquid is proportional to the amount of water to be evaporated, *i.e.*, to the volume of the drop which, in turn, is proportional to the cube of the radius. Second, this amount of time is also inversely proportional to the surface of the drop which is, in turn, proportional to the square of the radius. Hence if Γ designates the icing time and r represents the radius of the drop,

$$\Gamma = kr \tag{4}$$

where k is the factor of proportionality, which Bleeker says is dependent mainly on the vapor pressure existing in the air surrounding the drop. He then calls attention to the fact that in applying these results to practice, very nearly half of the surface of the drop will not be contributing to this evaporation. He points out, however, that this circumstance can, at most, lead to a doubling of the icing time and that the true icing time will probably be much less than twice that at first computed.

Having then established the fact that the icing time concept retains its significance in practice, Bleeker then explains the failure of an airplane to accumulate any considerable deposit of ice in heavy undercooled rain as follows: "If, now, with a large drop radius, great relative humidity and a temperature in the neighborhood of the freezing point, the icing time is great, the drops then have sufficient time to coalesce and blow off from the airplane." Although he does not say so, a little consideration will show that in order to explain the small ice accumulation, it must be assumed that a considerable portion of the ice formed when the drops collide with the airplane must be carried away when the coalesced drops are blown off. For, if no other factors are changed, simply increasing of the size of the drops cannot result in the formation of less ice since the same amount of heat will be withdrawn by the processes of evaporation and conduction when the drops are small as when they are large, assuming the same temperature and vapor pressure differences for the small drop deposit as for the large drop deposit. Although nothing is known as to which portion of the drop freezes upon impact, there seems to be no valid reason for supposing that all of the ice formed as a consequence of the impact adheres to the plane. As has been said, it is quite probable that the true explanation of the light ice deposit experienced in heavy undercooled rain lies in the supposition that much of the ice formed is washed away by the excess liquid water.

It may be pointed out, however, that Bleeker's claims as to the importance of the process of evaporation for the removal of the latent heat of fusion seem to be refuted when some of the equations developed by Schumann[3] in his recent paper on hailstone formation are applied to this problem. Letting h_1 be the heat lost per unit time by conduction and h_2 be the heat lost per unit time by evaporation, Schumann finds

$$h_1 = 4\pi r^2 K\theta/B \tag{5}$$

and

$$h_2 = 4\pi r^2 \varphi\lambda(C_1 - C_2)/B \tag{6}$$

where r = the radius in cm. of the spherical hailstone,

* In reviewing an abridged form of this paper which was presented before the annual meeting of the Institute of the Aeronautical Sciences in January, Klemin[12] raises the objection that the conclusion drawn from Eq. (3) is inapplicable to flow around an airfoil since Bleeker's results in connection with the flow around a cylinder were used in deriving the equation. Regarding this, it is to be pointed out that the only use made of Bleeker's results was that of justifying the assumption that the acceleration of gravity is negligible compared with the centrifugal accelerations experienced by the drop. Since it appears permissible to assume that the centrifugal accelerations suffered by the drop in the flow around the forward part of an airfoil and those suffered by the drop in the flow around a cylinder are of the same order of magnitude, Eq. (3) is in no way invalidated by the use of Bleeker's results.

Fig. 2

Fig. 3

Fig. 4

K = the coefficient of thermal conductivity of the air in cal. per cm. sec. °C., θ = the temperature difference in °C. between the hailstone surface and the free air, B = the thickness of the boundary layer in cm., φ = coefficient of diffusion of water vapor into air in cm.^{2} per sec., λ = the latent heat of fusion in cal. per gm., C_1 = the absolute humidity in gms. per cu. cm. of saturated air which has the same temperature as that of the hailstone surface, and C_2 = the absolute humidity in gms. per cu. cm. of the free air surrounding the boundary layer of the hailstone.

In order to compare the magnitudes of h_1 and h_2, it is necessary to consider only the values of the functions $K\theta$ and $\varphi\lambda(C_1 - C_2)$. Values of these functions for various values of the temperature (°C.) are given in Table 1.

From these values it is evident that, under the conditions assumed and throughout the temperature range −2°C. to −20°C., the process of conduction is about twice as effective as the process of evaporation in removing the latent heat of fusion liberated in freezing the surplus liquid water. This, of course, means that the validity of Eq. (4) and the deductions made from it must be reconsidered. When this is done, it is seen that the icing time T is still proportional to the radius of the drop, for, regardless of whether conduction or evaporation is the main factor acting in the heat absorption, the time required is still proportional to the amount of water present and is inversely proportional to the surface presented to the free air. Hence the form of Eq. (4) remains unchanged. The proportionality factor k, however, can no longer be said to depend mainly upon the vapor pressure but must, instead, be said to increase as the quantity

$$H = [K\theta + \varphi\lambda(C_1 - C_2)]/B \qquad (7)$$

decreases.

It is to be remarked, in addition, that the objections offered by Relf[4] with respect to Schumann's use of the quantity B in Eqs. (5) and (6) are to be borne in mind when considering Eq. (7). If, as seems likely, Relf's assertions in this connection are true, it is evident that B, in an equation of this sort, must be regarded as the "equivalent boundary layer thickness," *i.e.*, as the thickness of a layer of air surrounding the moving body which is stationary with respect to the moving body and which, assuming that no velocity gradient with respect to the moving body exists beyond the supposed layer, would give rise to the evaporation and conduction rates actually observed.

Table 1

t(°C.)	$K\theta \cdot 10^5$	$\varphi\lambda(C_1-C_2)\cdot 10^5$
− 1	5.33	0.78
− 2	10.66	4.53
− 3	15.99	8.16
− 4	21.32	11.78
− 5	26.65	15.15
−10	53.30	28.89
−15	79.95	38.59
−20	106.60	45.58

Bleeker's "icing time" concept is of some help in explaining the various shapes taken by aircraft ice accumulations. Figs. 2, 3, and 4 show the three different types of ice accumulation given by Noth and Polte.[5] Bleeker has already pointed out that the peculiar vertical extensions shown in Fig. 3 are to be explained by the fact that the upper and lower parts of the formation are subjected to a greater ventilation than their intermediate points. This, of course, means that the value of B in Eq. (7) is smaller for the upper and lower parts than it is for the intermediate part, and that, therefore, the icing time is smaller at the shoulders than it is in the intermediate region. The preponderance of the accumulation on the lower edge in Fig. 3 over that on the upper edge can be explained by the fact that only the larger drops possess sufficient inertia to penetrate the thick boundary layer or stagnation zone in front of the intermediate region. Since the icing time of these drops is large and the ventilation in the region is comparatively poor, the liquid water remaining over after the impact of the drops drains down into the region of greater ventilation near the lower edge and freezes.

The differences in the formation shown in Figs. 2 and 3 may possibly be explained by one or both of two factors. The first is the difference in the design of the two airfoils. The second is the possibility that the free air temperature for the deposit shown in Fig. 2 may be much lower than that for the deposit shown in Fig. 3. This latter possibility would, of course, mean that the icing time would be small regardless of the position on the airfoil on which the drop is deposited and that the accumulation would grow practically as rapidly in the intermediate region as in the upper and lower regions.

Noth and Polte state that the deposit shown in Fig. 4 occurs at low temperatures, which means, of course, that the icing time was small. Furthermore, freezing

will occur in a short time, regardless of the position of impact. If the differences in airfoil design of Figs. 2 and 4 do not explain the differences in the deposits, it seems possible that the size of the droplets for Fig. 4 might have been uniformly large enough to hit the airfoil with no appreciable deflection, while, in Fig. 2, the smaller droplets are deflected to a greater extent and thus create a better distribution of the deposit.

Finally, contrary to statements made by Bigg in his recent paper on aircraft ice formation[6] and by McNeal in a similar paper,[7] the salt content of the droplets should bring about no noteworthy reduction in the freezing point of the aircraft ice deposits. The truth of this statement is evident when the statements made by Köhler in summarizing the results of his analyses of the ice deposits produced by fog at the Haldde Observatory are considered.[8] In it Köhler says: "The most commonly occurring chlorine content was about 3.5 milligrams per liter of melted ice," and that, "The highest and lowest concentrations of chlorine were 56.33 and about 0.067 milligrams per liter, respectively." Köhler next states that, "On the presumption that all sea salts are present, we get the concentration of these salts per liter of melted ice on multiplying by Knudsen's factor of 1.805." Multiplying Köhler's maximum chlorine concentration by this number and assuming complete dissociation of the salts in solution, it is found that such a salt concentration would reduce the freezing point of the droplet by less than 0.01°C. These results may at first appear to contradict Köhler's statement quoted in McNeal's article with regard to the effects of the introduction of salt particles into liquid hydrometers. This statement reads as follows: "The introduction of salt particles here makes it very clear that fluid water can and must exist in the atmosphere at very low temperatures." The apparent paradox between what is said here and the foregoing is to be understood when a figure which appears in Köhler's paper, "On the Thermodynamics of the Condensation on Hygroscopic Nuclei,"[9] and the results of his droplet size measurements both at the Haldde Observatory[10] and on the Pårtetjåkko Mountain[11] are considered. The diagram referred to is given, with slight modification, in Fig. 5. In it the various curves show how the vapor pressure at the surface of a droplet containing a salt nucleus varies as condensation takes place, the temperature being assumed to remain at 0°C. The equation which Köhler uses in plotting these curves is:

$$\ln e = \ln e_m + \ln\left(\frac{2^n + A\cdot 2^p}{2^n + B\cdot 2^p}\right) + \frac{2S}{R_1 rT}\left(\frac{2^n}{2^n + C\cdot 2^p}\right)$$

in which T is the absolute temperature of the droplet, e is the vapor pressure in mm. Hg at the surface of the salt solution droplet (which is equal to the vapor pressure in the atmosphere at the temperature T), e_m is the vapor pressure in mm. Hg over a plane pure water surface at the temperature T, r is the radius of the droplet in cm., S is the surface tension of the solution in dynes per cm., R_1 is the characteristic gas constant for water vapor, 2^n is the cube of the radius multiplied by 1.4383×10^{39}, 2^p is the mass of the salt nucleus (in gm.) multiplied by 5.4142×10^{13}, and A, B, and C are constants which have the values 1.8341×10^{-6}, 2.1222×10^{-6}, and 4.5861×10^{-6}, respectively.

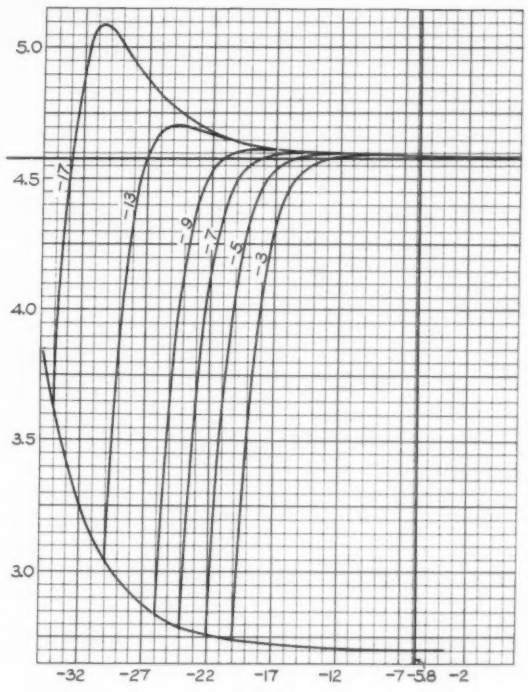

FIG. 5.

In the figure, e is used as the ordinate and n is used as the abscissa. Using p as a parameter, the various curves are then obtained, the values of the parameter being indicated for the respective curves. The curve in the lower part of the figure which intersects the vapor pressure curves is a curve of constant concentration. The heavy line drawn horizontally in the upper portion of the figure indicates the value of e for a plane pure water surface at 0°C. (4.58 mm. Hg). It will be noted that as n increases the various vapor pressure curves rapidly approach this value and then go above it, after which they approach it asymptotically from above. The heavy vertical line indicates the minimum value of n found by Köhler in his 9500 droplet size observations on the Haldde and on the Pårtetjåkko. From the position of this line it is evident that although, as is asserted in Köhler's statement quoted by McNeal, droplets with vapor pressures far below 4.58 mm. Hg do occur in the atmosphere, the size of the droplets which exhibit these vapor pressures is far below that of the visible droplets and, in consideration of the conclusions to be drawn from Eq. (3), this droplet size is still farther below the size of the droplets which will cause any significant ice deposit either on solid objects in a fog or on

aircraft flying in clouds. It is further evident from the figure that, considering droplets of a visible size, the vapor pressures will be slightly in excess of 4.58 mm. Hg, this excess being due, of course, to the great curvature of the droplet surface. After such a droplet is deposited on the surface of an airplane, the curvature will practically vanish and freezing point reductions of the negligible order of magnitude previously mentioned will be produced.

Summarizing, it has been shown that: (1) As the size of the droplets decrease the amount of aircraft icing becomes vanishingly small. (2) Under certain conditions, it is possible for undercooled drops to become so large that the excess liquid water remaining after their impact will wash away a great part of the ice formed. (3) Assuming that a plane is flying in a cloud in which the usual high humidities prevail, a consideration of certain equations set up by Schumann for the dissipation of the heat of fusion from a hailstone indicates that conduction plays a part considerably more important than that played by evaporation in dissipating the heat of fusion from the ice deposit on the plane. (4) The "icing time" concept of Bleeker offers a possible basis for explaining the peculiarities in shape of the various aircraft ice deposits. (5) No noteworthy reduction of the freezing point of droplets of the sizes which contribute to aircraft icing results from the presence of salt nuclei in them.

References

[1] Noth. H., *Die Vereisungsgefahr bei Flugzeugen*, Die Arbeiten des preussischen Aeronautischen Observatoriums bei Lindenberg, Bd. 16, Heft G, 1930.

[2] Bleeker, W., *Einige Bemerkungen über Eisansatz an Flugzeugen*, Meteorologische Zeitschrift, 49 Jahrgang, pages 349–354, Braunschweig, 1932.

[3] Schumann, T. E. W., *The Theory of Hailstone Formation*, Quarterly Journal of the Royal Meteorological Society, Vol. 64, page 11, London, 1938.

[4] Relf, E. F., Discussion of paper cited in reference 3, Quarterly Journal of the Royal Meteorological Society, Vol. 64, page 17, London, 1938.

[5] Noth, H., and Polte, W., *Über die Vereisung von Luftfahrzeugen*, Deutsche Luftwacht, Ausgabe: Luftwissen, Bd. 2, page 305, Berlin, 1935.

[6] Bigg, W. H., *Ice Formation in Clouds in Great Britain*, page 3, Professional Notes No. 81, British Meteorological Office, London, 1937.

[7] McNeal, Don, *Ice Formation in the Atmosphere*, Journal of the Aeronautical Sciences, Vol. 4, page 119, 1937.

[8] Köhler, Hilding, *The Nucleus in and the Growth of Hygroscopic Droplets*, Transactions of the Faraday Society, Vol. 32, page 1153, London, 1936.

[9] Köhler, Hilding, *Zur Thermodynamik der Kondensation an hygroskopischen Kernen und Bemerkungen über das Zusammenfliessen der Tropfen*, page 7, Meddelanden från Statens Meteorologisk-Hydrografiska Anstalt, Bd. 3, No. 8, Stockholm, 1926.

[10] Köhler, Hilding, *Untersuchungen über die Elemente des Nebels und der Wolken*, Meddelanden från Statens Meteorologisk-Hydrografiska Anstalt, Bd. 2, No. 5, Stockholm, 1925.

[11] Köhler, Hilding, *Untersuchungen über die Wolkenbildung auf dem Pårtetjåkko im August, 1928 nebst einer erweiterten Untersuchung der Tropfengruppen*, Naturwissenschaftliche Untersuchungen des Sarekgebirges in Schwedisch-Lappland, Bd. 2, No. 21, Stockholm, 1930.

[12] Klemin, Alexander, The I. Ae. S. Annual Meeting, Aircraft Engineering, Vol. 10, No. 109, page 69, London, 1938.

(*continued from page 441*)

recorders are given by *W. Drude* (D.V.L.). Induction type balance beams are discussed by *Wieselsberger* (T.H., Aachen).

Structures. (Comments by Dr. E. Reissner.)

The section on Structures contains a number of valuable theoretical and experimental contributions toward rational solutions of the problems involved in all-metal plane construction.

The stress distribution and the allowable stresses of shell wings are discussed in a very thorough way by *H. Ebner* (see also Lufo 14, 1937).

E. Seydel gives a comparative weight analysis of the different types of wing construction. His conclusion is that for a wing with given loading and given maximum stress, the shell wing can be made about 15 percent lighter than the other types, provided it is possible to make the compression skin effective.

Along similar lines is a paper by *M. Schrenk*, (deceased), written in 1930, which contains quantitative studies on the theoretical minimum weight of cantilever wings.

Articles by *O. Heck* and by *H. Ebner* and *H. Koller* (the former especially clear) deal with the analysis of monocoque structures as frameworks in which some of the members (the diagonals) are replaced by shear resistant flat sheets. The shear in each of these members is assumed to be constant. The analysis is along the lines of the classical theory of structures.

An investigation of the stresses in plates after buckling by means of the large deflection theory of elasticity is made by *K. Marguerre* and *E. Trefftz* (see also, Zeitschr f. ang. Math. u. Mech., Bd. 17, 1937, pages 85–100). These problems, which demand the solution of non-linear partial differential equations, are mathematically very complicated.

R. Kappus presents a new, simple derivation of the equations of the problem of failure of open-section columns. He uses the conditions of equilibrium for the elements of the slightly deformed columns, instead of starting from energy considerations as in his earlier work (Lufo 14, 1937). He points to unsolved problems in this field: (1) The redistribution of stress after failure in columns with ends which are not pin-jointed; (2) the problem of failure if the column is riveted to the skin; (3) failure under stresses beyond the limits of proportionality.

Buckling tests with corrugated reinforced shells have been made by *O. Nissen*. The agreement with theoretical results (*Dschou*, Lufo Bd. 12, 1935), is considerably better than for the uncorrugated shell (see, *L. H. Donnell*, A.S.M.E. Trans.). Plausible reasons for this better agreement are mentioned.

K. Thorn has measured the stresses and deflections in the skin of some reinforced shell fuselages. His results are in fair agreement with those of the "Incomplete Tension Field Theory" (*E. Schapitz*, Jahrb. d. Lilienthal Ges., 1936).

J. C. Hunsaker

Stainless Steel in Aircraft

HERBERT V. THADEN, *Carnegie-Illinois Steel Corporation*

(Received May 19, 1938)

IT IS natural to question the use of stainless steel in aircraft in view of the popularity and success achieved by the lightweight metals currently employed. The answer to the question involves a number of factors.

(1) The favorable strength-weight ratio of stainless steel is an important one and, while it is unquestionably true that structural weight can be saved in a thin high speed or heavily loaded or high aspect ratio wing, or in fact wherever there are high stresses necessarily resisted within restricted dimensions, this favorable factor, alone, may not seem to some sufficient to justify the substitution of stainless steel for the currently used material.

(2) Another factor is that of the superior corrosion resistance of stainless steel. Here again, however, this advantage in itself may not seem to warrant a consideration of stainless steel, even though such material is ideally suited for seaplanes and flying boats. Its use for land planes is evidently not essential, although from a maintenance standpoint clearly desirable.

(3) Recent research in aerodynamics indicates the practical necessity of eliminating all external-surface rivet heads, sheet lap-joints, and the obtaining of a smooth airfoil to promote high speed. While it is true that stainless steel fabricated by spot welding fulfills all of these requirements and thereby offers a third advantage it is only where high speed and efficiency is mandatory that sufficient benefit may be shown to warrant the use of stainless steel for this reason alone.

(4) The factor of comparative cost is of particular importance. Survey indicates that aircraft in general cost so much to build and operate that adequate profits, either to the manufacturer or the operator, are scarcely the rule.

This being evident, the question is, can the use of stainless steel as a structural material ameliorate this situation? In view of the developments, it is the author's conviction that it can. Cost, from a fabricating standpoint, should be reducible because of the unique adaptability of stainless steel to the process of high-speed spot welding. Cost from an operating standpoint, should be reducible because of the longer service life of a stainless steel structure, materially lowering depreciation charges. Lowered maintenance charges also, could be anticipated.

The cost factor then, in itself, appears to justify consideration of stainless steel; and indeed, when combined with the favorable strength-weight ratio, favorable corrosion resistance, and the ease with which a smooth surface can be obtained, its consideration as an aircraft material is definitely warranted. The following discussion supports this conclusion.

It is generally conceded that successful aircraft must be a compromise in design and material. An all-wood, or an all-aluminum alloy or an all-stainless steel aircraft cannot be as efficient as one in which each of the component parts has been fabricated of that particular material best adapted to the individual requirements of structural strength, safety, aerodynamics, appearance, fabricating, and operating costs.

No one type of material can be the complete answer. The technique of good wood design is as inapplicable to good aluminum alloy design, as the latter is to stainless steel design.

Considering the contention that stainless steel, as a material, has low fabricating cost potentialities, it can be noted first that relative to the aluminum alloys, stainless steel has a considerable cost advantage on a weight-strength basis. Secondly, when the material is combined with a fast spot-welding process, the labor cost is reducible in average hourly rate as well as in total hours. The former because relatively inexperienced workmen can be trained to operate spot-welders safely in stainless steel with only a short training period; and the latter, because of the uniform type of machine operations inherent in a spot-welded design.

The elimination of any processing, such as anodizing and heat treating of the material (it comes ready for use direct from the mill) and the relative absence of concern about scratching or marring the hard, tough surface of stainless steel are both conducive toward lowered cost.

The cost of aluminum alloy riveting is variously estimated at from 3 cents to 5 cents a rivet and spot-welding at $^1/_{10}$ to $^1/_{100}$ of this figure. Even on the assumption of many spot welds replacing one rivet, there is a significant relative margin justifying the confident expectation of a very considerable saving in the total production cost. Any chance of offsetting this particular advantage, now inherent in stainless steel, would seem to lie in the general replacement of riveting in the aluminum alloy by spot welding. Much progress toward this goal has been made, but in the author's opinion, it is still far away, for reasons of the inherent electrical and physical characteristics of the material.

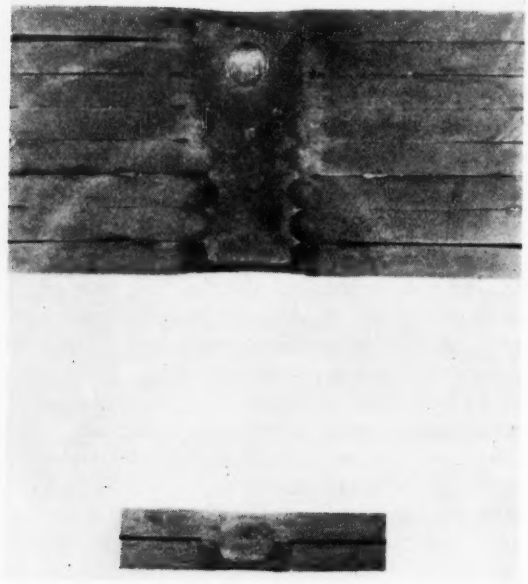

FIG. 1.

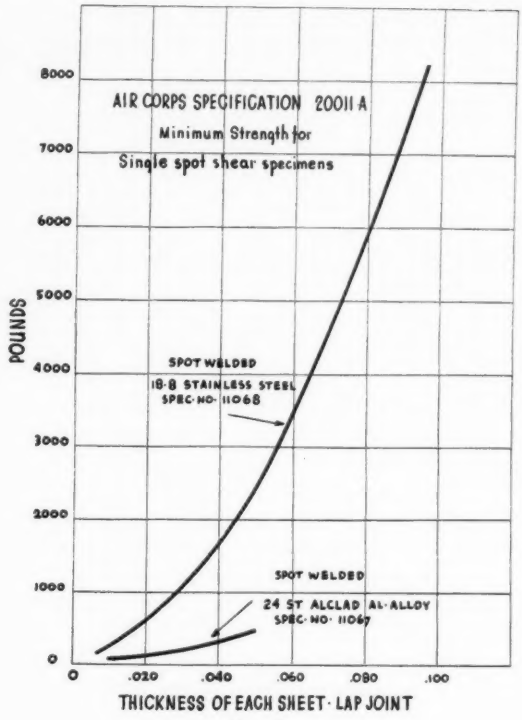

FIG. 2.

WELDING CHARACTERISTICS

The prime requisite of resistance welding is that there be electrical resistance offered to the welding current by the material to be joined. Assuming the relative electrical resistance of silver as one, aluminum has a value of two, and 18–8 stainless steel, fifty; or twenty-five times the resistance of aluminum, and, incidentally, eight times the resistance of mild steel. Stainless, in keeping with its high electrical resistance, has a low heat conductivity. Both of these properties tend to aid spot welding; the former lessening the required current, the latter concentrating and conserving the fusion heat during welding.

This fact explains the adaptability of stainless steel to spot welding and is the reason why the use of a machine of approximately 10 k.v.a. capacity is adequate in the fabrication of a large portion of a stainless steel aircraft. The low current requirements permit the use of relatively light and long secondary leads facilitating the use of small portable hand tools.

On the other hand, aluminum alloy spot welding machines necessarily begin around 100 k.v.a. capacity, frequently require as high as 500 k.v.a. capacity because of aluminum being characterized by low electrical resistance and high heat conductivity.

One of the characteristics of stainless steel is that when heated to or above the annealing temperature (approximately 2000°F.) and then quenched or cooled rapidly, the material acquires the physical properties of very high ductility and toughness and a tensile strength around 80,000 to 90,000 pounds per square inch.

In the act of spot welding, an analagous process takes place. The heat developed by the current flow causes the metal at the point of contact of the adjacent pieces of stainless steel to become molten and fuse together, and then with termination of the current flow, the fused metal chills to the surrounding cold wall, forming a small "ingot" or button. This is pictured in Fig. 1. Two or more pieces can be thus welded together and as a demonstration of versatility a sample is pictured in Fig. 1, of eight pieces of $^1/_8$ inch stainless steel welded together with one spot. Both of these particular samples were made on a standard spot-welding machine.

The experience of many fabricators and spot welding researchers indicate that the most satisfactory welds in stainless steel are made with a very short and accurately gaged time interval; and that reasonably accurate control of the electrode pressure, size, and temperature, and of the voltage must be maintained for consistent quality of welding. Both mechanical and thermionic timing devices are in current use.

As a demonstration, or a production shop inspection procedure, the ductility and toughness of a weld can readily be determined by spot welding two strips of the metal together with a single spot. A good stainless steel weld is indicated if one piece of metal can be twisted 90 degrees with respect to the other before rupture. Carbon steels, chrome-molybdenum, and aluminum alloy materials rarely exceed one-quarter of this angular twist before rupture.

In addition to this test of ductility and toughness, weld strength is generally determined, in the production shop, by frequent checks of the physical shear strength of test strips spot welded together, with a

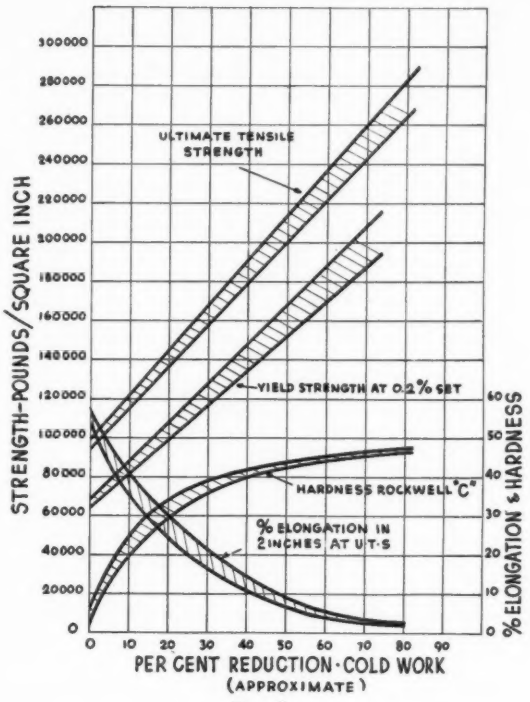

FIG. 3.

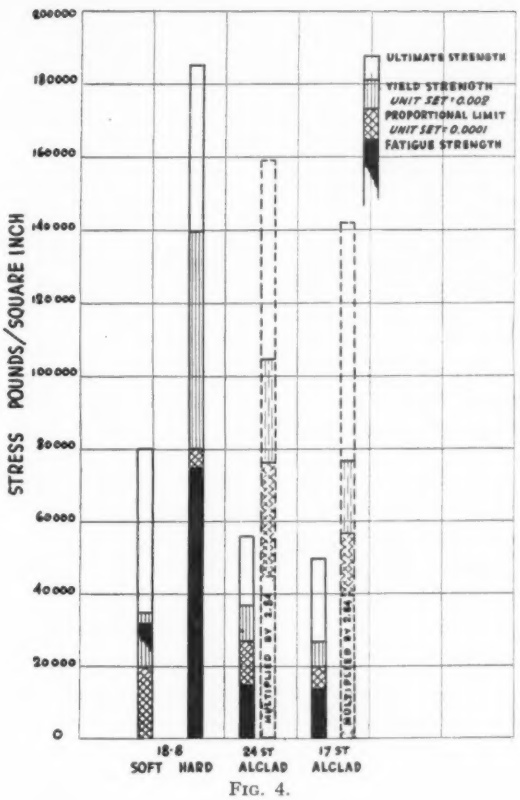

FIG. 4.

single spot, on a standard size lap joint in which the strips are made of the same gage material as is being production welded.

The shear strength of a single spot weld in stainless steel is indicated in Fig. 2 which is a curve of the minimum strength requirements for various thicknesses of sheet, as specified by the U. S. Army Air Corps. The magnitude of the required strengths is significant.

Metallurgical Characteristics

The rustless or stainless steels and irons may, for convenience, be divided into three fairly distinct groups.

The first group, and the earliest in point of time, comprises the stainless steels which are properly called steels because they are hardenable through appropriate heat treatment. They contain 12 percent to 14 percent of chromium with relatively high carbon and are used mainly for cutlery.

The second group comprises the stainless low carbon steels, the chromium-iron alloys, some of which are not hardenable to any appreciable degree by heat treatment. They are rustless under many circumstances, but are not entirely satisfactory under the severest conditions of exposure; their use is, therefore, limited largely to special industrial applications. These steels are magnetic and are wholly ferritic or partly martensitic depending on analysis and heat treatment.

The third and most important group, from an aviation standpoint, are the austenitic alloys containing iron, chromium, and nickel with relatively low carbon. The most commonly used contains about 18 percent chromium and about 8 percent nickel with relatively little carbon; it is often called simply 18–8 though there are a number of trade names. They may be work hardened, are non-magnetic in the quenched state and characterized by high strength, toughness, and ductility.

Physical Characteristics

The specific information now available on the physical properties of cold worked 18–8 is indicated in Fig. 3. The average spread of values is as given in the hatched areas. The relation between the tensile strength and hardness as determined on Rockwell "C" scale is also indicated. For flat rolled products today's commercial practice limits ultimate tensile strength to approximately 185,000 lbs. per sq. in.

An interesting graphical presentation of the relative strength characteristic of 18–8 stainless steel and the most prevalently used aluminum alloys in aircraft work is indicated in Fig. 4.

The allowable design stress values for the ultimate strength; yield strength (0.2 percent set); proportional limit (0.01 percent set) and fatigue strength are plotted in solid lined bars. Adjacent to each of the aluminum alloy bars is plotted a dotted line bar indicating the allowable stress of an equivalent weight of the respective aluminum alloy to that of the stainless steel. Obviously this is a hypothetical value and indicative only

TABLE 1
Properties U.S.S. 18–8 (.10 Max. C)

	Annealed	Cold Worked
Weight per cu. in. (lbs.)	0.286	0.284 (extreme CW)
Specific Gravity	7.92	7.86
Melting Range, °F.	2550–2590	2550–2590
Melting Range, °C.	1400–1420	1400–1420
Specific Electrical Resistance, Michrohms in.^{3}	27	32
Specific Electrical Resistance, Michrohms cm.^{3}	70	81
Magnetic Permeability	1.003	2.0
Specific Heat B$_t$t.u./°F./lb. (32–212°F.)	.12	.12
Specific Heat Cals./°C./gm. (0–100°C.)	.12	.12
Thermal conductivity B.t.u./in.^{2}/sec/°F./in. at 212°F.	.00022	.00022
Thermal conductivity Cals./cm.^{2}/sec./°C./cm. at 100°C.	.039	.039
Coefficient linear thermal expansion per °F. (32–212°F.)	.0000096	.0000096
Coefficient linear thermal expansion per °C. (0–100°C.) (Longitudinal and Transverse Equal)	.0000173	.0000173
Endurance Limit, lbs. per sq. in.	35,000	93,000 (150,000 UTS)
Modulus of Elasticity in Tension and Compression, lbs. per sq. in. (At comparatively low stress, 15,000 lbs. per sq. in., to insure elastic behavior.)	28–29 × 10^6	28–29 × 10^6

of the relative strength-weight ratio of the materials.

The comparable allowable yield and fatigue strengths are especially noteworthy.

In connection with the latter it is known that the fatigue strength or endurance limit is strongly affected by the nature of the surface and the strength of the surface layers. It has, for example, been conclusively proved that decarburized surfaces on ordinary steel, materially lower the endurance limit through failure starting in the weak ferrite surface and communicating to the stronger material beneath. This derives increased importance from the fact that the surface layers are ordinarily the most highly stressed of all. The figures given for the aluminum alloy are for the material without the soft aluminum cladding.

It is also a fact that stress concentration due to surface irregularities, sharp changes of section, or other notch effects will seriously affect the fatigue resistance of many materials. Data are not at hand on the resistance of aluminum to this "notch sensitivity." It is well known, however, that the work hardening capacity of 18–8 stainless steel results in relative insensitivity to notches.

In Table 1 are given some of the other characteristics of 18–8 stainless steel in the annealed and the cold-worked state. None of these values require any discussion here except those for the elastic properties, with respect to which there have been some misconceptions.

ELASTIC PROPERTIES

Stainless steel in the purely elastic range of deformation has, like ordinary carbon steel, a Young's modulus of twenty-eight to twenty-nine million, the higher figure being in all probability the more exact. This holds not only for annealed, but also for cold-worked material. The fact that figures considerably lower have been reported from time to time is probably due to a combination of two circumstances: (1) the stress range for purely elastic behavior, and hence the proportional limit is comparatively low, as will be discussed later in greater detail; (2) many of the measurements, upon cold-worked material particularly, have been made on thin strip or sheet specimens, which may not have been entirely flat, and accordingly the stress in some parts of the material is very much higher than in the remainder which was near a convex surface at the beginning of the test. As a result, when the mean load is still in the comparatively low stress range, certain parts of the material are really exhibiting behavior corresponding to much higher loads; and this gives the impression of a low modulus. This is borne out by the fact that the most careful tests, performed upon standard specimens of circular cross-section prepared in such a way as to be essentially straight, invariably show the higher modulus. It is thought that low figures such as twenty-five to twenty-six million should not be given consideration when the fundamental properties of the material are in question; such figures are only an apparent modulus, erroneous because the phenomenon is not wholly elastic.

With either high-carbon or low-carbon ordinary steel there is, in general, a definite linear relation between stress and strain (load versus elongation) over a moderate stress range. With soft steel this strict proportionality holds up to the sudden marked yield at which the stress-strain curve abruptly drops. With strong, heat-treated, high carbon steels which do not show any such sudden marked yield, a still more extended linear relation is observed. Stainless steel differs from these

markedly, its range of proportionality being relatively short but without a marked yield point. Its stress-strain diagram has certain characteristics resulting from its extraordinary ductility, combined with the very high ultimate strength manifest in the test, and indeed, developed in part during the test. At only a moderate load, generally in the vicinity of 20,000 to 25,000 lbs. per sq. in., the stress-strain curve begins to depart from absolute linearity, thus giving evidence of a slight permanent set; from this point on until the maximum load is applied, the curve continuously bends away more and more from the straight line corresponding to a modulus of 29 million but shows no abrupt "knee." There is some reason to believe that under a load only slightly in excess of 25,000 pounds the cold-worked material may, in spite of its much greater maximum strength, yield slightly more than the annealed material, and no doubt it is this which has given rise to the belief that cold-worked material has a lower proportional limit than annealed material. It should be borne in mind that these phenomena can be observed only with a testing technique of the highest possible accuracy. Even with ordinary equipment it is easy to observe that the stress required for some small, definite permanent deformation increases continuously with the degree of cold work.

One may say that the proportional limit actually observed on stainless steel depends only upon the sensitivity of the length measurement during the test; the greater its precision, the lower the apparent proportional limit. But this appears to be true in principle also with other metals; the point of difference is merely that austenitic stainless steel departs from observable strict proportionality of elongation and stress at a load which is a somewhat smaller proportion of its ultimate strength than that of some of the more familiar materials. Indeed one cannot escape the conclusion that present exceedingly precise methods of testing cannot possibly result in a strictly linear relation between load and elongation, as at present plotted, even for a purely elastic body. Moreover, it follows that the only figure for modulus which can be defended as having a fundamentally sound basis is the slope of the stress-elongation curve for an axially loaded specimen extrapolated to zero load. When this is approached experimentally the figure for the austenitic stainless steel is found systematically to approach about 29,000,000.

Because of the curvature of the stress-strain relation, and because the proportional limit is indefinite, it is now considered that the most useful criterion for design is the stress required to cause some definite predetermined degree of permanent elongation, under recognized proper conditions of test. The criterion generally accepted in aircraft work is that the yield point of a metal, such as the stainless steels and aluminum alloys, shall be the unit stress at which the material acquires a permanent set of 0.2 percent equal to a strain of 2 thousandths of an inch per inch.

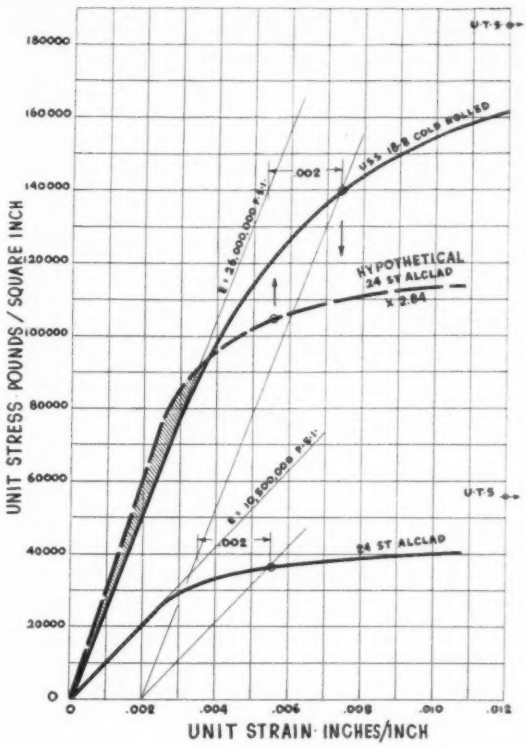

FIG. 5.

In Fig. 5 there have been drawn two synthetic stress-strain curves, one for 18–8 cold rolled stainless steel and one for 24 ST Alclad Aluminum Alloy, in both cases indicating the maximum design values as allowed by the Army Air Corps, in the absence of test data qualifying higher values.

For present purposes it will be assumed that these values are comparably conservative.

In order to place the two metals on an equal weight basis the unit tensile values of the 24 ST Alclad have been multiplied by 2.84 (neglecting influence of required weight of protective paint on the aluminum alloy) arriving at the hypothetical curve indicated. Obviously the unit stress for such a hypothetical curve is actually no longer in lbs. per sq. in. even though this nomenclature is used.

It will be noted that for equivalent strains (deflection) both metals are on a par at a unit stress of approximately 95,000 lbs. per sq. in. At higher values the equivalent weight hypothetical aluminum alloy markedly increases its rate of elongation while the stainless steel rises at a slower rate, reaching a value of approximately 20,000 lbs. per sq. in. greater unit stress at the equivalent yield point total strain than that of the aluminum alloy and a value of 35,000 lbs. per sq. in. greater unit stress than that of the aluminum alloy at the respective allowable maximum yield points.

At values below 95,000 lbs. per sq. in., the equivalent weight hypothetical aluminum alloy deflects to a some-

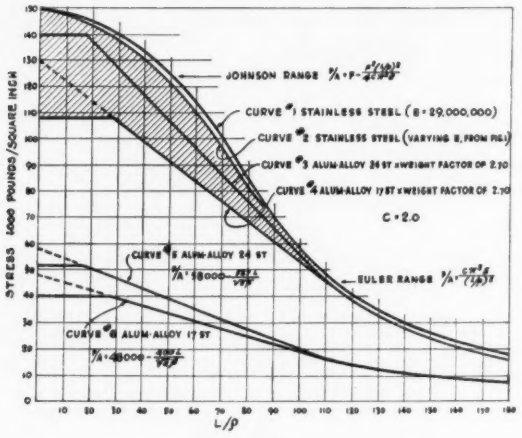
STRESS 1000 POUNDS/SQUARE INCH
JOHNSON RANGE
CURVE #1 STAINLESS STEEL (E = 29,000,000)
CURVE #2 STAINLESS STEEL (VARYING E, FROM FIG.)
CURVE #3 ALUM-ALLOY 24 ST x WEIGHT FACTOR OF 2.70
CURVE #4 ALUM-ALLOY 17 ST x WEIGHT FACTOR OF 2.70
C = 2.0
CURVE #5 ALUM-ALLOY 24 ST
EULER RANGE
CURVE #6 ALUM-ALLOY 17 ST
L/ρ

FIG. 6.

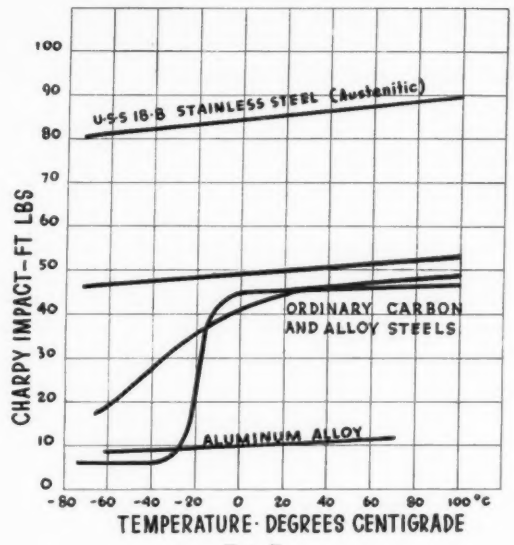

FIG. 7.

what lesser degree than the stainless steel, in the amount as indicated by the shaded area.

It is apparent from this that at low values of unit stress, the aluminum alloy would deflect slightly less than the stainless steel, but that after a certain critical value (approximately 95,000 lbs. per sq. in.) stainless steel would deflect to a much less degree; and in addition, for equivalent strains the stainless steel would have an allowable unit stress conservatively of 30,000 to 35,000 lbs. per sq. in. greater than the aluminum alloy of equivalent weight of stainless steel.

Considering the fact that, in a last analysis, all of our aircraft structures must be so designed as to successfully withstand a full static load test, it is contended that in the lower unit stress region the favorable, lesser elongation, of aluminum alloy, is markedly overshadowed by the considerably lesser elongation of the stainless steel in the higher unit stress region, and incidentally the usual design stress region.

The foregoing applies generally to tension stresses, the compressive stress picture has been ably presented by W. L. Sutton and Carl de Ganahl, in various publications including the January, 1935, Journal of the Aeronautical Sciences. One of the charts presented by de Ganahl therein is reproduced in Fig. 6 with the following quoted description: "The chart shows the usual Johnson-Euler curve for steel compression columns. The upper curve shows the allowable stress based on a constant modulus of 29,000,000. The curve immediately below is based on a varying modulus taken from a previous chart in which the modulus was indicated as varying from 29,000,000 to 21,000,000 between a unit stress of zero and 150,000 lbs. per sq. in. Throughout the Johnson range the yield point is of primary importance and the effect of the low modulus on the allowable unit stress is negligible.

"In the Euler range where the modulus is of importance, the allowable unit stresses have fallen to a point where the 18–8 again has its high modulus of 29,000,000 and there is no difference between the curve for stainless and any other steel of equal tensile strength.

"The lowest two curves indicate the allowable stresses for 17 ST and 24 ST Aluminum Alloy as generally used in Army and Navy practice. In order to compare these allowable stresses on an equal footing with stainless they have been multiplied by a factor of 2.70 representing the ratio between the specific weight of steel and aluminum alloy, with 5 percent added to the latter for paint and corrosion protection requirements. In this way the allowable stress curves for steel and light metals can be compared on an equal weight basis as shown here. It will be noted that the steel and light metal alloy curves are about equal in the long column or Euler range and that the steel has a distinct advantage in the short column or Johnson range.

"From these charts, therefore, it would seem that structures can be built as light in stainless as in the aluminum alloys, and, where the unit stresses are high, the advantage is materially in favor of stainless."

An additional factor in connection with stainless steel structures is that owing to the high degree of corrosion resistance, highly efficient box-type sections can be used.

Properties at Elevated and Reduced Temperatures

With regard to the characteristics at other than room temperature, it can be said that a reduced temperature causes an increase, and an elevated temperature a decrease in the tensile strength of 18–8 and in fact of other metals. Accompanied with a decrease in temperature there is usually, except in the case of 18–8 stainless steel and certain other alloys, a marked decrease in impact or shock strength. In Fig. 7 there is

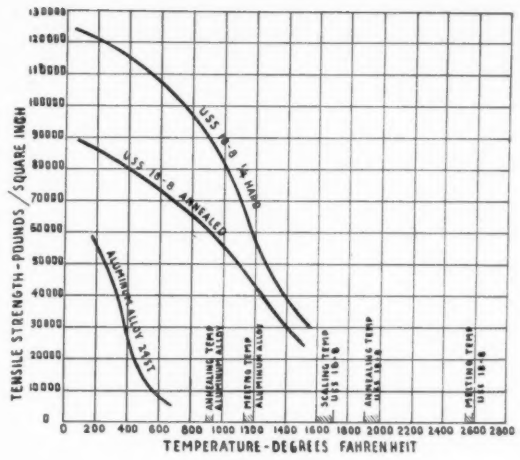

FIG. 8.

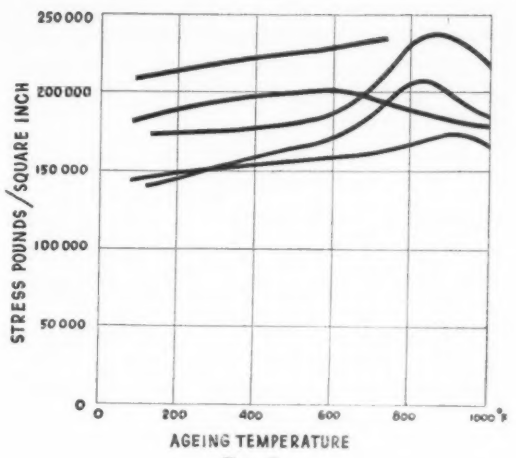

FIG. 9.

indicated typical Charpy impact figures determined at reduced temperatures for some of the ordinary carbon and alloy steels. On the same chart is indicated the typical variation in impact strength of an austenitic type 18–8 stainless steel and an aluminum alloy at reduced temperature. The shock resistance and toughness of the 18–8 is strikingly obvious.

With regard to the tensile strength, it has been determined that at reduced temperatures, the aluminum alloys, to a moderate degree and the stainless steels to a very large degree, increase in their strength properties. A typical 18–8 stainless steel annealed sample increased in ultimate tensile strength from 100,000 lbs. per sq. in. at room temperature to 180,000 lbs. per sq. in. at −80°C.

A cold-rolled sample increased from 150,000 lbs. per sq. in. to over 220,000 lbs. per sq. in. in going from room temperature to −80°C. Unfortunately this increase has no practical significance, but it is at least reassuring to know that the strength of stainless steel improves at high altitude and in cold climates and most important of all, retains its extremely high impact strength characteristics.

In Fig. 8 there are indicated the pertinent strength characteristics of 18–8 stainless steel and aluminum alloys at elevated temperatures. One of the most significant facts about cold worked 18–8 stainless steel is that it retains its normal room temperature annealed strength when practically red hot.

This fact is quite reassuring when consideration is given to the fire hazard involved in accidental high temperatures, as near an exhaust or in an engine nacelle while in flight. Also in view of the high melting temperature of stainless steel, the improbability of its igniting and burning, as after a crash, is reassuring.

HEAT-AGE HARDENING

One of the most interesting characteristics of stainless steel of the 18–8 types, especially those having slight additions of titanium or columbium, is the ability of certain heat-aging treatments to appreciably raise the yield and ultimate strength of the material. Some experiments reported to date indicate that material originally cold rolled to 170,000 lbs. per sq. in., heated at 900°F. for a few hours and then cooled, resulted in ultimate strength values above 200,000 lbs. per sq. in., and an elastic modulus recovery of about two million from 27 million to 29 million lbs. per sq. in. A number of typical curves of different 18–8 alloys showing this relation between aging temperature and tensile properties are indicated in Fig. 9.

The temperature range for the heat aging is approximately that which is currently used to heat treat aluminum alloy and is not high enough to cause distortion of a fabricated stainless steel structure. The infinitesimal oxidation formed is of a straw tint typical of temper colors, easily removed if desired, in hot dilute nitric acid.

Stainless steel does not age at room temperature; tests made on a straight 18–8 stainless steel strip material shortly after fabrication and again 20 months later showed no significant change in mechanical properties. In another test of the same material at elevated temperatures, aging for periods up to three days at 700°F. resulted in an increase of yield strength and ultimate tensile strength by an amount of the order of 5 percent to 10 percent and a lowering of the proportional limit and elongation by an amount slightly greater.

Most important, in addition to the very considerable increase in strength of the columbium and titanium bearing 18–8 steels, and the more moderate increase in the straight 18–8 materials, is the fact that the heat aging process tends to relieve the structure of such fabricating and welding stresses as may have developed.

While it is true that this proposal of heating and aging stainless steel necessitates some of the heating facilities as were earlier claimed eliminated by the use of stainless steel, one cannot lightly dismiss a 10 per-

cent to 20 percent or more increase in tensile strength, and such heating facilities may actually prove quite inexpensive. In any event, more will be heard from this unique characteristic of stainless steel as a clearer understanding of the phenomenon develops.

Life Cost

Proper consideration of the cost of any piece of equipment includes not only the raw material and fabricating labor but also the operating cost during the life of the equipment.

In this regard, stainless steel as a material offers some very clear advantages over other metals. Of first advantage is a fact that the bare metal is corrosion resistant to a very superior degree even in the presence of salt water. Given normal maintenance and a surface kept reasonably clear from deposits, stainless steel should last indefinitely. Disregard of these precautions has in certain instances induced a form of pitting corrosion when contaminated salt water has lain stagnant in contact with stainless steel. Corrosion generally indicates its presence by a visible localized rust discoloration.

The ability to use the bare metal has the obvious advantage of saving painting cost initially and in service maintenance, but just as important is the saving in weight and the increase in pay load. On a large ship this may amount to the weight of a number of passengers.

An indirect advantage accrues from the hardness and stiffness of the material, that of resisting scratching and marring, as well as improved resistance to deformation and penetration of the surface either by casual contacts on the ground or by striking hailstones or birds in flight. The fact that water and gas tightness, as well as minor repairs can be effected by soldering patches on the material is a very definite maintenance advantage.

Letters to the Editor

August 20, 1938

Dear Sir:

Kindly place the following comment regarding the recent paper by von Kármán and Sears (*Airfoil Theory for Non-Uniform Motion*, Journal of the Aeronautical Sciences, Vol. 5, No. 10, August, 1938) before the readers of this Journal.

I would like, in future papers on this subject, to see the simplification carried to still greater length by altogether dispensing with the division of the forces and moments into several parts. The airfoil is occupied by vortices v moving with individual velocities w relative to the fluid. In a fluid of unit density, to each vortex is then to be ascribed a force equal to v times w, acting at the place of the vortex, at right angles to w. No further appeal to dynamics is necessary.

The integrations over the airfoil are simplified by writing

$$L = \int vwdx = \int (\partial v/\partial T)xdx + |vx| \quad (1)$$

$$M = \int vwxdx = \int (\partial v/\partial T)x^2dx + |vx^2| \quad (2)$$

I will illustrate this suggestion by proving that the moment coefficient of any thin wing section about the 25 percent point is constant, even when moving through fluid slightly disturbed by any system of stationary vortices (not necessarily concentrated along the trailing wake line).

Let u denote the impressed cross velocity, and $u' = \partial u/\partial T = \partial u/\partial x$ (velocity of advance = 1) its derivatives with respect to both time and x coordinate. This impressed velocity is arbitrarily chosen, subjected however to the Kutta condition of vanishing trailing edge velocity

$$\int [u(1+x)/\sqrt{1-x^2}]dx = 0 \quad (3)$$

This gives the vorticity fluxion distribution

$$\partial v/\partial T = \int u'\sqrt{1-x^2}\,dx(\cos\delta/\sin\delta) + \int u'x\sqrt{1-x^2}\,dx(\cos 2\delta/\sin\delta) + \ldots \quad (4)$$

and that, substituted in Eqs. (1) and (2), gives expressions proportional to

$$L = \int u'\sqrt{1-x^2}\,dx = \int (ux/\sqrt{1-x^2})\,dx \quad (5)$$

$$M = -2\int u'x\sqrt{1-x^2}dx = -2\int (u/\sqrt{1-x^2})\,dx \quad (6)$$

From Eqs. (3), (5), and (6) it follows that $L + M/2 = 0$, which proves the proposition for a straight airfoil, and hence for all.

Max M. Munk

August 22, 1938

Dear Sir:

To avoid possible misunderstandings the author of the article entitled, "A Study of Available Flap Data," in the June, 1938, issue of the Journal, would appreciate the opportunity of a reply to the statements contained in the letter of H. D. Fowler in the August issue.

Mr. Fowler has reported that the effectiveness of the Fowler flap increases with flap chords greater than 20 percent. This is in agreement with the author's statement, on page 311 of the June issue of the Journal, that "The external-airfoil, like the Fowler and Zap flaps, becomes much more effective as regards $\Delta C_{L_{max.}}$ with increasing flap chord." The statement that "among the usual types of flap there is little to be gained in $C_{L_{max.}}$ where the flap chord exceeds 20 percent," mentioned by Mr. Fowler, does not appear in the paper, so far as the author is aware.

As to scale effect with the Fowler flap, it is interesting to learn that there are favorable trends. Information on this point does not appear in the published flap literature which was depended upon for the data used in the analysis of flap characteristics.

The writer feels that we have a great deal yet to learn about flaps and high-lift devices.

Richard C. Molloy
United Aircraft Corporation

Editorial Note: In the Letter to the Editor from Harlan D. Fowler, in the August issue of the Journal, the words "As the paper states" should be deleted from the second sentence of the first paragraph. This phrase was not in Mr. Fowler's letter as submitted, but was an editorial insertion to improve the continuity. The sentence should stand as Mr. Fowler's own opinion.

Institute Notes

Wright Brothers Lecture

Hugh L. Dryden, a Fellow of the Institute, has been selected to deliver the Wright Brothers Lecture at the Honors Night Dinner on Dec. 17, 1938.

The members of the committee making the selection are D. W. Douglas, W. F. Durand, J. C. Hunsaker, Th. von Kármán, Glenn L. Martin, and William P. McCracken, all of whom have given the Wilbur Wright Memorial Lecture before the Royal Aeronautical Society.

The subject of the lecture will be "Turbulence and the Boundary Layer." Dr. Dryden occupies a preeminent position in this field of aerodynamic research. His investigations of Turbulence are considered classics, both from the standpoint of their theoretical importance in Fluid Mechanics, and of their wide practical application, where their far-reaching effects on the technique of model testing, particularly, are universally recognized.

Dr. Dryden is at present Chief of the Mechanics and Sound Division and of the Aerodynamics Section at the National Bureau of Standards. He entered that bureau from The Johns Hopkins University in 1918. He is an Associate Fellow of the Royal Aeronautical Society, and a Member of the American Society of Mechanical Engineers.

Dr. Dryden's selection as Wright Brothers Lecturer is considered particularly fortunate from the standpoint of maintaining the high standard set for that lecture by Prof. B. M. Jones in 1937.

Meetings

The Fifth International Congress for Applied Mechanics is meeting in Cambridge, Massachusetts, from Monday, September 12 through Friday, September 16, 1938, as guests of Harvard University and the Massachusetts Institute of Technology. The program comprises one hundred and thirty papers, together with six general lectures, covering all phases of Applied Mechanics.

A joint meeting of the Institute and the Applied Mechanics Division of the American Society of Mechanical Engineers will be held on the Pacific Coast, from September 28 to September 30, 1938, in the Los Angeles area.

An "Air Transport Meeting" of the Institute will be held in Chicago on October 21 and 22, 1938. Papers describing new transport planes, problems of high altitude flight, radio, meteorology, and instruments will be presented.

The Philadelphia Branch of the Institute will hold a meeting on September 23 and 24, 1938. The technical sessions will be devoted to papers on rotary-wing aircraft.

Books Received

The Institute acknowledges with appreciation the receipt of the following books for its library.

Aerial Navigation, by Albert F. Zahm; D. Appleton and Company, New York, 1911; 497 pages, illus. Presented by Lt. Clyde W. Smith, Bureau of Aeronautics, Navy Department.

Charts of the Atmosphere for Aeronauts and Aviators, by A. Lawrence Rotch and Andrew H. Palmer; John Wiley and Sons, New York, 1911; 92 pages, illus. Presented by Lt. Clyde W. Smith, Bureau of Aeronautics, Navy Department.

Air Transportation, Part I, by A. F. Bonnalie; Boeing School of Aeronautics, Oakland, California, 1938; 134 pages. Presented by A. F. Bonnalie, Boeing School of Aeronautics.

Twenty-Third Annual Report of the National Advisory Committee for Aeronautics, 1937; United States Government Printing Office, 1938; 741 pages, illus., $2.50. Presented by the N.A.C.A.

The Century Illustrated Monthly Magazine, May, 1891 to October, 1891; The Century Co., New York, 1891. Presented by William Rickett, Shellburn, Massachusetts.

Necrology

Edward Earl Wyman

Edward Earl Wyman, an Industrial Member of the Institute, was a passenger on the Hawaii Clipper, lost over the Pacific Ocean on July 30, 1938.

Mr. Wyman was born in Evanston, Illinois, on April 9, 1893. He was graduated from Yale University with a Ph.B. degree, and in 1917 studied aeronautical engineering at the Massachusetts Institute of Technology. He served as a wartime commissioned pilot in the Navy and, at the time of his death, held the rank of Lieutenant Commander in the U. S. Naval Reserve.

Mr. Wyman was, successively, vice-president and director of Pacific-Alaska Airways, Inc., vice-president and director of the Marine Airport Corporation, assistant to the president of Pan American Airways, Inc., and was, at the time of his death, a vice-president of the Curtiss-Wright Corporation.

Leo Terletzky

Leo Terletzky, a Pilot Member of the Institute, was captain of the Hawaii Clipper, lost over the Pacific Ocean on July 30, 1938.

Mr. Terletzky was born in Samara, Russia, on Feb. 1, 1895. He was a naturalized United States citizen. He was graduated from the gymnasium in Samara, Russia, and, after his immigration to this country, was a student in the Liberal Arts College at New York University.

In 1929, Mr. Terletzky became associated with Pan American Airways, Inc., as air line pilot. For the past two years he had been captain of one of the Trans-Pacific Clippers on regular flight duty between Alameda, California, and Hong Kong, China.

Frank Monroe Hawks

Frank Monroe Hawks, a Pilot Member of the Institute, was fatally injured on August 23, 1938, when his plane crashed near East Aurora, New York.

Mr. Hawks was born in Marshalltown, Iowa, on March 28, 1897. He attended high school at Long Beach, California, and entered the University of California in 1916. In 1917, he enlisted in the army and was instructor and test pilot in the Air Section of the Signal Corps. He attained the rank of Captain.

After the war Mr. Hawks set many records, outstanding of which were his trans-continental records made in 1930 and 1932. He also established a total of 225 city to city records in the United States and Europe. In 1930, he was awarded the Harman Trophy as the outstanding aviator in the United States.

Mr. Hawks was the author of two books, "Speed" (1931) and "Once to Every Pilot" (1936), and was a contributor to the Encyclopedia Britannica.

He was, until recently, head of the Aviation Division of the Texas Oil Company, and, at the time of his death, was a vice-president of the Gwinn Aircar Company. He held the rank of Lieutenant Commander in the U. S. Naval Reserve.

Exchanges

The Institute exchanges the Journal with many other aeronautical periodicals. They are kept on file at the Skyport in Rockefeller Center, New York City, where members may read them. As readers of the Journal may wish to subscribe to some of them, a list of these periodicals with their addresses is published here. Information regarding subscription prices may be secured from the Secretary of the Institute.

Aero, Maneesikatu 2, Helsingfors, Finland.

Aero Digest, 515 Madison Ave., New York City.

Aeronautica Argentina, Velez Sarsfield 57, Cordoba, Argentina.

L'Aéronautique, 55 Quai des Grands-Augustins, Paris, France.

L'Aérophile, 7 Rue Sainte-Lazare, Paris, France.

The Aeroplane, 175 Piccadilly, London, W.1, England.

L'Aerotecnica, Via delle Coppelle 35, Rome, Italy.

Les Ailes, 77 Boulevard Malesherbes, Paris, France.

L'Air, 71, Champs-Élysées, Paris, France.

Aircraft Engineering, 2 Bloomsbury Place, London, E.C.1, England.

Air Law Review, Washington Square East, New York City.

American Aviation, Earle Building, Washington, D. C.

Asas, Caixa Postal 1967, Rio de Janeiro, Brazil.

Astronautics, American Rocket Society, 31 West 86th Street, New York, N. Y.

Aviation, 330 West 42nd St., New York City.

L'Aviazione, Corso Umberto 504, Rome, Italy.

Bradshaw's International Air Guide, Surrey St., Strand, London, W.C.2, England.

Boletin de Aeronautica Civil, Calle Azcuenga 923, Buenos Aires, Argentina.

Bulletin du Service Technique de l'Aéronautique, 72 Chaussee de Waterloo, Rhode-Saint-Genese, Belgium.

Bulletin of the American Meteorological Society, Blue Hill Observatory, Milton, Massachusetts.

Bulletin Technique du Bureau Veritas, 31 Rue Henri-Rochfort, Paris (17), France.

Canadian Aviation, Journal Building, Ottawa, Canada.

Contact, Fort Lee, N. J.

Deutsche Luftwacht, Schoeneberger Ufer 46, Berlin W35, Germany.

Der Deutsche Sportflieger, Peterssteinweg 19, Leipzig C1, Germany.

Les Fiches Aéronautiques, 6 Rue Galilee, Paris, France.

Flight, Dorset House, Stamford St., London, S.E.1, England.

Indian Aviation, P. O. Box 2361, Calcutta, India.

Interavia, 13, Corraterie, Geneva, Switzerland.

Journal of Air Law, Northwestern University, Chicago.

Journal of the Institute of Engineers, Australia, Science House, Gloucester and Essex Sts., Sydney, N. S. W., Australia.

Journal of Research of the National Bureau of Standards, U. S. Govt. Printing Office, Washington, D. C.

Journal of the Royal Aeronautical Society, 7 Albemarle St., Piccadilly, London, W.1, England.

Journal of Scientific Instruments, 1 Lowther Gardens, Exhibition Rd., London, S.W.7, England.

Journal of the Society of Automotive Engineers, 29 West 39th St., New York City.

L'Ala d'Italia, L'Aquilone, La Rivista di Diritto Aeronautico, La Rivista di Meteorologia Aeronautica, Le Vie dell'Aria, Viale dell'Universita 4, Rome, Italy.

Letectvi, Celetna 13, Praha I, Czechoslovakia.

Luftfahrt-Forschung, Verlag Oldenbourg, Munich 1, Germany.

Die Luftreise, Lindenstr. 35, Berlin SW68, Germany.

Luftfahrt-Literaturschau, Z.W.B. bei der D.V.L., Berlin-Adlershof, Germany.

Model Airplane News, 551 Fifth Avenue, New York City.

Monthly Weather Review, U. S. Dept. of Agriculture, Washington, D. C.

Motor and Flying, 24 Bond St., Sydney, N. S. W., Australia.

National Aeronautics, Dupont Circle, Washington, D. C.

Official Aviation Guide, 608 S. Dearborn St., Chicago, Illinois.

The Pilot, Grand Central Air Terminal, Glendale, California.

Popular Aviation, 608 S. Dearborn St., Chicago, Illinois.

Proceedings of Institute of Radio Engineers, 330 W. 42nd St., New York City.

Publications Scientifiques et Techniques du Ministère de l'Air, 55 Quai des Grands-Augustins, Paris, France.

Review of Scientific Instruments, 175 Fifth Ave., New York City.

Revue de l'Armée de l'Air, 55 Quai des Grands-Augustins, Paris, France.

Revue du Ministère de l'Air, 71 Avenue des Champs-Elysees, Paris (8), France.

Rivista Aeronautica, Ministero dell'Aeronautica, Rome, Italy.

The Royal Air Force Quarterly, Gale & Polden Ltd., 2 Amen Corner, London, E.C.4, England.

Schweizer Aero-Revue Suisse, Gubelhangstrasse 22, Zürich-Oerlikon, Switzerland.

Soaring, 1614 Delaware Ave., Wilmington, Del.

Southern Flight, Ledger Building, Fort Worth, Texas.

Sportsman Pilot, 515 Madison Ave., New York City.

Technical News Bulletin of the National Bureau of Standards, U. S. Govt. Printing Office, Washington, D. C.

Technika Lotnicza, Czerwonego Kryza 21/23 m.6, Warsaw, Poland.

Technika Vosdushnogo Flota, U1. Radio 16, Moscow 16, U. S. S. R.

La Technique Aéronautique, 2 Rue Blanche, Paris (9), France.

U. S. Air Services, Transportation Building, Washington, D. C.

Western Flying, 420 S. San Pedro St., Los Angeles, California.

Wirtschaft Technik Verkehr, Alte Jakobstr. 148/155, Berlin, SW68, Germany.

Zeitschrift für angewandte Mathematik und Mechanik, Kulmstr. 1, Dresden A24, Germany.

AERONAUTICAL REVIEWS

These brief reviews of recent articles on aviation subjects are published by the Army Air Corps for the information of its officers, and are printed here each month by permission of the Chief of the Air Corps.

Aerodynamics

Experiments with the Two-Bore Slipstream-Measuring Apparatus for Determining Flow Direction. H. Muttray. First experiments in measuring slipstream were made with the Christiani two-bore instrument comprising a 20-mm.-diameter tube having two openings, one above the other and at a center angle of about 60° to each other. The "two-finger" instrument is an improvement on this device and consists of two pitot tubes arranged at about right angles to each other, with their ends very close together. Accuracy is ±0.05°. Experiments made with both the instruments described. A.V.A. (Goettingen) report. Brief abstract from Luftfahrtforschung, March 20. Aircraft Engineering, June, 1938, page 193.

Wind Tunnel of the Dornier Company. H. Schlichting. Experimental chamber of the Dornier tunnel, now in operation, has an elliptical section 3 × 4 meters and 7 meters long. Maximum wind velocity is 60 meters/sec. Local uniformity of velocity, static pressure, direction of flow, and turbulence of the tunnel are up to good German and foreign standards. Three-component and six-component balances are used. Brief abstract from Luftfahrtforschung, March 20. Aircraft Engineering, June, 1938, page 193.

Aircraft Design

Distribution of Wing Torque over the Span. J. Kleinwaechter. Lift distribution is first calculated and plotted and from the result distribution of torsional moment is plotted in a graph shown in the original article. Report of the Technischen Hochschule, Danzig. Very brief abstract from Luftfahrtforschung, March 20. Aircraft Engineering, June, 1938, page 193.

High Wing-Loading. H. Belart. Designer's problem of deciding on the wing area necessary for his purpose. Optimum wing loading giving highest level speed and best aerodynamic efficiency (range) for any given set of design and operating conditions is determined analytically. For a variable-wing-area airplane flying a given power output, the condition for highest level speed is shown to coincide with the one for best aerodynamic efficiency. Reduction of parasite drag is very beneficial if corresponding increase in wing loading can be allowed, gain being far greater than for a fixed-wing airplane. Conditions given for a flying wing operating at 0.7 times sound speed indicate that high optimum wing loadings required at low values decrease to very reasonable values at great heights and power output is moderate. Aircraft Engineering, June, 1938, pages 173–176, 191, 8 illus., 1 table, 8 equations.

Investigation of the Slipstream Behind a Trapezoidal Wing with Fuselage and Propeller. H. Muttray. Ideal form of fuselage with a low-wing model had only a negligible influence on the slipsteam in comparison to tests with wing alone. With a fuselage, the section of which shows angles, the influence was very great. With rotating propeller fitted the torsional movement of the slipstream was found to be still very strong in the neighborhood of the elevators in spite of the straightening effect of the wing. Further troubled zones were found on both sides of this torsional region. Low-wing model with angular section fuselage proved to have better stability qualities. A.V.A., Goettingen, report. Short abstract from Luftfahrtforschung, March 20. Aircraft Engineering, June, 1938, page 193.

Some Conclusions on the Non-Polar Method. J. Kleinwaechter. Shrenk's nonpolar method for calculation of flight characteristics results in formulas with which effect of various constructional dimensions can be determined. Examples of calculation of drag and range are shown in the original article. Report of the Technischen Hochschule, Danzig. Very brief abstract from Luftfahrtforschung, March 20. Aircraft Engineering, June, 1938, page 193.

Wing and Propeller Slipstream. A. Franke and F. Weinig. Conditions of flow on an airplane wing are greatly influenced by propeller slipstream, and the slipstream boundary is subject to special conditions. These boundary conditions are represented and it is explained how they may be met by consideration of the axial supplementary velocity, slipstream rotation and the oblique wind. Change in effective angle of attack due to influence of the slipstream, and the variations of lift, drag, and longitudinal moment on the wing elements are demonstrated. DVL report. Luftfahrtforschung, June 6, 1938, pages 303–314, 16 illus., 47 equations.

Large Aeroplanes. H. R. Cox. On structural grounds a limiting weight of 680 tons is possible, but even if certain difficulties of the engine-propeller group can be overcome this propulsion group limits the weight to 446 tons. Reasons are given for believing that successful airplanes of an enormous size can be built. Discussion includes: square-cube rule; consideration of an airplane of conventional layout; effects of changes in layout with attainment of size; and apparent limitations to size which are dependent on systems of propulsion. Journal Royal Aeronautical Soc., July, 1938, pages 591–602, 9 illus., many equations.

Recent Research on the Improvement of the Aerodynamic Characteristics of Aircraft. E. F. Relf. Paper and discussion. Journal Royal Aeronautical Soc., June, 1938, pages 512–535, 7 illus.

A Tea and Tattle at Teddington. Brief reference only to research being conducted at the National Physical Laboratory on balancing of flaps by insetting the hinge point from the leading edge of the control surface, and general account of visit. Aeroplane, July 6, 1938, page 6.

Rotary-Wing Aircraft

Contribution to the Aerodynamics of Rotary-Wing Aircraft. G. Sissingh. Existing methods of calculation for rotors with articulated coupled blades are extended and improved according to various points of view. Principal disadvantage of investigations made so far has been due to the more or less arbitrary assumption of an "average" drag coefficient for all blade elements. This negligence is prevented by substituting for the constant coefficient a function of greater order corresponding to the polars of the profile used. This substitution makes it possible to extend the theory in general to the entire field from the rotary wing without power drive to the driven rotor with blade axis inclined forward. Rectangular blades that may be twisted and the nontwisted trapezoidal blades are discussed. Investigation is based on work by Wheatley which in turn is based on the well-known Glauert and Lock methods of calculation. Luftfahrtforschung, June 6, 1938, pages 290–302, 7 illus., 77 equations.

Static Longitudinal Stability and Elevator Control of Rotary Wings. M. Schrenk. Three types of elevator control and their efficiency in regard to stability and controllability are investigated, including the normal tail-surface control, the Cierva blade control, and the new center-of-gravity control. Nature and balancing of control forces are discussed and bases for constructive development given. DVL report first published in 1933. Luftfahrtforschung, June 6, 1938, pages 283–289, 19 illus., 8 equations.

The Stressing of Rotor Blades. J. Morris and W. Tye. Loading over the blade is assumed as steady at any instant of a given flight condition. Subject to this restriction, stresses in the blade may be found to any required degree of approximation by the generalized theorem of three moments suitably modified. Gyroscopic moments of a blade and its frequency of "flapping" vibration is found on the assumption that blade is rigid and with regard to imposed rotation. Aircraft Engineering, June, 1938, pages 177–179, 4 illus., 3 tables, many equations.

Stress Analysis and Structures

Manipulation of Stainless Steel for Aircraft. C. de Ganahl and W. L. Sutton. Tapered cantilever wing panel of 18-8 stainless steel recently constructed for the Army Air Corps. Tests proved it to be light in weight, stiff in bending, and exceptionally rigid torsionally, and its elastic center was sufficiently far forward to offer inherent stability against flutter. Wing was designed for quantity production. Long description of wing design, welding, and other processes used in construction, and the construction difficulties which were eliminated. Aero Digest, July, 1938, pages 44–45, 10 illus.

Good Arguments in Defense of the Airplane of All-Wood or Mixed-Construction. J. J. Turc. Technical arguments are based on the practical equality of one or the other form, and on the possibility of a far more simple fabrication than that permitted in metal construction. Les Ailes, June 16, 1938, page 7.

The Elastic Stability of a Curved Plate under Axial Thrusts. S. C. Redshaw. Theoretical critical stresses have been obtained for four cases in each of which a curved panel has been subjected to a compressive stress, parallel in direction to a generator and uniformly distributed around its top and bottom circumferential edges. In each case critical stress may be expressed by $p = [\pi^2 . t^2/12\ (1 - \sigma^2)\ b^2]\ EK$ where coefficient K is split into flat and curved plate coefficients, both depending on the ratio of axial length of plate divided by product of circumferential length of plate and number of half waves in the axial direction. Curved plate coefficient is also dependent on the curvature of plates which has a most marked effect on its numerical value. Journal Royal Aeronautical Soc., June, 1938, pages 536–553, 7 illus., 1 table, 106 equations.

Force Distribution in Riveted Connections of Constant Cross Section under Tensile Loads. Method for approximate determination of force distribution in simple butt straps of constant cross section up to tensile breaking load. Expressions developed permit determination of displacements of the straps for both elastic and plastic deformation of the rivets. Tests were made on displacements taking place in double-shear connections, each consisting of ten duralumin rivets disposed in line with the pull and connecting plates of different thicknesses, and on various types of single-rivet connections. Short abstract from Luftfahrtforschung, January 20, pages 41–47. Journal Royal Aeronautical Soc., June, 1938, page 568.

Aircraft Alighting Gear

Aeorplane Undercarriages. E. Jones and F. G. R. Cook. Operational load on main and tail wheels; high and intermediate pressure tires; tires for service and civil airplanes; load deflection curves; energy absorbed by tires and elastic rate; tire clearances; effect of increased weight; tests; ground contact pressure; tests of wheels; brake design and operation; differential brake unit; rebound control of shock-absorber struts; constant and variable orifice struts; and tests of struts. Review of current practice and notes on design. To be continued. Aircraft Engineering, June, 1938, pages 165–172, 18 illus.

Hydraulic Controls. Lockheed complete hydraulic system for operating both main and auxiliary services. Engine-driven and emergency hand pumps, selector and flow-control valves, hydraulic jacks, emergency selector valve, undercarriage indicator, and operating fluid used are discussed in detail. Diagrammetric arrangement of complete system and layout in an airplane of Lockheed controls for operation of undercarriage, flaps and tail wheel are illustrated. Photograph of Lockheed jacks in position on the Ensign airplane included. Aircraft Engineering, June, 1938, pages 189–191, 3 illus.

Hydraulic Filters. Cuno filters for hydraulic flap and landing-gear operating systems of both direct-acting and accumulator types. Few details. Aviation, July, 1938, page 44, 1 illus.

Light Plane Tail Wheels. Three types of Universal Alloy tail wheels, consisting of Type H-60 non-swivelling all-metal assembly attaching to the conventional spring-leaf skid, Type H-3 designed to provide complete maneuverability for light aircraft, and Type H-2 designed for attachment to the Aeronca K. Few details. Aviation, July, 1938, page 47, 2 illus.

Malleable Iron Wheel Assemblies. Two types of Lancaster tail-wheel assemblies, one for attachment to the tail spring leaf of a Rearwin airplane and the other for the skid tube on the Aeroncas. Few details. Aero Digest, July, 1938, page 85, 1 illus.

Aircraft

Continental Touring Aeroplanes. Arado Ar. 79 two-seater low-wing monoplane (105-hp. Hirth H.M.504 A.2 engine, top speed 143 m.p.h.). Breda 79S four-seater high-wing monoplane (200-hp. Alfa Romeo 115 6-cylinder inverted inline engine, maximum speed 161 m.p.h.). Construction, characteristics, performance. Additional photographs of the Arado Ar. 79 are given on another page with a reference to four class records recently set up with it. Aeroplane, July 20, 1938, pages 83, 95, 6 illus., 2 tables.

Fast Transport Aeroplanes. Lockheed Super-Electra Model 14WG3 14-seater transport (two Wright GR.1820G-3 Cyclone engines, top speed 264 m.p.h. at 8700 ft.), and the Savoia-Marchetti S.M.83 14-seater transport (tnree 780-hp. Alfa-Romeo 126 R.C.34 engines, top speed 276 m.p.h. at 13,123 ft.). Construction, characteristics, and performance. Aeroplane, July 20, 1938, page 87, 4 illus., 2 tables.

Imperial Airways' "Ensign." Comparison of the Armstrong-Whitworth "Ensign" 40-passenger land plane (four Armstrong-Siddeley 900-hp. engines, top speed 200 m.p.h., and cruising range 800 miles) and the Douglas DC-4 42-passenger land plane. Short note. U.S. Air Services, July, 1938, page 31.

A Clutch of Records. Commandant Rossi piloting an Amiot 370 (two Hispano-Suiza 12Y21 900-hp. engines) established three new long-distance records over a closed circuit of 5000 km. (3107 miles), with 1000-kg. load, 1012 gal. gasoline and 62 gal. oil, making an average speed of 249.16 m.p.h.

Major Udet covered 62 miles at an average speed of 394 m.p.h. Machine is said to be a special Heinkel, possibly derived from the Heinkel He 112.

A Junkers Ju.90 (four Daimler-Benz inverted-vee twelve engines of about 1000-hp. each) has broken an altitude record for machines carrying a 5000-kg. load, reaching 30,550 ft. Short note. Flight, June 23, 1938, page 615.

Account of Rossi's flight in the Amiot 370 with 1000-kg. load, breaking the Soviet record by 75 km./hr. Les Ailes, June 16, 1938, pages 3–4, 1 illus.

General Udet's record and the Junkers Ju.90 altitude record. Les Ailes, June 16, 1938, page 5, 2 illus.

Brief references to all three records, as well as to Hanna Reitsch's round-trip glider record of 155 miles in 5½ hours. Aero Digest, July, 1938, page 38.

BELGIUM

"Les Ailes" in Belgium. Tests of the Renard R-6 single-seater pursuit have been pushed. Of the six versions being built, one has a reduced wing, one is equipped as a two-seater for training and dual control, and one has a radial engine (probably a Gnôme Rhône K-14). Renard is searching for the best version of his design, the prototype of which exceeded 500 km./hr.

A Percival Vega Gull and the Messerschmidt are being tested by Belgian military authorities as trainers in piloting low-wing airplanes.

A small bimotored Peterman S.E.A.-1 has been completely transformed into a single-engined plane and retractable landing gear has been replaced by a fixed gear. The L.A.C.A.B. GR-8 equipped with two K-14 engines is also mentioned.

New Browning machine gun firing 1800 shots per minute has been constructed by the Fabrique Nationale d'Armes de Guerre, and has been tested on the Fairey Kangouroo single-seater pursuit which has an Hispano-Suiza 12 Xbrs engine and four non-synchronized machine guns in the upper wing. Short notes. Les Ailes, July 7, 1938, page 4.

FRANCE

Airplanes in Test. Brief references only to the following aircraft undergoing tests. First issue—Hanriot 510 three-seater prototype (two Gnôme Rhône K-9 engines) presented to the President of the Republic. Delanne flying model of the pursuit prototype. Farman 223 bomber (four Hispano Suiza 12-Y liquid-cooled engines). Bloch 131 bomber. Nieuport 161 pursuit (Hispano-Suiza 12-Ycrs engine cannon). Morane-Saulnier 406 pursuit. Bréguet 690 three-seater combat and light bomber. Latè 523 flying boat. LeO-45 bomber. Farman 470 trainer (two Gnôme Rhône Jupiter engines). Brief references only to these aircraft undergoing tests. Les Ailes, June 30, 1938, page 7.

Morane-Saulnier 406 (Hispano Suiza engine cannon). LeO-301 autogiro (Salmson 9-N.E. engine). M.S.-278 (Clerget heavy-oil 500-hp. engine) attaining an altitude of 5000 meters. Les Ailes, July 7, 1938, page 7.

Coming Along in France. Potez 63 neat new twin-motor fighter (two 670-hp. Hispano-Suiza 14-HB engines) which does about 280 m.p.h. Photographs only. Aeroplane, July 13, 1938, page 45.

Flying Model of the Potez-CAMS-161 Made its First Flights at Sartrouville. Performance of the Potez-CAMS 160, flying model of the 40-ton 161 transatlantic flying boat for Air France, during tests. Questions of similitude are also discussed and a large model of the hull of the 161 is briefly described. Les Ailes, June 30, 1938, pages 5–6, 1, 3 illus.

Great Expectations. The newly formed Société Coopérative d'Études et Production Aéronautique is producing an airplane to compete in the race for the Coupe Deutsch de la Meurthe in 1939. Prototype is called the Payen "Flèchair" PA-112 and will have two Salmson engines driving oppositely rotating propellers. A two-motored cannon fighter (designed speed 435 m.p.h.) and the Payen PA-240 high-speed mail plane for the North Atlantic will be produced. Brief reference. Aeroplane, July 13, 1938, page 43.

The S.F.A.N. with the Billioque Stabilizer Descends Like a Parachute. L. J. Boudet. Performance of an airplane having a horizontal control surface located in front as a stabilizer. Les Ailes, July 7, 1938, page 12, 1 illus.

Technical Notes. New Gerin monoplane prototype recently designed has a very thin triangular wing, the lifting surface of which will be variable from 3.6 to 15 square meters in a ratio of 1 to 4.2. Mechanism has been very much simplified. A 140-hp. engine will be used to power the airplane.

Two prototypes, the Latécoère 690 and the S.E. 200 of 60 tons, have finally been passed. Latter has been modified to make its performance similar to that of the Latè 690 and will have a P-18 engine of 1700 hp. Brief references. Les Ailes, July 7, 1938, page 7.

Villacoublay—1938. Potez 63 twin-motored three-seater fighter (two 670-hp. Hispano engines, top speed 295 m.p.h.) is armed with two 0.75-in. guns in front and a machine gun in the rear, and has nearly the same performance as the best single-seater fighter. Bréguet 690 three-seater twin-motored fighter (two 1100-hp. Hispanos) is bigger but probably not quite so fast. Morane 406 single-seater fighter (860-hp. Hispano engine) has two machine guns and a 0.75-in. gun all firing forward. Bloch 150 single-seater fighter (945-hp. Gnôme Rhône engine) looks nearly as fast as the Morane 406, is much quieter, and has a very low landing speed. Amiot 340-370 midwing medium bomber (two 1000-hp. Gnôme Rhône engines) and LeO-45 low-wing bomber (two 1078-hp. Hispano engines), both have top speeds of 300–310 m.p.h. Brief comments on these airplanes exhibited at the Fête de l'Air in which nine Hawker Hurricanes and three Gloster Gladiators of the Royal Air Force also took part. Aerobatic flight of the French flying school is described. Aeroplane, July 20, 1938, pages 79–80, 4 illus.

GERMANY

Heinkel 112 pursuit is announced as reaching 480 km./hr. with a Junkers Jumo 210 Ea-660-hp. engine. In reality the airplane slightly exceeded 450 km./hr., but with a reduced wing and a Daimler-Benz engine group of more than 1000 hp., it permitted Major Udet to attain 634 km./hr. over 100 km. Photograph only. Les Ailes, June 30, 1938, page 5, 1 illus.

230 Km. in a Helicopter. Focke-Wulf FW-61, equipped with a Bramo 160-hp. engine, has raised its distance record from 108 km. to 230 km. Brief reference. Les Ailes, June 30, 1938, page 6.

No Burning and Slow Landing. T. James. In an account of a visit to the Deutsche Luft Hansa maintenance depot, comments are given on the Diesel engines used in the airplanes. Diesels are in service for periods of 55 to 288 hours running. Only trouble experienced with Diesel aircraft engines comes from the fire rings or fire plates, one-piece cast-iron rings on the top of the lower pistons which close and open the exhaust ports. A few details of the Focke helicopter and a trip in the Focke-Wulf Condor are described and controls and instrument panels of the latter are illustrated. Aeroplane, July 6, 1938, pages 23–27, 7 illus.

Flight at More Than 700 Km./Hr. with 4000 Hp. New Messerschmidt bimotored fighter was recently discussed in "The Aeroplane" as being capable of attaining 715 km./hr. with two 2000-hp. engines. Messerschmidt B.f.109-C single-seater fighter, derived from the airplane holding the speed record of 610 km./hr., should attain a maximum speed of 715 km./hr. at 4000 meters. Dornier Do-17 bomber now powered with Daimler-Benz engines has exceeded 400 to 460, 470 and now 535 km./hr. with a useful load of 900 kg. Few details from various sources. Les Ailes, June 30, 1938, page 6.

The Focke Helicopter. H. Focke. Fundamental considerations which guided the designer in his work, and preliminary work and experiments leading to the final success. Translation from Luftwissen, February, pages 33–39. Journal Royal Aeronautical Soc., July, 1938, pages 577–590, 12 illus.

New Military Aircraft. Arado Ar.95-See catapultable two- or three-seater multipurpose seaplane (B.M.W. 132 Dc 880-hp. 9-cylinder aircooled radial engine, top speed 310 km.–hr. at 3000 meters) carries one torpedo of 800 kg. or 500 kg. bombs. Arado Ar.95-Land catapultable two- or three-seater multipurpose airplane for aircraft carriers (B.M.W. 132 Dc 880-hp. engine, top speed 328 km./hr.). Junkers Ju-87 two-seater dive fighter for ground attack (liquid-cooled engine of 680 to 950 hp.). Construction and armament of all three and performance and characteristics of the two Arado aircraft. Luftwehr, June, 1938, pages 250–252, 5 illus., 2 tables.

Hamburg Ha-142 airplane is being constructed by Blohm and Voss. It is derived from the Hamburg Ha-139 seaplane but is equipped with four gasoline engines instead of Diesels. Brief reference. Les Ailes, June 9, 1938, page 6.

Germany's Big Bombers. "Germany has not given up the big four-motor bomber entirely, perhaps because the smaller two-motor bomber cannot yet be made to carry the load required for the range needed at the speed wanted." Details are given for the following: Junkers Ju.89 bombers (four 640-hp. Jumo 210 12-cylinder inverted-vee liquid-cooled engines, estimated top speed 225 m.p.h., load 16,500 lb., outward bombing range 950 miles against a 37-m.p.h. headwind with 2205-lb. bomb load) in quantity production for the Luftwaffe; Dornier Do.19 bomber (four 715-hp. Bramo 322H-2 radials, maximum speed about 236 m.p.h., similar ranges and bomb load) believed to be in quantity production; Focke-Wulf Condor (four 750-hp. B.M.W. 132G engines) showed how quietly and quickly these four-motored craft can fly. Short note. Aeroplane, June 29, 1938, page 815.

Junkers Bomber in South Africa. Junkers Ju. 86K bomber (two B.M.W. Hornet engines) recently delivered to South Africa for demonstration purposes, made the outward trip in 31 hours 34 minutes at an average speed of over 200 m.p.h., thereby setting up a new record between Central Europe and South Africa. Brief reference. Flight, June 16, 1938, page 592.

GREAT BRITAIN

All Is Not Wheel. Close-up, with part of fairing removed, of the Westland Lysander's undercarriage having a Dunlop-tired Dowty internally-sprung wheel, a concealed machine gun and Harley landing light. Photograph only. Flight, June 16, 1938, page 604, 1 illus.

Fairey Fantome at Martlesham. Fairey Fantome single-seater fighter biplane with a Hispano-Suiza 12 Ycrs liquid-cooled engine is now at Martlesham for armament experiments. Speed should be around 270 m.p.h. Armament normally comprises a shell gun firing through the propeller boss and four Browning guns. Brief reference. Flight, June 30, 1938, page 638.

An Imperial Albatross. Successful test flights have been carried out on the Frobisher, first of five DeHavilland Albatross high-speed transports which will transport 22 passengers and crew of four at 210 m.p.h. at 10,000 ft. using 1320 hp. (four Gipsy Twelve engines giving 525 hp. for take-off). Brief reference. Aeroplane, June 29, 1938, page 820.

Photographs, one pointing out curious wing-fuselage fillets. Aeroplane, June 22, 1938, pages 766–767, 769, 3 illus.

The Miles Monarch. Monarch two- or three-seater enclosed-cabin low-wing cantilever monoplane (130-hp. Gipsy Major I 4-cylinder inline engine, maximum speed 145 m.p.h., cruising speed 130 m.p.h.). Glide Control is an arrangement of flaps so that glide is completely controlled at all times. Split trailing-edge flaps are in five portions extending all the way under the fuselage from aileron to aileron and worked from a Theed vacuum ram. Some parts are interchangeable with those of other Miles types. Long detailed description with drawing of the Glide Control. A second article describes flight performance. Aeroplane, June 22, 1938, pages 779–782, 5 illus.

Long description with drawings of layout of controls, operation of the interconnection and gate arrangement of throttle and flap controls, and Mentor-type magnesium-alloy tail wheel. Flight, June 23, 1938, pages 612a–612d, 7 illus., 1 table.

Modern Trainer. Airspeed Oxford twin-engined trainer (two Armstrong-Siddeley Cheetah X 350-hp. engines, top speed 192 m.p.h. at 8000 ft.) for flying instruction in piloting high-speed first-line military aircraft, and in navigation, night flying, radio, direction finding, gunnery, and vertical photography. Large number are to be produced at the Airspeed Portsmouth plant, and at the DeHavilland and Percival plants. Long description of design, flying qualities, pilot's cockpit and controls, equipment and methods of construction and construction equipment used. Table shows performance and the navigation, bombing, and gunnery loads. Flight, June 30, 1938, pages 628–632, 8 illus., 1 table.

Our Fastest Fighter in Production: The Vickers-Supermarine Spitfire. Spitfire fighter (Rolls-Royce 1050-hp. Merlin) developed from the design of the Supermarine racing seaplanes which won the Schneider Trophy. Photographs of the airplane taken during flight tests. Attention is called to the ducted radiators situated beneath the wing. Flight, June 30, 1938, pages 636, 636a–636b, 5 illus.

Perseus for the Burnelli. Two Bristol Perseus XIVC sleeve-valve aircooled engines (similar to the XIIC except for gear ratio) are specified for the Burnelli transport which should be flying in a few weeks. Brief reference. Flight, June 30, 1938, page 640.

Handley Page Hampden Bomber. All-metal day and night fighting bomber has a maximum speed comparable with that of the fighting machines now in service. Special tapered form of wings are fitted with the atest form of Handley Page slot. Wing-tip slots give complete lateral stability and immunity from spin when flying near stalling condition. While dimensions are only half those of the Harrow bomber, the Hampden is capable of carrying a bigger load over a longer distance at much higher speed. Few details only. Engineering, July 1, 1938, pages 7–8, 1 illus.

New slotted and flapped Handley-Page Hampden (two 1050-hp. Pegasus engines), newest bomber to go into the Service. "The downstairs gun position under the stern of the body is notable." Photographs also of the production version of the Hampden pointing out the clean lines of the gun station in the nose and above the wings as well as the slots and flaps as noteworthy. Aeroplane, June 8, 1938, pages 706–707 716, 5 illus.

Account of the baptism and photographs. Aeroplane, June 29, 1938, page 816, 2 illus.

The New Autogiro. Successful trial flights of the latest Cierva Autogiro have been made. The Cierva C.40 is a two-seater semi-enclosed model with a 203-hp. Salmson 9.ND 9-cylinder radial engine. Direct take-off is a marked improvement on earlier gyroplanes. Five have been ordered by the Air Ministry for Army Cooperation duties. Brief reference. Aeroplane, July 6, 1938, page 34.

The Long Range Flight. Nonstop flight of 4300 miles made by a formation of four Vickers Wellesley monoplanes (Bristol Pegasus XXII 1010-hp. engine) of the R.A.F. Long-Range Development Unit, between Cramwell and Ismailia, Egypt. Average ground speed was 135 m.p.h. and flight was made at an average altitude of 10,000 ft. Engine, long-chord cowling and bulges behind the engine differ from those of the standard Wellesley. Short note and photograph.

A second note describes engine and its cooling. Aeroplane, July 13, 1938, pages 49 and 66, 1 illus.

HOLLAND

New Military Aircraft. Fokker T.5 5-seater heavy bomber (two aircooled engines from 800 to 1000 hp., top speed with two Gnôme Rhône 14 N.1 engines 445 km./hr.). Construction, armament, bomb load and characteristics and performance are given for the bomber when powered by two Gnôme Rhône, 14 N.1, two Bristol Pegasus XXVI, and two Armstrong-Siddeley Tiger VIII engines, respectively.

Fokker G-1 two- or three-seater multipurpose airplane. New characteristics and performances are given for the airplane equipped with two Bristol Mercury VIII 830-hp. engines, with two Hispano-Suiza 14 AB.02 750-hp. engines, and with two Pratt & Whitney Twin Wasp, Jr. engines, respectively, both when the airplane is equipped as a multipurpose airplane and when it is fitted out as a light bomber. Two photographs are given of the Fokker C.10 single-seater fighter, reconnaissance and light day bomber, and of the Fokker T.8-W. torpedo, bomber and scout twin-float seaplane. Luftwehr, June, 1938, pages 254–256, 5 illus., many tables.

Really Running. Koolhoven 55 single-seater fighter (one Lorraine engine driving two propellers in opposite directions). Photographs only. Aeroplane, July 13, 1938, page 43, 2 illus.

The Twin-Screw Koolhoven. Koolhoven FK-55 single-seater fighter (special Lorraine Petrel vee-twelve mounted in the fuselage and driving coaxial propellers in opposite directions) has made its first taxying tests. Machine is now a high-wing monoplane and has ailerons instead of "spoilers" for lateral control. Brief reference. Flight, June 16, 1938, page 592.

ITALY

A Fast Foreign Bomber. Breda 88 two-engined high-speed attack bomber (two 1000-hp. Piaggio radial engines). Handley-Page slots and slotted flaps are used to give stability at slow speeds and what is claimed to be one of the greatest speed ranges yet achieved by an airplane. Maximum speed without military load must be about 350 m.p.h. which makes it about as fast as any bomber in the world today, and stalling speed must be about 81 m.p.h. Normal bomb load is about 2205 lb. for 1000-mile range. Short description. Aeroplane, June 29, 1938, page 826, 1 illus.

Few details. Flight, June 16, 1938, page 602.

Fiat Fighter-Bomber. Small series of twin-engined fighter-bomber-attack airplanes going through the Fiat shops, are about the size of a Blenheim but of low-wing design fitted with two-row Fiat A.74 840-hp. radials. Armament is variable but for ground attack there are four fixed guns in the nose and fifth firing through a trap in the floor. Internal stowage is provided for perhaps 1000 lb. of bombs. Top speed is said to be 280 m.p.h. Brief reference. Flight, June 16, 1938, page 592a.

A Fast Freighter. Sabena's new Savoia-Marchetti S.M. 83 transport (three Wright Cyclones) carries $1^1/_2$ tons of payload for 1200 miles and $2^1/_2$ tons for 200 miles. Photograph only. Aeroplane, June 29, 1938, page 817, 1 illus.

Savoia-Marchetti S.83 transport has a top speed of 268 m.p.h. Photograph only. Flight, June 23, 1938, page 612, 1 illus.

Italian Airplane with Tricycle Landing Gear. S.A.I.M.A.N. LB-2 small two seater sport airplane having tricycle landing gear and powered by an Alfa-Romeo 110-hp. engine driving a pusher propeller. Top speed 215 km./hr. Short description. Les Ailes, June 30, 1938, page 12, 1 illus.

When Fiats Go Forth. Flt. Lt. R. C. Preston. Fiat BR-20 bombers (two 1000-hp. Fiat A.80 RC engines, top speed 260 m.p.h.) are being turned out at the rate of about 20 per month, and the Fiat CR-32 single-seater combat airplanes (600-hp. V-type A.30R engines) at the rate of 45 per month. Latter airplanes are being sent to Spain. Short description of these airplanes, and a few comments on the engine altitude test chamber, and other points of interest observed on a trip through the plant. Aeroplane, July 6, 1938, pages 37–38, 4 illus.

POLAND

P.Z.L. 37 Bimotored Bomber. P.Z.L.37 all-metal four-seater medium bomber (two Bristol Pegasus XII or XX, or Gnôme Rhône 14N-25 engines) is armed with three machine guns and carries a load of bombs located entirely within the wing. Powered with two Gnôme Rhône 14 N.25 900-hp. engines the airplane has a speed of 460 km./hr. at 4600 meters and range with full bomb load (2200 kg.) of 1600 km. Long description, bomb loads and performances with three different types of engines. Rev. de l'Armee de l'Air, June, 1938, pages 704–710, 4 illus., 2 tables.

Very long description. Aircraft Engineering, July, 1938, pages 225–226, 3 illus., 1 table.

U. S. A.

A Curtiss Fighter. Curtiss XP-37 single-seater "fighter" has, according to report, a top speed of 355 m.p.h. and cruises at 325 m.p.h. for 621 miles. "Armament is two fixed machine-guns which fire through the airscrew disc. There is provision for a 37-mm. cannon to fire through the airscrew shaft." Brief reference. Aeroplane, July 20, 1938, page 86.

Very long description. Les Ailes, July 7, 1938, page 9, 2 illus., 1 table.

Becoming Acquainted with the D.C.4. Earl of Cottenham. Eight-page description from the British point of view of the Douglas D.C.4, tests during construction, test flights, and the author's opinion of the behavior of the D.C. 4 in the air. Test equipment in the D.C.4 for the flight test and weight of each part are listed, and performance and characteristics of the Douglas, Armstrong Whitworth Ensign, Boeing 314, Junkers Ju-90 and Short Empire boat are compared. Aeroplane, July 13, 1938, pages 53–60, 11 illus., 2 tables.

New Military Aircraft. Martin 166 heavy bomber. Construction, armament, characteristics, and performance. Luftwehr, June, 1938, pages 256–257, 2 illus.

330-Hp. Beechcraft F17D. Beechcraft biplane for sportsman pilots has ailerons on upper panels and flaps on the lower. Jacobs L-6 330-hp. engine, cruising speed 177 m.p.h., service ceiling 18,000 ft. Brief description. Aero Digest, July, 1938, page 81, 1 illus., 1 table. Aviation, July, 1938, page 39, 1 illus., 1 table. Western Flying, July, 1938, page 38.

Airplane Made from Plastic-Bonded Plywood. Airplane whose fuselage is made from two premolded pieces of plywood bonded by a synthetic resin developed in Germany has been built by the Clark Aircraft Corporation. An airplane of similar construction is being tested by the Materiel Division of the Air Corps. Brief note. Science News Letter, July 2, 1938, page 8.

The Boeing 314 and Douglas DC-4 Transports. Frank E. Samuels. Twin rudders instead of the single rudder used during initial tests and slight modification of the angle and span of the hydrostabilizers are being incorporated in the Boeing 314 74-passenger flying boat as test program proceeds. Few details of flight test of the flying boat as well as details of the Douglas DC-4 42-passenger land plane recently tested. Aero Digest. July, 1938, pages 42–43, 6 illus.

Long description of both aircraft, test flights, characteristics and performance. Aviation, July, 1938, pages 20–21, 30–33, 13 illus., 2 tables.

Curtiss-Wright Develops Craft. Twin-engined 30-passenger pressure-cabin plane being built by the St. Louis Division for 20,000-ft. altitude performance will be powered by two Wright 1500-hp. engines. Brief reference. Western Flying, July, 1938, page 40.

Menasco-Powered Spencer-Larsen Amphibion. Model SL-12C all-wood two-seater amphibion is designed for sportsmen pilots, commercial training and general utility purposes and has a pusher propeller and retractable tricycle landing gear. Menasco C4 inverted inline 125-hp. engine is mounted in the hull and may be tilted up approximately 90° for servicing. Kirkham gear transmission unit contains two vertical shafts encased in a streamlined aluminum-alloy casting. Long description but no performances. Aero Digest, July, 1938, page 78, 2 illus., 1 table. Aviation, July, 1938, pages 35–36, 7 illus., 3 tables.

A New Little Douglas. Douglas DC-5 14-passenger airplane (Wright G-100 1000-hp. engines) is said to be going to fly shortly. It is similar to the DC-3. Brief reference. Aeroplane, June 29, 1938, page 815. Flight, June 23, 1938, page 612.

Retractable Wing Built. Single-seater midwing airplane designed by C. Ellingston incorporates both a retractable wing and retractable landing gear. Outer wing sections can be telescoped in the air, retracting approximately one-third of their span. LeBlond 90-hp. engine, crusing speed 130 (extended) and 175 m.p.h. (retracted). Short description. Western Flying, July, 1938, page 38, 2 illus.

Today's Design, Tomorrow's Airplane—100 Passengers, 300 Miles Per Hour. Artist's conception of proposals submitted to Pan American Airways for a huge transoceanic aircraft, including the Consolidated four-engined, Boeing and Sikorsky flying boats, and the Douglas landplane. Drawings only of exterior and interior views. Western Flying, July, 1938, pages 12–13, 12 illus.

Two-Place Grumman "Gulfhawk." Grumman G-32 "Gulfhawk III" two-seater airplane delivered to the Gulf Oil Corporation is basically similar to the Navy's shipboard fighters. Wright Cyclone 1000-hp. engine. maximum speed 280 m.p.h. at 7000 ft., cruising speed 210 m.p.h., cruising range 700 miles, and service ceiling 32,000 ft. Short description. Aero Digest, July, 1938, page 81, 2 illus.

Air Transportation

Foreign News in Brief. France has obtained temporary authority to use the Botwood, Newfoundland, base and refueling facilities to test the feasibility of a transatlantic service. A large land plane and a seaplane will be used. A second brief reference refers to the rights obtained from Portugal for use of the Azores as a seaplane base. Aero Digest. July, 1938, page 38.

France's Atlantic Plans. Leaving on August 10 the Latécoère flying boat, Lieutenant-de Vaisseau Paris, will make the first of a series of three double crossings of the Atlantic by way of the Azores and Bermuda. When the new Farmans with airtight cabins are ready the company will start operations over the northern route to Newfoundland. Brief note. Flight. June 23, 1938, page 612.

Norwegian Interlude. Account of a flight, across the North Sea on an Allied Airways airplane, work of the D.N.L. airline, and Norway's new civil airports. Flight, June 16, 1938, pages 592b–592d, 7 illus.

Airships

Directional Stability of an Airship in Level Flight. W. Bader. New airships have no positive directional stability as a result of structural limitations of the rudder unit which are increased by use of helium. Dynamic behavior of an airship in level flight is investigated for the purpose of dimensioning the rudder unit. Equations of motion are compiled and time factors of dynamic equilibrium conditions determined. Divisions of the stability equation formulated allows the mechanical significance of the separate roots to be recognized and emphasizes the value of static directional stability. Luftfahrtforschung, June 6, 1938, pages 275–282, 4 illus., 2 tables, many equations.

There is Helium in France. G. Houard. There is said to be enough helium in France to place it in a better position than the United States to produce this gas. Short note. Les Ailes, June 30, 1938, page 8.

Propellers

Aerodynamic Considerations Affecting Propellers for Large Engines. G. W. Brady. Paper and discussion by T. P. Wright who stressed the need for shank fairing. S.A.E. Jour., July, 1938, pages 293–300, 10 illus.

Propeller Factors Tending to Limit Aircraft-Engine Powers. G. T. Lampton. Paper and discussion by T. P. Wright who stressed the necessity for propeller weight reduction. S.A.E. Jour., July, 1938, pages 289–292, 10 illus.

Propeller Problems Imposed by Substratosphere Flight Requirements. C. F. Baker, S.A.E. Jour., July, 1938, pages 285–288, 300, 6 illus., 3 tables.

Hamilton Standard Hydromatic Propeller. F. W. Caldwell. Hydromatic propeller developed to meet requirements for greater pitch-angle range during normal operation and for full feathering in emergencies. Engine oil which has been boosted to higher pressure by the constant-speed governor pump is used to overcome the centrifugal twisting moment when it is necessary to increase pitch. Adjustment toward low pitch is also accomplished by oil pressure supplementing and augmenting the centrifugal force on the blades. An auxiliary pressure supply system is put in operation when it is desired to feather the blades. Long description. Aviation, July, 1938, pages 28–29, 76, 4 illus.

Similar long description. Aero Digest, July, 1938, pages 69–70, 114, 4 illus.

Short description. U.S. Air Services, July, 1938, page 27, 1 illus. Aeroplane, July 6, 1938, page 28, 2 illus.

One Blade—Twice. Test of Everel single-blade propellers fitted to the two 40-hp. Continental engines on the Hordern Richmond Autoplane. Tests were made to determine if there would be any difficulty in effecting synchronization on the two motors since the Everel is, in effect, an automatically variable-pitch design and has approximate constant-speed characteristics. Flight Lieutenant Hordern reported that there was absolutely no difficulty in effecting correct synchronization. In fact he found it easier than with normal fixed-pitch propellers. Short note. Flight, June, 16, 1938, page 602. Aeroplane, July 6, 1938, page 34.

Miscellaneous

Aircraft Manufacture and Research in Finland. E. Wegelius. Development of the aircraft industry in Finland, and research on wood and metal construction. A second article describes the Air Show in Finland. Luftwissen, June, 1938, pages 193–196, 7 illus.

Aircraft Instruments and Navigation

Astronomical Navigation. Sqn. Ldr. E. H. D. Spence. Further simple explanations for the student. Right ascension method is worked out, the equation of time explained, and use of the "Air Almanac" and book of Nautical Tables described with examples. Concluded. Flight, June 16, 1938, pages 596–597, 10 illus.

Flying Classroom. Interior of a D.H.86B, two of which have been specially equipped for instructing Cramwell cadets in aircraft radio operation (including D/F) and working of the automatic pilot. Photograph only. Flight, June 23, 1938, page 610, 1 illus.

The French Air Service Discards the "Cheval." New units are used on all new aircraft instruments. Scales of manifold pressure gages are divided into piezes and those of oil-pressure gages into heptopiezes. Power of aircraft engines will no longer be expressed in horsepowers of 75 kilogrammeters per second, the new unit being the kilowatt. French official horsepower differed considerably from the British unit. Pressures are to be expressed in pieze and heptopieze and forces in sthenes instead of kilograms. Brief note from La Technique Moderne, June 1. Automotive Industries, July 2, 1938, page 7.

Kollsman Improves Altimeter. Side-window barometric scale is a feature of the Kollsman sensitive altimeter. Few details. Western Flying, July, 1938, page 38.

Position Finder. Stark's position finder, announced by Air-Track, consists of a circular frame containing three movable discs, the uppermost carrying a removable map. Pilot tunes in a range or broadcast station on his direction finder and transfers the compass bearing of that station to the position finder by lining up one disc bearing parallel lines. A bearing from another station is transferred to the other movable disc of the position finder. Where lines intersect is exact position of the airplane. Few details. Western Flying, July, 1938, pages 38, 40.

Torque Indicators for Aircraft Engines. Flight tests have been made with the Poincare-Farman torque indicator on a Potez 25 with Farman engine and on a Potez 541 with the Gnôme Rhône 14K engine. Mention is made of the Farman torque indicator, the A.C.O.M.E. indicator (based on the change of magnetic permeability of a steel shaft when subjected to stress), other investigations, and to the DVL torque indicator. Short note from "La Technique Moderne" June 15. Automotive Industries, July 9, 1938, pages 45–46.

Flight Impact Pressure Calibration by Means of Total-Pressure Apparatus and a Static Sounder Trailing under the Airplane. G. Kiel. Simple method for calibration of airplane impact pressure based on Bernoulli's law. Measuring apparatus required is described and method of carrying out the impact pressure calibration is explained. It is shown how the accuracy of the impact pressure calibration can be estimated in a simple manner. Luftwissen, June, 1938, pages 219–223, 9 illus., 5 equations.

Round-the-World Flight Gave Test to Navigation Robot. Operation of the Army Air Corps' new aerial navigation mechanism invented by W. L. Maxson and used by Lt. T. Thurlow on Hughes' flight around the world. Science News Letter, July 23, 1938, pages 52–53, 2 illus.

Miscellaneous Equipment

15 Ton Beaching Gear. Kenilworth beaching gear developed for the Boeing 314 Clippers. Few details. Aviation, July, 1938, pages 44, 47, 1 illus.

Bearings

Silver Bearings for Aero Engines. Best results are obtained with the purest silver, and alloying with another metal merely results in inferior antifrictional qualities. Silver is a very effective alloy hardener of the solution-forming type, and certain alloys, in addition, have interesting age-hardening properties. Brief abstract from Progress Report of the American Silver Producers' Research, reported by the Journal of the Franklin Institute. Metal Industry, July 1, 1938, page 10.

Film Lubrication of Finite Curved Surfaces. S. M. Skinner. Statements of Boswall and apparent belief of many engineers notwithstanding, it is shown that computable solutions to Reynolds' three-dimensional equation are possible in many cases, and several such solutions are given which seem particularly useful for studies in bearing design and lubricants. Equations cover: curvature only in direction of motion and curvature both normal to and in the direction of motion, motion in an arbitrary direction with respect to sides of the plate, and sector shaped surfaces in rotation. Michell thrust bearing and the journal bearing also discussed. Jour. Applied Physics, June, 1938, pages 409–421, 2 illus., 2 tables, 46 equations.

The Graphoid Layer on Bearing Surfaces. G. I. Finch and E. J. Whitmore. Graphite is actually absorbed into the amorphous surface layer of the metal formed during running in with an oil containing colloidal graphite. Experiments described were carried out on a wear-testing machine, corresponding surface changes being followed by means of the electron-diffraction camera. Mild steel, lead, copper, and two widely differing white metals were tested. Electron diffraction patterns are illustrated. Engineering, July 22, 1938, page 91, 8 illus.

The National Physical Laboratory. Research in the Engineering Department. Tests of non-metallic bearings; four-ball top for testing qualities of extreme-pressure and low-pressure lubricants; tests of seizure characteristics showing superiority of extreme-pressure lubricants over oils containing zinc oxide or castor oil or even mineral oils; and tests on the behavior of driving belts. Engineering, July 22, 1938, pages 107–108, 4 illus.

The Theory of the Thick Film Lubrication of a Complete Journal Bearing of Finite Length. M. Muskat and F. Morgan. Successive approximation theory is developed for the hydrodynamics of journal bearing systems of finite length, the expansion parameter being the journal eccentricity, and is applied to full journal bearings of lengths exceeding bearing parameter. Existence of lubricant source and associated end leakage is taken into account. General formulas are also developed for asymptotic behavior of friction coefficients on both journal and bearing at very low eccentricities or large values of the Sommerfeld variable. Jour. Applied Physics, June, 1938, pages 393–409, 5 illus., 40 equations.

Fuels and Lubricants

Composition of Lubricating Oil. F. L. Carnahan. Composition of Pennsylvania and other oils studied at Pennsylvania State College. Properties of cuts of a Pennsylvania and a commercial oil in vacuum fractionation; molecular types in various oils; classification of oils; reflux extraction of a Pennsylvania neutral and a Mid-Continent neutral; and high viscosity index constituents in oils. Pennsylvania Grade Crude Oil Association paper. Oil & Gas Jour., June 30, 1938, pages 66, 68–70, 6 tables.

Theory of the Viscosity of Unimolecular Films. W. J. Moore, Jr., and H. Eyring. Equation for fluidity of a liquid based on the reaction rate theory of viscous flow is modified to interpret the viscosity data for liquid films. Equations are given for pressure and temperature effect on surface viscosity. Knowledge of these effects may be used to interpret structure of films and to separate and evaluate contributions to the free energy of activation due to lateral association, solvation and hydrogen bonds. Jour. Chemical Physics, July, 1938, pages 391–394.

Viscosity of Hydrocarbon Solutions. B. H. Sage and W. N. Lacey. Effect of pressure on the viscosity of liquid and gaseous propane was determined at five temperatures between 100° and 220°F. Measurements throughout the superheated gas region and the condensed liquid region at pressures up to 2000 lb. per sq. in. were included. Part of research being conducted by Research Project 37 of the American Petroleum Institute. Industrial and Engineering Chemistry, Ind. Ed., July, 1938, pages 832–834, 6 illus., 1 table.

Metals

Metals in the Aircraft Industry. J. R. Goldstein. Steel alone accounts for about 17½ percent of the structural weight of the empty Douglas DC-3. Chrome-moly and stainless steel, nickel steel and nickel alloys, and aluminum and magnesium alloys used in aircraft are discussed. Applications of extruded shapes and castings of aluminum alloys, and die castings for small parts are described. Metal parts of the Douglas DC-4 are illustrated. Long abstract of Western Metals Congress paper. Aero Digest, July, 1938, pages 46–47, 50, 6 illus.

The National Physical Laboratory. Research on properties of engineering materials carried on in the Engineering Department, some of it at request of the British Air Ministry. Mechanism of deformation and fracture in metals by means of X-ray; behavior of materials under combined bending and torsional stresses; fatigue strength of steel strip with special reference to influence of various types of commercial surface finish (for the Air Ministry); frettage or fretting corrosion; effect of mean stress of the cycle on resistance of metals to corrosion fatigue (six metals used in aircraft construction for which resistance to cycles of reversed direct stress, in air and in corrosive environment were tested, including carbon-steel, chrome and chrome-nickel steel, duralumin and magnesium alloy); welded pressure vessels; and lubrication. Engineering, July 15, 1938, pages 62–65, 8 illus.

Résumés of Recent Research. Recent experiments on the variation of electron mass with velocity; ideas concerning field and motion; and studies of the magnetic structure of cobalt. Short notes. Jour. Applied Physics, June, 1938, pages 352–353, 2 illus.

Present Status and Future Potentialities of Die Casting. T. Lynn. Die-casting process, and applications of aluminum, magnesium and brass die castings in aircraft construction. Comparative tables giving alloy number, composition and physical properties of these alloys were jointly prepared by the Harvill Company and Aircraft Accessories Corporation. General characteristics, die requirements, and production costs also considered. Aero Digest, July, 1938, pages 54, 57, 58, 5 illus., 3 tables.

Effect of Copper on Some Alloy Steels. R. Harrison. Preliminary survey of the possibility of utilizing the temper-hardening effect of copper in steels containing other alloy elements, to develop a steel of high yield strength. Copper may prove a useful alloy element in steels used in the oil-quenched and tempered condition, and the mechanical properties after these treatments were also examined. British Iron and Steel Institute paper. Heat Treating & Forging, June, 1938, pages 286–292, 8 illus., 2 tables.

Nonferrous Alloys

Age Hardening Mechanism. Structural changes in copper-aluminum alloys in the earlier stages of aging, as found by Wassermann and Hartnagel. Short discussion of articles in Z. Metallkunde, 1938, 30, 62. Metal Industry, July 15, 1938, page 66.

New Investigations on the Aluminum-Silicon Alloy, Silumin-Gamma, with Reference to Requirements for Aircraft-Engine Construction. P. Koetzschke. Influence of copper additions up to 2.5 per cent on strength properties of eutectic Silumin Gamma. Original expectations of attaining, or exceeding, by low copper additions to Silumin Gamma alloy, the heat resistance properties of aluminum-copper-nickel alloys (such as used for cylinder heads of aircooled aircraft engines), have not been fulfilled in extended laboratory tests. Good casting properties of eutectic Silumin Gamma can largely be lost by copper addition. Application of eutectic Silumin Gamma alloy with or without high thermal load, as in cylinder heads, cannot be recommended. These laboratory investigations as well as results of tests on crankcases of eutectic Silumin-Gamma alloy having manganese and cobalt additions are described. The lower eutectic Silumin Gamma alloy had approximately 1 kg./mm.² greater alternating bending resistance than the alloy with the eutectic composition. Luftwissen, June, 1938, pages 205–211, 12 illus., 6 tables.

Aluminum Casting Alloys. G. Guertler. Problems of foundry and metallurgical practice. First issue—Gases in aluminum; laboratory experiment; supersonic vibrations for effective liberation of gas; changes occurring in a sand mold; experimental apparatus designed to provide a picture of what was taking place in the mold; and effect of rapid cooling.

Second issue—Influence of titanium, and age hardening by Mg_2Si and by $MgZn_2$. Variation of fatigue strength of Alpax-Gamma containing

12 percent and 6 percent Si with Ti content, static and dynamic property variations, and various structures of Alpax-Gamma are illustrated. Institute of British Foundrymen paper. Metal Industry, June 24 and July 1, 1938, pages 656–658 and 11–13, 17 illus.

The Constitution of Magnesium Alloys. First issue—Constitution of magnesium alloys is discussed in the light of new data with particular attention to initial portions of the liquidus and solidus curves and range of magnesium-rich solid-solution field.

Second issue—Reduced solubility of the elements of Group Four B to Group Six B as attributed by Hume-Rothery and Raynor to the tendency for these elements to form stable compounds of the ionic type with magnesium, at expense of primary solid solutions. Short discussions of papers by Hume-Rothery and Raynor before the British Institute of Metals. Metal Industry, June 24 and July 1, 1938, pages 651 and 4.

Determination of Compressive Yield Point in Light Metal Profiles of Strips of the Hammer-Forged Aluminum Alloy Al-Cu-Mg. H. Moechel. Results obtained in tests are reported by the Zeppelin Airship Company, Friedrichshafen, Germany. Luftfahrtforschung, June 6, 1938, page 315, 2 illus., 5 tables.

Surface Protection of Magnesium Alloys. E. J. Pike. Nearly all the commercial protective dips in use today are based on dichromate dips evolved by Sutton and Le Brocq at the Royal Aircraft Establishment. Different methods outlined include: preparation of surface; R.A.E. long-period bath; a short-period bath; chrome pickle treatment; selenium treatment; magnesium sulphate-bichromate bath; nickel sulphate-bichromate bath developed at High Duty Alloys, Ltd.; anodic treatments developed by Buzzard and Wilson and several under development in Germany; and recommended methods for treatment of parts to be painted. Flight, Aircraft Engineer, Sup., June 30, 1938, pages 43–44.

Miscellaneous Materials

Applications and Testing of Transparent Materials Used in Aircraft Construction. K. Riechers and J. Olms. Heat treatment of single-layer safety glass (hard glass) so that on shattering the splinters would adhere together and not fly around; multi-layer safety glass consisting of two glass plates combined by a transparent elastic intermediate layer consisting of safety glass; combination of glass and synthetic-resin substance; celluloid, cellulose acetate, mixed polymerized and poly-acrylic-acid-ester transparent synthetic-resin materials; processes for these materials; and methods of testing window materials.

Second article gives a German translation of "The Study of Transparent Plastics for Use on Aircraft," B. M. Axilrod and G. M. Kline, Bureau of Standards. Luftwissen, June, 1938, pages 197–202, 10 illus., 3 tables, and pages 202–204, 3 illus.

Fiber Glass. J. H. Plummer. Mechanical development of fiber glass. This is a mineral fiber resistant to all acids except hydrofluoric and capable of standing much higher temperatures than any other textile fiber. It will not mildew, rot or support combustion. Industrial and Engineering Chemistry, Ind. Ed., July, 1938, pages 726–729, 7 illus.

Improvements in Plywood. Bakelite Plybond takes the form of a thin sheet of paper specially impregnated with Bakelite resinoid which possesses the property of first becoming fluid under influence of heat and then re-hardening to an infusible and insoluble state when heating is continued. Various plies are interweaved with Plybond and the whole is formed into a homogeneous board in a heated press. Sheet is water- and steam-resistant and resistant to insects and fungus. Short note. Aeroplane, July 6, 1938, page 34.

Wood as a Homogeneous Material. O. Kraemer. Conditions to be satisfied by wood glues and synthetic-resin glues; hot gluing process, including technique of applying both types of glues, and strength properties obtained; cold gluing with "Kaurit," its strength properties compared with ordinary glues, applications of synthetic-resin gluing, and water- and fungus-resisting glue obtained with mixture of "Kaurit" and blood albumin; and example in which shaping of wooden parts is carried out at same time as gluing process. Concluded. Aircraft Engineering. June, 1938, pages 183–186, 14 illus., 2 tables.

Meteorology

Comparisons of Soundings with Radio-Meteorographs, Aerographs and Meteorographs. H. Diamond, W. S. Hinman, Jr., and E. G. Lapham. Because of possible lack of lateral homogeneity of an air mass, comparison soundings using two instruments on the same balloon give more reliable results than comparisons of a balloon instrument with aerograph. Results compared, accuracy of the radio-meteorograph observations estimated, and method of radio meteorography reviewed. Am. Meteorological Soc., Bulletin, April, 1938, pages 129–141, 10 illus., 1 table.

Hurricanes, Their Nature and History. I. R. Tannehill. Review of book by Chief of the Marine Division of the United States Weather Bureau. Also bibliography of books most likely to be of use to Weather Bureau officials in their meteorological work and studies also given. Monthly Weather Rev., March, 1938, pages 73–74.

On the Thermodynamic Interpretation of Isentropic Charts. H. R. Byers. Advantages of the thermodynamic isentropic chart over the chart based on elevations and specific humidities; construction of the atmospheric cross sections; and the moist-adiabatic process. Monthly Weather Rev., March, 1938, pages 63–68, 4 illus., 15 equations.

Problems Connected with the Condensation and Precipitation Processes in the Atmosphere. H. G. Houghton. Most important causes for appearance of cloud particles of different size at the same point seem due to presence of a number of extremely large hygroscopic nuclei of condensation, turbulent mixing within the cloud and the growth of ice crystals by sublimation at expense of coexistent supercooled liquid drops. Condensation and causes of precipitation, and stability of clouds. Present state of knowledge concerning condensation and precipitation, and problems to be studied at M.I.T. Am. Meteorological Soc., Bull., April, 1938, pages 152–159.

Relation of Pressure Tendencies to Cyclones and Fronts. W. R. Stevens. Value of the three-hour pressure tendencies in analysis as well as in prognosis is illustrated by a set of model moving Cyclones with and without frontal structures. Since pressure tendencies are composed of two parts, one due to deepening or filling and other due to movement, a good estimate of subsequent displacement of the center over a period of 12–24 hours can quickly be made. Monthly Weather Rev., March, 1938, pages 68–70, 4 illus.

Engine Design and Research

The Internal Combustion Engine. H. R. Ricardo. Advent of the internal-combustion turbine is considered not very far distant. The low-compression highly-supercharged Diesel engine and the single-piston two-cycle Diesel engine even lighter per horsepower than the gasoline engine and combining a somewhat lower specific fuel consumption are regarded as possibilities for aircraft. General discussion of recent progress in detonation, combustion in the Diesel engine, the light high-speed Diesel, aircraft engines, Diesel engines for aircraft, and steam versus internal combustion. Excerpts from paper presented before the International Engineering Congress. Engineer, June 24, 1938, pages 702–703.

Investigation of Engine Combustion by Spectroscopic Methods. E. Czerlinsky and M. Seibt. Most essential results of spectral investigations on open flames are given as a basis for the survey of the present status of research on the combustion process in Diesel and gasoline engines by the spectroscopic method. Based on a comprehensive bibliography, the research is reviewed particularly in regard to detonation phenomena. Number of spectrograms are included. Luftfahrtforschung, June 6, 1938, pages 316–320, 3 illus.

An Opinion on the Engine Crisis. M. Victor. American engines are superior in mechanical operation and the French engines are superior in aerodynamic efficiency. In their efforts to reduce the maximum cross section of their radial engines the French designers encountered the greatest difficulties, but American engineers have retained the large diameter and long connecting rods. Bore, stroke and coefficient of elongation of cylinder are compared for the Gnôme 14N, Wright Cyclone and "Twin Cyclone," Hispano 14AA, Pratt and Whitney Hornet and Twin Hornet, Hispano 14AB and Gnôme 14 Mars. Maximum diameters are compared with connecting-rod length for these engines. Discussion of difficulties of French designs, and description of Wright G-100 Cyclone. Les Ailes, June 16, 1938, page 8, 5 illus.

Diesels for Distance. With a 15-hr. flight and 3000 hp., gasoline engines would require 19,000 lb. of fuel, and Diesels 14,500 lb., resulting in a saving of 4500 lb. Brief reference to advantages of Diesel engines for transatlantic aircraft in a general talk by Lord Sempill. Automotive Industries, July 16, 1938, page 92.

Engines. Ricardo patents for reducing height of cylinder sleeve and for a two-cycle engine with double effect in which cylinder has exhaust ports for two faces of the piston and an opening to the scavenging collector. Miller 1150-hp. marine engine weighing 885 kg. (description and comparison with Rolls-Royce Merlin and Gnôme-Rhône 14M engines). Supercharging as decreasing thermal fatigue in parts of heavy-oil engines. These subjects are discussed and brief reference made to a recent article on the Clerget engine and to results reported in the United States by the "Power Plant Committee" on a two-cycle engine with gasoline injection. Les Ailes, July 7, 1938, page 7, 2 illus.

The Lightening of Fuel-Injection Engines by Supercharging. J. Jalbert. A volumetric supercharger of relatively slow operation, having two speeds and supercharging at altitudes is considered necessary for a fuel-injection engine to be used on pursuit airplanes. Conditions for adapting a supercharger to the fuel-injection engine in operation on the ground with a view to raising the mass output are considered. Volumetric ratio and pressure and temperature at the end of compression are computed for a single cylinder with fuel injection but without supercharging and for the same cylinder with supercharging, and heating of air produced by supercharging, volumetric ratio and pressure at end of compression, combustion pressure, and economic efficiency are calculated. Formulas are applied to the case of a 1000-hp. engine. A fuel-injection engine of 24 cylinders in H with 105-mm. bore and stroke giving 1000 hp. at 3750 r.p.m., supercharged at a ratio of 1.8 atmospheres for a weight of 550 kg. is predicted. L'Aéronautique, L'Aérotechnique Sup., June, 1938, pages 73–78, 8 illus., 15 equations.

Some Notes on the Results Obtained up to the Present with Heavy-Oil Engines for Aircraft. L. Keuleyan. Results obtained on single-cylinder 4- and 2-cycle Diesels by the N.A.C.A., and reported by Whitney and Foster to the S.A.E. are compared with horsepower per liter obtained by various European Diesels, including: Junkers Jumo 205D two-cycle engine; Ricardo injection-engine with "Vortex" combustion chamber; L.O.F.-6; and M.A.N.Z.129 two-cycle marine engine. References are also made to the Daimler-Benz D.V.600, Coatalan, Rolls-Royce Condor, and the Bristol Phoenix engine tested on a Westland biplane which reached an altitude of 8370 meters.

Drawings include the Ricardo, L.O.F.-6, General Motors two-cycle, and M.A.N. Difficulties with the four-cycle Diesel engine are pointed out. Author concludes with a note saying that "certain American manufacturers of gasoline aircraft engines . . . have been summoned by the Army Air Corps to discuss the construction of a heavy-oil engine. . . . It is probable that the Army Air Corps will be interested in an engine of the order of 2000 hp." L'Aéronautique, June, 1938, pages 117–120, 5 illus.

Supercharger Installations for High-Output Internal-Combustion Engines Particularly Aircraft Engines. W. von der Nuell. Status of development of aircraft-engine superchargers; flow over the vanes of r.p.m.-controlled centrifugal superchargers; supercharger control; mounting and form of rotor; examples of designs of aircraft-engine superchargers; utilization of exhaust-gas energy; and supercharging of motor-vehicle engines.

Illustrations include the DVL rotor, and superchargers for the following engines: Hispano-Suiza, Rolls-Royce, Mercedes-Benz D.B.600, Junkers Jumo 210, Wright Cyclone, Bramo, Packard Roots, Rateau supercharger for the Potez aircraft engine, Buechi, and Graham. Long article. A.T.Z., June 10, 1938, pages 282–295, 30 illus., 1 table, many equations.

Engine, Fuel and Lubricant Testing

Diesel Deposits as Influenced by Fuels and Operating Conditions. J. R. MacGregor and W. V. Hanley. S.A.E. Jour., July, 1938, pages 272–280, 19 illus., 4 tables.

Laboratory Tests of Lubricants and Their Tendency to Piston-Ring Gumming. M. Richter. Process of piston-ring gumming based on D.V.L. tests. Principal cause of gumming is the return movement of the unevaporated unburned oil residue. Aging method described permitted measurements of relative volatility and tendency towards oxidation. Simple apparatus tested weighed portion of 10 g. in air in a temperature range of from 200° to 300° and in a 4-hour test period. Laboratory values are compared with operating the time of a small Siemens test engine up to piston-ring gumming, best conformity being obtained at a test temperature of 275°. Tests and results described. Luftwissen, June, 1938, pages 213–218, 11 illus., 4 tables.

The Measurement of Mechanical Power. C. V. Drysdale. Modified form of Ford torsionmeter suitable for mounting on airplanes and developed at the Royal Aircraft Establishment. Propeller is fixed to rim of a forged steel wheel having 24 radial spring arms cut from a solid forging. Second device described is used for testing propellers and was developed by the author and completed at the Royal Aircraft Establishment. It consists of two 20-pole inductors mounted on two ends of a shaft designed to give the most accurate relations between torsion angle and torque. Alternators are

excited by magnetizing coils and micrometer-screw attachment to one stator is used for zero adjustment. Detailed description. Engineering, July 15, 1938, pages 69–71, 6 illus.

Studying Engine Combustion by Physical Methods. L. Withrow and G. M. Rassweiler. Application of spectrographic and photographic methods at the General Motors Research Laboratory to the study of combustion within the engine. High-speed cinematography; camera requirements; emission spectra obtained by mounting a spectrograph above a window in top of engine and by using a stroboscopic shutter synchronized with the engine; temperature measurements by sodium line reversal method; nature of engine knock; time-displacement photographs showing pressure waves in the inflamed charge; and absorption spectra of noninflamed portions of charge revealing distinct differences between knocking and nonknocking explosions even before spontaneous inflammation sets in. Jour. Applied Physics, June, 1938, pages 362–372, 12 illus.

New "Weather" Tunnel and Test Tracks. Huge new weather tunnel put into operation at the Ford Engineering Laboratories is equipped to produce at any time every conceivable weather condition for cold-weather tests of engine, oil, battery, and starter. Refrigeration system (500-ton), rain machine, sand and dust blower, and a cold chamber for temperatures as low as −40° F. are installed. Short description. Industrial and Engineering Chemistry, News Ed., July 10, 1938, page 377.

Unique Engine Test Stand. Aircraft-engine test stand of Northwest Air Services uses the engine being tested to move the stand. Engine is overhauled and assembled on an engine plate in the engine shop and plate is mounted on the engine stand in rubber to reduce strains or stresses. Western Flying, July, 1938, page 40, 1 illus.

Engines

Marcel Bloch Bureau of Engine Research has developed a four-cylinder inverted 95-hp. engine and a 12-cylinder inverted 12-liter engine with supercharger and reduction gear which should develop 450 hp. at 3200 r.p.m. Brief reference. Les Ailes, June 30, 1938, page 7.

A Junkers Jumo 205-C heavy-oil engine, first of a series of six bought by the French government, has successfully completed its acceptance tests at the Peugeot plant. The Junkers two-meter transmission used in the tests was similar to that of the rear motor of the Dornier 18 recently beating the world's distance record. Brief reference. Les Ailes, June 30, 1938, page 9.

The DeHavilland Gipsy Twelve Aero Engine. Another long description of the Gipsy Twelve engine (rated at 405–420 hp. at 2400 r.p.m. at 7500 ft.) with photographs of engine and parts including supercharger. Engineering, July 8, 1938, pages 48–50, 6 illus.

Experiments on the Hesselman Engine. W. Wilke. Engines are divided into five categories from the low-compression Otto engine with spark ignition to the high-compression compression-ignition Diesel using heavy fuel. Hesselman engine is in the central category with medium compression, medium fuel, spark ignition and pump injection. In the original, main characteristics of Otto and Diesel engines are compared in regard to increase of knocking in one and decrease of knocking in the other. Latest Hesselman arrangements with spark advance linked to a fuel pump for partial load operation is illustrated. Short abstract from A.T.Z., January 25, pages 25–30. Royal Aeronautical Soc., Jour., June, 1938, page 560.

Imperially Proved. Successful 200-hr. endurance test of the Armstrong-Siddeley Tiger IX 880-hp. engine for Imperial Airways. Tests results are discussed and special features of the engine, designed to eliminate wear, are described. Parts of engine and supercharger illustrated. Aeroplane, July 20, 1938, pages 85–86, 7 illus.

New Stratosphere Engine Invented in Sweden. Engine is designed for operation at altitudes ranging from 39,000 to 59,000 ft. and is expected to give the airplane an air speed of about 465 m.p.h. A 12-cylinder inverted vee operating normally at 1900 r.p.m., it is capable of developing 800 to 900 hp. Precompression problem is solved by combination of specially constructed compressors. Brief reference. Automotive Industries, July 23, 1938, page 97.

British Diesel Engines. Descriptions of British Diesels for marine and road transport services. Other articles describe European and American Diesels with tables. Foreign aircraft Diesel engines described include: Mercedes Benz, Clerget, Coatalen, Salmson-Szydlowski two-stroke and Zbrojovka two-stroke engines. Automobile Engineer, June, 1938, pages 190–240, 106 illus., many tables.

Crankless Engine. Four-cylinder crankless two-stroke liquid-cooled aircraft engine designed by H. Alfaro and built in cooperation with the Indian Motorcycle Company. Engine has double opposed pistons, fuel injection and spark ignition. (Output 115 hp. at 2000 r.p.m., weight 240 lb., diameter 15½ in.) Engine cylinders are parallel to the shaft. An eight-cylinder model could be built with closer grouping of cylinders, which would weigh 300 lb. and would deliver about 300 hp. at 2400 r.p.m. Description of 115-hp. engine and test results at M.I.T. Aviation, July, 1938, pages 39, 75. Science News Letter, July 16, 1938, page 37.

A New Aircooled Motor. DeHavilland Gipsy Twelve inverted-vee 12-cylinder 525-hp. engine was specifically designed to be cooled by air from ducts led into the back part of the engine and is said to have cleaner entry of air and cost less in power to cool than any other engine in the world. Thrust-weight ratio is another advantage. Improvements for ease of maintenance also included. Swept volume 1121.2 cu. in., net weight dry 1058 lb., take-off 505/525 hp. at 2600 r.p.m. at 3½ lb./sq. in. boost pressure, maximum power 410/425 hp. at 2450 r.p.m. at 7750 ft. at zero boost. Very long detailed description. Photograph shows the Gipsy Twelve installed in the D. H. Albatross. Aeroplane, June 22, 1938, pages 776–778, 790, 10 illus.

Detailed description with two-page cutaway drawing showing location of parts, and photographs including the supercharger impeller. Flight, June 23, 1938, pages 612e–612h, 613–615, 11 illus., 2 tables.

The Junkers Jumo 210 Inverted-Vee Engine. Twelve-cylinder liquid-cooled engine with 6.5:1 compression ratio and developing 690 hp. at sea level and 700 hp. at 5000 ft. Characteristics, drawings of engine, shafting and gear trains (with speeds of components and drives), and photographs of section of two-speed supercharger and Junkers automatic boost control. No text. Aircraft Engineering, June, 1938, pages 180–181, 5 illus.

Two Engines. Unitwin power plant in the Lockheed Altair. Two Menasco 260-hp. engines mounted side by side drive a single propeller. Photographs only of engines in the airplane. Automotive Industries, July 16, 1938, page 71, 2 illus.

The Wellesley Achievement. Bristol Pegasus XXII engines were used in the four Vickers Wellesley long-range airplanes which flew nonstop from Cranwell to Ismailia. Nose of airplane was modified to take this engine with the latest Bristol long-chord cowling, front exhaust-collector ring and controllable-gill cowlings, giving considerably less drag than ring cowlings on standard Wellesleys. Fuel consumptions were reduced below those already achieved with sleeve-valve engines. Details of engine. Short note. Aeroplane, July 15, 1938, page 66.

Parts and Accessories

Bendix Enters the Injection-Equipment Field. Scintilla fuel-injection equipment for Diesel engines includes injection pumps of the port-controlled type and spray nozzles of the differential type. Description. Automotive Industries, July 25, 1938, page 121, 2 illus.

Cutting Out Vibration. Metalastik rubber-bonded-to-metal mounting units developed for aircraft engines to prevent transfer of vibrations. Joint between rubber and metal is so strong that under tensile loads rubber will tear before the joined surfaces part. Process also applied to joinings of aluminum and rubber as well as use of synthetic rubber. Few details. Aeroplane, July 6, 1938.

The Oetiker Engine Brake. F. Weiner. Construction and action of the Oetiker brake system which depends upon the pressure in the exhaust pipe acting on a cylinder piston system with the usual linkage. Brake system includes a hand lever operating a slide valve on the exhaust pipe and a control on the inlet pipe, which in carburetor engines, opens an air valve and in Diesels cuts out the fuel pump. When operation is by hand lever, a storage cylinder is charged with filtered exhaust gas. Short abstract from A.T.Z., January 25, pages 31–33. Jour. Royal Aeronautical Soc., June, 1938, pages 559–560.

A Family of Motor-Mountings. R. Vogt. New type of engine mount which the author developed for the inverted Jumo gasoline engines and the Jumo Diesels. Motors hang from the top of the crankcase and are left free to spring up and down like the wheels of a motor car which has independent springing. Last mounting is for the new Blohm and Voss landplane version of the transatlantic seaplane. Aeroplane, June 29, 1938, pages 813–815, 7 illus.

Multi-Engine Control Devices. "The Materiel Division at Wright Field has two experimental devices under development for automatic control of engines with special reference to four-engined aircraft." Few details of automatic engine synchronizer and automatic engineer. Aero Digest, July, 1938, page 85.

Aircraft Radio

Aircraft Radio. Learadio Model R3AB crystal-controlled receiver, and Air-Track position finder eliminating all calculations in radio-compass flying. Descriptions of this equipment, progress report on the Metcalf-M.I.T. new blind landing system, and photograph of tiny receiver designed and built by J. T. Lee, Coast Guard Chief Radioman. Aviation, July, 1938, pages 40–41, 4 illus.

Status of Instrument Landing Systems. W. E. Jackson. System using ultra-high frequencies for each of the three elements outlined is most satisfactory. Straight localizer courses may be obtained using ultra-high frequencies with either vertically or horizontally polarized waves, latter being necessary with the glide path. Developments of the Bureau of Standards-Airways Division, Department of Commerce, Army (Hegenberger), Washington Institute of Technology, TWA, Bureau of Air Commerce, and later Lorenz system; Indianapolis tests; United Airlines and Bendix developments; and fundamental elements and projected development. Inst. Radio Engrs., Proc., June, 1938, pages 681–699.

Characteristics of Propagation and Field of Utilization for Different Wavelengths for Guiding Aircraft. Characteristics, advantages, and disadvantages of four categories of wave lengths, and uses to which they can be employed for guiding aircraft. Long waves above 100 meters, short waves between 10 and 100 meters, ultra-short waves between 1 and 10 meters, and microwaves or centimeter waves. Rev. de l'Armée de l'Air, June, 1938, pages 685–688.

"Panoramic Reception" Shows Promise in Radio Navigation. Panoramic reception system developed by M. Wallace. Radio receiver is tuned periodically from one end of a given band of frequencies to the other, by some such system as a motor-driven condenser at a rate perhaps 30 times per second. Receiver reveals relative signal strength and frequency separation of all stations within the band. Cathode-ray tube is used as an indicator to allow simultaneous indication both of signal strength and frequency separation. Electronics, July, 1938, pages 36, 38, 40, 42, 4 illus.

The Practical Use of Radio as a Direct Aid to the Landing Approach in Conditions of Low Visibility. Squadron Leader R. S. Blucke. Paper and discussion. Jour., Royal Aeronautical Soc., June, 1938, pages 483–511, 21 illus.

Short-Wave Radio Communications Set for Pursuit Airplanes. G. Jacquet. British Standard Telephones and Cables R.10 set described requires a minimum of attention from the pilot, and weighs only 23 kg. Four wavelengths which can be selected instantaneously by a manipulation of a single lever are given for both transmitter and receiver without other adjustment. Rev. de l'Armée de l'Air, June, 1938, pages 711–713, 3 illus.

Aeronautical Industry and Production

Four Months' Production Beats 1937 by 55 Per Cent. Production statistics on military and civil airplanes and engines. Aviation, July, 1938, page 57, 1 table.

Pilots

Prediction of a Good Pilot by Psychotechnics. Tests described were recommended by H. Spreng of Switzerland to predict whether or not a student would become a good pilot. Sense of pressure, sense of motion with and without rhythm, emotivity, coordination of movements, observation and intelligence are determined. Les Ailes, June 9, 1938, page 8, 6 illus.

Here and There. Physiological laboratory for aeronautics has been established near the École des Hautes-Études and will be devoted to experimental research on medical-physiological problems relating to aviation. Médecin-general J. Beynes of the Armée de l'Air is director. Brief reference. Les Ailes, June 30, 1938, page 4.